CHEMICAL REVIEWS

pubs.acs.org/CR

Review

RNA: The Unsuspected Conductor in the Orchestra of Macromolecular Crowding

Published as part of Chemical Reviews virtual special issue "Molecular Crowding".

Elsa Zacco, Laura Broglia, Misuzu Kurihara, Michele Monti, Stefano Gustincich, Annalisa Pastore, Kathrin Plath, Shinichi Nagakawa, Andrea Cerase, Natalia Sanchez de Groot, and Gian Gaetano Tartaglia*

Cite This: https://doi.org/10.1021/acs.chemrev.3c00575

Read Online

ACCESS | Metrics & More | Article Recommendations

ABSTRACT: This comprehensive Review delves into the chemical principles governing RNA-mediated crowding events, commonly referred to as granules or biological condensates. We explore the pivotal role played by RNA sequence, structure, and chemical modifications in these processes, uncovering their correlation with crowding phenomena under physiological conditions. Additionally, we investigate instances where crowding deviates from its intended function, leading to pathological consequences. By deepening our understanding of the delicate balance that governs molecular crowding driven by RNA and its implications for cellular homeostasis, we aim to shed light on this intriguing area of research. Our exploration extends to the methodologies employed to decipher the composition and structural intricacies of RNA granules, offering a comprehensive overview of the techniques used to characterize them, including relevant computational approaches. Through two detailed examples highlighting the significance of noncoding RNAs, *NEAT1* and *XIST*, in the formation of phase-separated assemblies and their influence on the cellular landscape, we emphasize their crucial role in cellular organization and function. By elucidating the chemical underpinnings of RNA-mediated molecular crowding, investigating the role of modifications, structures, and composition of RNA granules, and exploring both physiological and aberrant phase separation phenomena, this Review provides a multifaceted understanding of the intriguing world of RNA-mediated biological condensates.

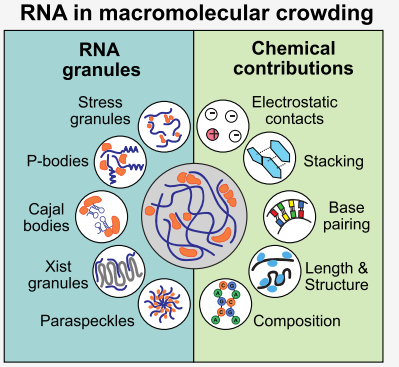

CONTENTS

Received: August 14, 2023
Revised: January 12, 2024
Accepted: January 18, 2024

1. INTRODUCTION

In this Review, we aim to shed light on the role of RNA in molecular crowding, a phenomenon that profoundly impacts the formation, dynamics, and functionality of protein−RNA assemblies in cells.[1,2] These assemblies play an essential role in cellular physiology, and their examination opens up a wealth of opportunities for understanding the molecular mechanisms of health and disease.

We will begin our exploration of the concept of RNA as a crowding driver by delving into the intricate world of gene expression, a fundamental cellular process responsible for translating the genetic code into functional proteins (see section RNA as the Crowding Agent of the Cell). This process follows a remarkably orchestrated procedure, both spatially and temporally. Facilitating this sophisticated coordination are the assemblies of ribonucleoproteins, which consist of RNA molecules and proteins that play a pivotal role in processing them. A central part of our discussion will be dedicated to understanding how RNA crowding and the formation of ribonucleoprotein hubs in specific cellular compartments can trigger the biophysical phenomenon known as liquid−liquid phase separation (LLPS).[3] In this context, the most frequently occurring and biologically relevant cellular event driven by RNA LLPS is the formation of membrane-less organelles, known as ribonucleoprotein (RNP) granules, that are unique cellular entities essential to numerous biological functions.[4]

Increment in local concentration of both RNA and proteins, and therefore controlled molecular crowding, is essential for granule formation and enables the molecules involved to exert their biological function. Together with this aspect, our discussion on LLPS will also analyze other factors that govern RNA-driven crowding and granule formation, highlighting the complex interplay between the inherent properties of the participating molecules, their concentration, and their dynamic interactions.[5] Importantly, the phenomenon of LLPS is not confined to the boundaries of cellular components alone; it is also heavily influenced by extrinsic factors such as temperature, pH, pressure, and salts.[6] These external stimuli can modulate LLPS by altering the physicochemical properties of the resulting droplets, thus opening up avenues for understanding processes in the cell. We will further discuss the role of molecular nucleators, weak interactions, and the unique chemical features of the involved molecules, all of which are vital to trigger and regulate phase separation within cells.[7−9]

Our investigation of crowding promoted by RNA will highlight its unique attributes and capabilities. Due to their intrinsic ability to form base pairs and create complex secondary and tertiary structures, RNA molecules can drive phase separation by themselves or with the support of other macromolecules, leading to the formation of RNA granules such as paraspeckles, Cajal bodies, stress granules, processing bodies, and XIST granules, all of which play critical roles in cellular function (see section RNA-Driven Physiological Crowding).[10−12] These granules are dynamic structures wherein multiple RNA molecules interact with each other to form complex networks. As more RNAs integrate into these networks, the resultant granule becomes increasingly stable and resilient. We will dive deep into the properties that define the functionality of RNA within these granules, such as its sequence and structure.[13,14]

We will pave the way for an exciting area of future investigations into the role of RNA in human disease (see section RNA-Driven Pathological Crowding). In fact, while the implications of RNA in physiological crowding have gained substantial recognition in the scientific community, its potential impact on pathological conditions, specifically neurodegeneration and cancer, is yet to be fully elucidated.

We will also look into the impact that enzymatic modifications on RNA molecules might have on the physical properties of RNA granules, thereby impacting their interactions with other molecules (see section Modifications Influencing RNA-Mediated Cellular Crowding). This makes them crucial players in the regulation of gene expression. Moreover, such modifications can also have far-reaching implications on cellular compartmentalization by influencing the formation of membrane-less organelles. Our Review will investigate these aspects,

https://doi.org/10.1021/acs.chemrev.3c00575
Chem. Rev. XXXX, XXX, XXX−XXX

enlightening on the significant role that RNA modifications play in cellular physiology and potentially in pathological conditions.[15,16]

This Review also offers insights into the methods used to investigate nature and properties of RNA-driven molecular crowding (see section Methods to Study RNA Crowding). We will first look into the physical properties of RNA granules and their rheological characteristics,[17,18] dissecting how these properties underpin their biological functions. To this end, we will examine a diverse array of experimental techniques, spanning from traditional approaches that have stood the test of time to novel techniques that are ushering in a new era of RNA research. We will then focus on the methods employed to investigate the structural features of RNA involved in biological condensates,[19] exploring how the power of light scattering and microscopy enables us to probe molecular interactions, structural attributes, and crowding potential of RNA at unprecedented resolutions. To conclude this section, we will take a closer look at the techniques for determining the composition of RNA granules, elaborating on the types of interactions established by RNA that stabilize its structure, playing a vital role in coordinating its biological functions.

To facilitate a better understanding of the centrality of RNA in attracting other molecules and regulating vital cellular processes , we provide specific examples related to *NEAT1*[20,21] (see section NEAT1: An Archetypical Case of RNA-Mediated Biological Condensation) and *XIST*[22,23] (see section XIST: A Recently Discovered Case of RNA-Mediated Biological Condensation).

Our broad introduction is thus intended to serve as a comprehensive overview, setting the stage for a deeper exploration of the diverse and multifaceted roles of RNA in health and disease, and potentially unlocking new therapeutic avenues.[24,25]

2. RNA AS THE CROWDING AGENT OF THE CELL

The spatiotemporal organization of gene expression at transcriptional and post-transcriptional levels occurs via the formation of supramolecular assemblies of ribonucleoproteins (RNPs), which are hubs of RNA molecules and proteins involved in RNA processing. The increment in local concentration of these components enables their compartmentalization into organelles. Unlike membrane-bound structures, membrane-less organelles (MLOs) exist as liquid droplets[4] and are highly specialized in the passage of molecules, allowing the execution of cellular functions that would not be possible in the dispersed environment of the cytoplasm. MLOs display an intrinsic fluidity that allows for molecular diffusion while guaranteeing specialized molecule recruitment and internal rearrangement. This also enables control over biochemical reactions, which are highly dependent on the type and concentration of reactants. Within the microenvironment of a liquid droplet, or condensate, the rate of *in vivo* reactions can be accelerated by as much as 2 orders of magnitude[26] by incrementing the concentration of essential molecules, making molecular crowding an excellent candidate to be the biological mechanism by which the cell tunes its reactions. The effects of this mechanism can be observed within the Cajal bodies, nuclear MLOs in which the preassembling of spliceosomal complexes can occur 11-times more efficiently than in the surrounding environment.[27] In addition, molecular condensates contribute to the regulation of cellular biochemistry by filtering molecular components in and out of the droplet. For instance, RNA can tune the composition of MLOs by means of length,[28] structure,[9] and sequence,[12] factors that also determine the partition of RNA itself. RNA acts as a scaffold by attracting different numbers and types of proteins, according to its sequence and the higher-order structures it can form. For this reason, RNAs critically affect the behavior of biomolecules within MLOs, promoting and regulating their phase separation. In fact, proteins might recognize single or double-stranded RNA and specific structural features or motifs while RNA can increase local protein concentration, acting as a scaffold for the recruitment of multivalent RNA-binding proteins (RBPs) and the increment of their local concentrations.

Condensation is also the means by which the cell compartmentalizes its biochemistry.[29] A pertinent example is offered by the biochemical communication at synapses, where formation and disassembly of clusters of neurotransmitter-containing synaptic vesicles are regulated by the organization, into droplets, of key proteins that function as scaffolding elements.[30] The formation of liquid droplets driven by RNA and proteins enables their confinement without the need of synthesis upregulation and despite the challenges posed by the neurons' large surface area.[31] Another example is given by the potential evolutionary advantage offered by molecular crowding in response to stress. For efficient energy production, mitochondrial respiration creates an excess of oxygen that can profoundly affect the function of all biological molecules. The modification of the phase behavior of macromolecules within liquid MLOs regulates oxidative imbalance through translational remodeling, activation of DNA repair mechanisms, and metabolic switching.[32] By temporarily trapping substrates of one cascade and excluding others, molecular condensation into droplets determines the activation of specific response pathways.[33]

2.1. Phase Separation Led by RNA

MLOs form by liquid−liquid phase separation (LLPS), a process that occurs when a boost of reagents leads to a supersaturated solution that spontaneously separates into differently concentrated phases.[3] In this context, the concept of phase separation coupled to percolation (PSCP) could play an important role.[34,35] Within MLOs, numerous weak homotypic and heterotypic interactions established by nucleic acids and proteins counteract the interfacial free energy cost of the phase boundary, creating an energetically favorable system.[36] This intricate interplay creates an energetically favorable environment, wherein PSCP, which can be intuitively understood as the spreading of molecular connectivity within these phases, becomes instrumental in regulating connectivity. As the polymers found in soft matter chemistry, RNA and proteins are natural polymers packed with interaction sites for other molecules. To reduce the free energy of a solution made of different macromolecules, the enthalpic contribution of electrostatic interactions−determined by charge−charge interactions and the movement of charged particles− and the entropic input−derived from hydrophobic interactions− enable the thermodynamically driven, reversible phenomenon of the demixing of miscible substances in two distinct liquid phases with different solute concentrations.[37,38] Here, PSCP explains the interconnectedness of these phases and their impact on overall system behavior. Despite the entropic cost, this phenomenon can be energetically favored if the interactions between the components of the phase-separated system overcome the interactions with the solvent.[39] Upon mixing, homophilic interactions determine the negative contribution of

https://doi.org/10.1021/acs.chemrev.3c00575
Chem. Rev. XXXX, XXX, XXX−XXX

changes in internal energy to changes in free energy.[40] The increasing gain of entropy and the release of internal energy upon solvation greatly contribute to droplet formation.

Increasing evidence suggests that homotypic and heterotypic RNA assemblies can be promoted by non-Watson−Crick, nonspecific RNA−RNA intermolecular interactions.[10,11,41] A messenger RNA (mRNA) scaffold could, therefore, recruit additional mRNAs irrespective of the nature of the protein component. Another way to explain how RNA might spatially organize itself would be by intermolecular RNA−RNA interactions bridged by RBPs or Watson−Crick base pairing, and by the contribution offered by the higher valency of long, nontranslating RNA in incrementing the likelihood of self-recruitment. RNA crowding could also occur via base stacking: RNA dimerization can be stabilized by stacking between bases of the same or opposite strands within adjoining base pairs.[42] The structure of the RNA can also play a role in facilitating or hindering phase separation: the G-quadruplex structure, formed by the interaction of aromatic rings of guanines via Hoogsteen-type hydrogen bonding, can change significantly according to the orientation of each guanine base and, as a consequence, the guanine stacking can alter the RNA architecture and thermodynamics of translation.[43,44] Understanding these intricacies, particularly in the context of PSCP, sheds light on the complex mechanisms governing phase separation and percolation within MLOs.

2.2. Chemical Forces of RNA-Mediated Crowding in the Cell

The structure and ability to interact with an RNA chain depend on the physicochemical properties of its nucleotide sequence. An RNA nucleotide contains a ribose sugar with two hydroxyl groups attached to the pentose ring in the position 2′ and 3′. The base is attached to the 1′ position and the phosphate group is attached to the 5′ position. The last one provides negative charge to form electrostatic contacts and, in a chain, connects with the 3′ hydroxyl group of the subsequent nucleotide, assembling a backbone able to form long-range interactions.[45,46] The planar shape of the base allows them to stack on top of each other to form stable pairs. The formation of hydrogen bonds between complementary nucleobases is essential to build secondary and tertiary structures. In addition, the 2′-hydroxyl group can act as both donor and acceptor of hydrogen bonds stabilizing RNA duplexes and other types of interactions.[45,46] Importantly, modifications at this position, such as methylation or acetylation, can regulate RNA function and stability.[47] Overall, the interactions between RNA molecules shape and stabilize the RNA structure allowing the display of precise binding sites to appropriate partners and the formation of complex three-dimensional structures (Figure 1).

The shape of the ssRNA is determined by a delicate balance between stacking forces within the strand and repulsion from neighboring phosphates.[46] Despite the electrostatic repulsion, the hydrophobic nature of nucleobases drives them to move closer to each other, leading to the formation of base pairs and stacks.[46] When complementary ssRNA strands encounter each other, they start forming seed pairs in the typical Watson−Crick geometry.[46] These pairs then propagate in both directions, creating a linear and antiparallel duplex.[46] This pairing process is the fundamental building block of RNA secondary structure. The formation of complex secondary and tertiary structures provides stability and functionality. These structures are sustained by long-range interactions between different regions of the molecule, which include base pairing, base stacking, and

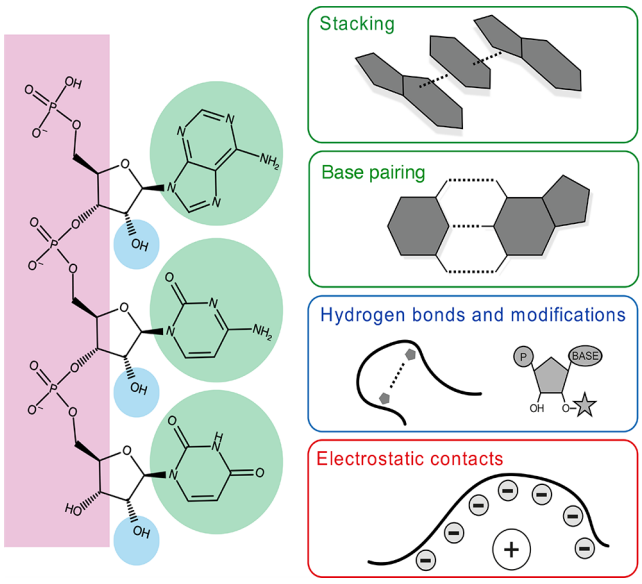

Figure 1. *Elements of the RNA chain involved in the formation of molecular interactions.* The bases can stack on top of each other and can form hydrogen bonds between complementary nucleobases. The hydroxyl groups can form hydrogen bonds and be modified. The phosphate groups form a chain of negative charges, enabling the formation of electrostatic contacts.

other types of interactions such as hydrogen bonding, electrostatic interactions, and van der Waals forces.

These same forces, together with the specific nucleotide sequence and the structure of the RNA molecules, are essential to initiate and scaffold LLPS. However, the occurrence of LLPS not only strongly depends on the nature and concentration of the molecules involved, but also on stimuli such as temperature, pH, pressure and salts.[6] These same variables can control the physicochemical properties of the droplets and may be able to either stabilize them or suppress them by affecting the interactions among the biopolymers or between the macromolecules and water.

Within the cell, phase separation is mainly achieved by three factors: presence of nucleators, establishment of weak interactions, and specific chemical features.

2.2.1. Presence of Nucleators. Biological condensation is promoted when the concentration of a "nucleator" goes beyond its saturation limits. Nucleic acids[48] and nucleic-acid-like molecules such as poly(ADP-ribose)[49] and polyphosphates[50] often seed the process of LLPS. RNA in particular can tune the MLO biophysical properties by attracting a different number and type of interactors. Indeed, RNA appears to strongly contribute to determine the distinct biophysical properties[7] and functionalities[51] of different MLOs and several organelles could be classified according to the type of RNA-centered process taking place in them (e.g., mRNA storage in Stress Granules (SGs), mRNA decay in Processing-bodies (P-bodies) or mRNA splicing in nuclear speckles)[29] (see section RNA-Driven Physiological Crowding). Examples are offered by the effect of reduced nuclear RNA levels on the propensity of RBPs such as FUS and TDP-43 to aberrantly aggregate,[8] and by the changes brought by variations of RNA structure on the recruitment of poly glutamine proteins within MLOs.[9]

2.2.2. Establishment of Weak Interactions. If intra- and inter-molecular interactions are favored over those with the solvent which, in the case of a cell, is almost always water,

https://doi.org/10.1021/acs.chemrev.3c00575
Chem. Rev. XXXX, XXX, XXX−XXX

biological polymers can condensate by largely secluding from the solvent. To counteract the energy cost of maintaining liquid compartmentalization, numerous noncovalent interactions must occur to create phase boundaries. For example, $\pi-\pi$ stacking is a major driving force for the formation of gel-like states, as occurs for the nuclear-pore complex.[52] Charge neutralization in molecular interactions, due to the proximity of oppositely charged polymers, can also induce the formation of coacervates, as shown *in vitro* by the mixture of positively charged peptides and RNA,[53] and as seen in cells for proteins such as nephrin, whose regions of high negative charge density drive its phase separation via interaction with positively charged partners.[53] Yet, it must be noted that protein−RNA interactions are not only driven by electrostatics.[54] Other weak interactions, including π−cation[55] and cross−β,[56] cooperate to confer stability or fluidity to MLOs.

2.2.3. Specific Chemical Features. The dynamic nature of MLOs implies high freedom of movement between the inside and outside of the droplets. Highly flexible, longer polymeric chains can more readily establish the numerous weak interactions essential for forming and maintaining the compartmentalization and for rapidly moving in and out of the MLO.[57] RNA can favor molecular crowding and condensation by acting as a scaffold for the recruitment of other RNA molecules, multiple copies of certain RBPs or different proteins.[58] Also, RNA concentration is correlated to its ability to promote or hinder phase separation: high RNA concentrations might inhibit, competitively or allosterically, the interactions between protein disordered regions, while low RNA concentrations might increase the possibility of establishing electrostatic interactions between the negatively charged RNA backbone and the positively charged protein regions.[8,59]

Proteins, with their varied chemistry, are crucial in the formation of most known MLOs. This is due to several key features:[60]

i) Intrinsically Disordered Regions (IDRs): Unstructured regions with a propensity to interact with other IDRs, significant in protein dynamics within MLOs.

ii) Prion-like Domains (PrLDs): These domains form amyloid-like structures crucial for phase transition in proteins, with a single PrLD often being sufficient for this process.

iii) RNA-binding Domains (RBDs): They facilitate interactions with nucleic acids, requiring multiple RBDs to modulate protein assembly dynamics within MLO.

iv) Post-translational Modifications: Altering the protein's charge, these modifications significantly impact the properties of the condensate and the protein's cellular interactions.

Additionally, the abundance of protein and RNA molecules influences complex formation in the cell, with implications for toxicity and cellular health.[61] Finally, the architecture of SGs and PBs is dynamic and adaptable, involving intricate networks of protein−RNA interactions.[62]

2.3. Physico-chemical Determinants of RNA-Mediated Interactions

The chemical features of RNA are sufficient to drive the formation of RNA-only granules. However, more frequently the biological functions of RNA condensates require the presence of key proteins that take an active part to the crowding process, either as scaffolds or as clients. The composition of the RNA molecules involved, their length and their structures determine the nature and concentration of proteins attracted within the granules.

2.3.1. Crowding of RNA Molecules. RNA molecules alone can drive phase separation and form granules thanks to their ability of base pairing and to form complex secondary and tertiary structures.[10−12] Base pairing can lead to the formation of RNA duplexes that can interact with other RNA molecules forming stable structures such as hairpins, loops, and stems, structures which can also interact with each other forming the network of interactions that sustains the RNA granule. The incorporation of more RNA molecules into this network improves its stability and half-life.[63−65]

The formation of RNA condensates without the contribution of proteins was initially observed with repeat RNAs associated with neurodegenerative diseases, such as Huntington's and Amyotrophic Lateral Sclerosis (ALS).[11,66] These RNAs contain long repeated segments able to form complex structures and multiple base pairing contacts that trigger the formation of RNA foci. Inside the cell, these foci can be dissolved by RNase A, demonstrating that their assembly is sustained by RNA.[11] In the case of the CAG triplet associated with Huntington's disease, phase separation is length dependent promoting an assembly sustained by a multivalent base-pairing.[11] In contrast, the hexanucleotide GGGGCC (G4C2), in addition to the length of the repetition, also depends on the structure, since it requires the formation of a G-quadruplex to trigger the granule assembly.[66] The capacity for phase separation without proteins extends beyond RNA repeats, enabling the creation of condensates using solutions of RNA homopolymers and purified cellular RNA.[10]

2.3.2. Crowding of Protein and RNA Molecules. The majority of biomolecular condensates are composed or sustained by both RNAs and proteins, defined as RNP granules.[12] Thanks to this combination, the two different molecules can exert a dual influence that regulates the structure and interaction network of each other.[7,12,67] Hence, the cell uses this as a mechanism to control granules formation in time and space. For example, although RNA molecules can self-assemble within the cell, the presence of RBPs can help bring them closer, increasing their local concentration and facilitating their interaction.[9]

The role of RNA in RNP condensates is diverse. For example, in the case of mRNA, it can trigger granule formation. When the translation stops and the mRNAs are released from the ribosome, their high numbers and inherent interactivity enable self-assembly and SG assembly.[64] RNA can also regulate the recruitment of RNA-binding partners or act as the main structural element of the granule.[63,64] Along these lines, many noncoding RNAs (ncRNAs) have been identified as scaffolds for the formation of intracellular structures.[68] In the cell nucleus, the so-called architectural RNAs (arcRNAs) are the core of nuclear bodies, such as nucleolus, Cajal bodies, and paraspeckles, contributing to the maintenance and three-dimensional organization of the genome.[68]

Regarding the protein side of the RNP complexes, the main properties associated with the granule-forming proteins is the presence of prion-like low-complexity regions and of RNA binding domains (RBDs). The first one provides flexibility and interactivity with different partners and the latter facilitates the interaction with RNA molecules.[69,70] Their sum promotes valency and interconnectivity within the granule. In the presence of RNA, the positively charged protein domains rich in lysines[71] and arginines[12] can interact with the negatively charged phosphate backbone. As single strands, RNA molecules might

https://doi.org/10.1021/acs.chemrev.3c00575
Chem. Rev. XXXX, XXX, XXX−XXX

resemble proteins' low-complexity regions, since they are highly flexible and can form specific and nonspecific interactions with many RBPs or RNAs.[72] Different RNA structures can be combined to form multiple binding sites for proteins and favor multivalency.[62,64] In an unstructured context, the specific physicochemical properties of single stranded RNAs and disordered proteins can promote interaction.[73,74] Intriguingly, the amino acids in a protein chain have been predicted to interact with combinations of nucleobases that correspond to the codons encoding them.[73,75] According to this model, when disordered protein regions and RNAs are available for interaction (e.g., during MLO formation), RNA sequences rich in pyrimidines interact with proteins enriched in hydrophobicity.[74]

Overall, known properties that determine RNA function and connections within the granules are (i) composition; (ii) length; and (iii) structure.[12]

2.3.3. The Effect of the RNA Composition on Phase Separation. The role of proteins in the formation of RNP condensates may be determined, with high efficiency, by analyzing their amino acid sequence and identifying specific regions such as low complexity regions or RNA binding domains.[76] However, this kind of approximation is not feasible with RNA, since all molecules are made up of only four different building block nucleotides, whereas proteins are chains of up to 20 different amino acids able to generate many different combinations. Nevertheless, the elements modulating the RNA interactivity go further than just the four-nucleotide code (Figure 2). There are connections involving nucleotides distant in sequence, tridimensional structures that expose specific areas and exclude others, and nucleotide modifications which may alter completely the chemistry behind their interactions.[77]

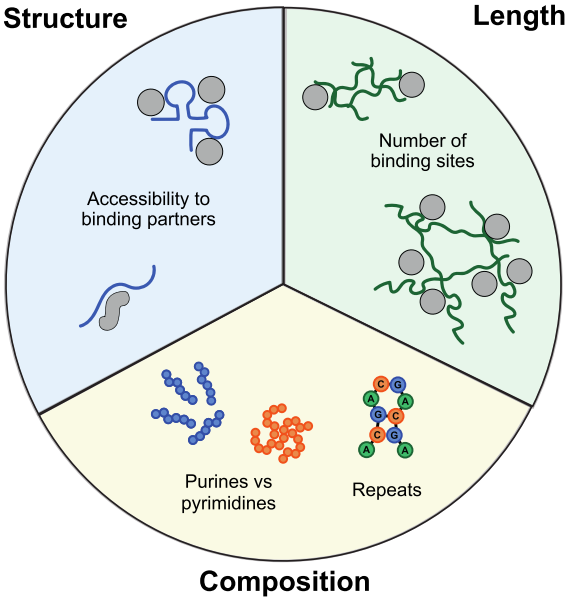

Figure 2. *Impact of RNA properties on macromolecular assembly.* (i) Nucleotide composition: Influences granule contact strength and dynamic behavior, with arrangements affecting local secondary structures in RNA repeats. (ii) Length: Directly influences local crowding and the number of available binding sites. (iii) Structure: Determines accessible regions for interactions with partner molecules, affecting the quantity and types of binding sites, thus influencing the range and number of potential partners. Binding partners (proteins and other molecules) are shown as gray objects.

Importantly, the presence of chemical modifications expands the RNA coding potential even beyond the 20 standard amino acids found in proteins.[77] They can alter the RNA physical properties, affecting its stability, folding, and interaction capabilities.[47]

A successful strategy to decipher the role of nucleotide sequence in the formation of RNP granules has been the study of homotypic RNAs. In 2019, Gitler and colleagues discovered that the ratio of purines to pyrimidines significantly impacts the forces driving phase separation in disordered RNA molecules.[12,78] They studied the phase separation of the combination of RNA homopolymers and poly(proline−arginine) and poly(glycine−arginine) protein repeats. In the case of arginine-rich proteins, *in vitro* phase separation is led by electrostatic and cation−π interactions.[79,80] In the presence of RNA, their results suggest that purines can act as "stickers", while pyrimidines can act as "spacers". This effect is associated with their ring structures, and, in the case of purines, the double ring can provide a stronger aromatic character. According to these results, assemblies formed by poly(G) and poly(A) were less dynamic than those formed by poly(C) or poly(U). In fact, poly(G) form fractal-like and gel-like structures while the other homotypic RNAs form liquid-like condensates. The combination of the different nucleotides can also alter the condensate properties. For example, poly(A) and poly(U) RNAs can base-pair and form solid-like gels.[11,12] Contrarily, poly(C) and poly(U) phase-separate independently, forming distinct droplets.[11]

2.3.4. The Effect of the RNA Length on Phase Separation. The length of an RNA isoform can determine its presence in a certain condensate.[63] For example, SGs exhibit a higher concentration of long and less translated mRNAs compared to short RNAs.[81] This has also been observed *in vitro* where, in a solution of polyethylene glycol (PEG) and dextran, RNA was able to form droplets that recruit ribozymes, however the longer RNAs phase separated more efficiently into droplets than the shorter ones.[28] In the case of the ncRNA *NEAT1*, a longer transcript isoform assembles into granules called paraspeckles, while the short one into different types of condensates, called microspeckles.[82,83]

Length affects the number of contacts that an RNA can form and has a direct effect on the size and stability of the condensate. Longer RNAs can form a larger number of interactions and cross-links with other RNA molecules, and can also contain more sites to bind RBPs. RBPs typically interact with one or more regions of around 10−20 nucleotides and just a duplication of this length will suffice to interact and attract multiple molecules.[84,85] On the contrary, small RNAs like microRNAs (miRNAs) and piwi-interacting RNAs (piRNAs) might lack the ability to independently initiate phase separation.[81,85,86] Overall, the length can bring biomolecules together and promote phase separation. This property can also affect the condensate dynamics, and, in general, longer RNAs tend to form more stable and less dynamic condensates.[64] In the case of the RNA helicases LAF-1 and DDX3X, found in coacervates called P-bodies, their activity and their way to interact with RNA is influenced by the RNA length.[40,87] RNA length is also closely connected with the concentration and number of RNA molecules inside a condensate, and the combination of these two variables relates to the number of RNA binding sites (Figure 2).

2.3.5. The Effect of the RNA Structure on Phase Separation. The formation of structural elements can expose or hide specific RNA sequences, determining both RNA−RNA

https://doi.org/10.1021/acs.chemrev.3c00575
Chem. Rev. XXXX, XXX, XXX−XXX

and RNA−protein interactions and influencing granules assembly, composition, and biophysical properties.[7,9,88] In the case of the protein Whi3 (from the multinucleated filamentous fungus *A. gossypii*), interaction with two RNAs having different sequence and structure (CLN3 and BNI1) results in the formation of immiscible granules with different viscosity that regulate the fungus branching sites.[9,89]

A trend known as 'structure-driven protein interactivity' has been identified, showing that RNAs with a greater number of double-stranded regions tend to establish more interactions with proteins compared to RNAs with less structure.[7] This trend does not just suggest that protein binding to RNA occurs exclusively in double-stranded regions; rather, it indicates that the structural context of the RNA contributes to the stability of these interactions. Indeed, in many cases, single-stranded binding sites are prevalent.[90] The structural content of RNAs is particularly relevant in distinguishing those involved in protein binding from those participating in the formation of ribonucleoprotein (RNP) assemblies. Remarkably, it has been observed that altering the structural content of RNAs involved in phase separation can lead to changes in the composition of protein aggregates.[7]

The analysis of the protein−RNA, protein−protein, and RNA−RNA interaction networks in MLOs such as SGs and P-bodies has shown that the proteins and RNAs that establish the largest number of contacts are enriched in disordered regions.[62] In this line, the authors observed that as protein disorder increases, also the number of single-stranded regions rises in their RNA-binding partners. These observations imply that SGs and P-bodies may have the capacity to rapidly assemble and disassemble, facilitated by dynamic interactions regulated by the unfolded domains of their constituent components.[62] This interactivity between unstructured regions recalls the observations behind the complementarity hypothesis in which most proteins interact specifically with their own mRNAs, especially if unstructured.[91,92] In this study, the analysis of CLIP-seq data shows an inherent attraction between nucleobases and amino acids that promotes the interaction between the mRNA coding regions and the proteins translated from them.[91]

3. RNA-DRIVEN PHYSIOLOGICAL CROWDING

MLOs such as SGs, P-bodies, and other RNP granules, represent a sophisticated cellular mechanism for coping with various stressors. These organelles, devoid of a surrounding membrane, form through intricate RNA−RNA and RNA−protein interactions.[93] RNA not only acts as a scaffold for protein assembly in these organelles but also participates in self-assembly, highlighting its dual role in the cellular stress response.[94] The formation of these organelles is a critical adaptive mechanism, allowing cells to regulate gene expression and protein synthesis under adverse conditions, thereby aiding in cell survival and maintenance of cellular homeostasis. Indeed, RNA can act as a scaffold that helps in the assembly of various proteins and other molecules. These granules form in response to stress conditions like heat shock, oxidative stress, or UV irradiation, providing a protective environment for mRNA.[95] By sequestering mRNA, SGs can regulate gene expression and protein synthesis, which is critical for cell survival under stress.[96]

However, the balance of these interactions is delicately poised. An overabundance of RNA−RNA interactions can lead to pathological states, particularly in the context of neurodegenerative diseases. Factors such as long repeat expansion RNAs or specific dipeptide repeats can disturb this balance, leading to the aggregation of SGs and contributing to disorders like ALS and Frontotemporal Dementia (FTD).[94] This underscores the importance of understanding the nuanced roles of RNA within these organelles, not only for insights into basic cellular biology but also for the implications they hold in the realm of disease pathology and potential therapeutic interventions. Thus, the study of stress-responsive membraneless organelles, particularly the role of RNA within them, is a rapidly evolving field that bridges fundamental biological processes with clinical relevance. Among the most commonly occurring MLOs there are the following.

3.1. Paraspeckles

Found in the nuclei of mammalian cells, within the interchromatin space, paraspeckles are built on the architecture of the long noncoding (lnc) RNA *NEAT1* (see section NEAT1: An Archetypical Case of RNA-Mediated Biological Condensation). Transcribed into two isoforms, a short one named *NEAT1_1* of 3.7 Kb and a long one called *NEAT1_2* of 22.7 kb, they each receive a differential 3′ end processing[20] and only *NEAT1_2*, with its specialized triple helix structure,[97] is found in paraspeckles. Knocking down *NEAT1* determines the disappearance of paraspeckles[82] and, in its absence, these RNA granules cannot be observed,[98] signifying that *NEAT1* is essential for paraspeckle formation and maintenance. In addition to *NEAT1*, other RNAs with given characteristics are found in paraspeckles: purine-rich sequences,[99] U1 small nuclear RNA,[100] and RNAs with long inverted repeats at their 3′ untranslated regions.[101] An example is the case of the RNA *Ctn*, which contains double-stranded hairpins generated by inverted repetitive elements.[102]

Despite not being direct sites of transcription, paraspeckles are intimately linked with this process since, among the proteins identified as part of paraspeckles, RNA Polymerase II (Pol II) is present, together with *de novo* synthesized RNAs. It is thought that the role of these RNA granules in transcription is exerted by retaining transcripts within the nucleus. In addition to Pol II, the proteins of the DBHS (*Drosophila melanogaster* behavior, human splicing) family (i.e., PSPC1, NONO and SFPQ), are also essential protein components of paraspeckles. Binding both single and double-stranded DNA and RNA, they are involved in many aspects of RNA processing, such as transcription initiation and termination, coactivation, and both constitutive and alternative splicing.

3.2. Cajal Bodies (CB)

One of the first MLOs to be discovered, CBs are multifunctional nuclear bodies (NBs) formed by concentration-dependent phase separation,[103] where the macromolecular crowding of given components enhances the processes necessary for the biogenesis of many subtypes of RNPs, in particular of small nuclear RNPs (snRNPs). These processes include transcription activation, RNA processing, enzymatic base modification and assembly of snRNPs: the enzymatic complexes responsible for the catalysis of RNA splicing.[27] CBs can directly upregulate the expression and 3′ end processing rate of snRNPs and of its associated RNAs through transcriptional activation and sequestration.[104] Telomerase RNPs are another important component found highly enriched in CBs, suggesting an active role of CBs in telomere maintenance. Within CBs, RNA-modifying enzymes such as 2′-*O*-methyltransferases and pseudouridine synthases contribute to the assembly of the spliceosome,[105] the macromolecular complex responsible for intron removal and splicing, together with small Cajal body-specific RNPs (scaRNPs). Both the RNA and protein

https://doi.org/10.1021/acs.chemrev.3c00575
Chem. Rev. XXXX, XXX, XXX−XXX

components of CBs are enriched in post-translational modifications that appear to affect the function of both elements. Recent studies have identified CBs in association with specific gene loci, in particular with chromosome 1, hinting at an organizational and architectural role of CBs in gene expression and regulation.[106]

3.3. Stress Granules (SGs)

SGs are cytoplasmic phase-separated RNP complexes that confer upon the cell the ability to adapt to change by tuning its biochemistry in response to intra- and extra-cellular inputs. Their formation is triggered by the phosphorylation of eIF2α and the consequent specific translational arrest of nonstress-related mRNAs. This enables the initiation of defense mechanisms that promote either survival or apoptosis, according to the type of stress.[107] SGs can form through a pathway that is independent of eIF2α phosphorylation. Indeed, when cells encounter stress, mature tRNAs are cleaved at the anticodon loop by the ribonuclease Angiogenin.[108−110] This cleavage generates tRNA-derived stress-induced RNAs (tiRNAs), which are able to displace translation initiation factors, such as the cap-binding eIF4F complexes, from the mRNA cap, inhibiting translation and thereby promoting SG formation.[108,111] Following stress-causing inputs, SGs allow the cell to store, temporarily, proteins and RNAs and to release them in a controlled manner. The way in which SGs exert their stress-dependent functions is by translational control over the fate of mRNAs, by entrapping translationally stalled mRNAs and translation initiation components,[95] and by regulating protein aberrant behavior, achieved by sequestration of potentially toxic misfolded proteins with a reversible process that is likely to be an adaptive response to cellular stress.[112] An essential point in the formation of SGs is the increment in local concentration of both RNAs and proteins, which are rich in low complexity domains (LCDs) that facilitate the interactions necessary for SG formation. This results in the generation of dynamic granules with droplet-like properties and implies that the concentration of RNAs and RBPs must be highly regulated in order to control SG formation. If, on the one hand, the presence of different amounts and species of RNPs inside the SGs increases the rate of rearrangement of RNPs within the MLO, on the other hand it reduces the concentration of the same molecules of RNA and proteins in the cytosol, affecting reaction rates. An example is represented by the SG-mediated inhibition of senescence by the sequestration, upon stress, of PAI-1, a protein strongly associated with aging due to its role in the hyper-activation of cellular proliferation.[113]

3.4. Processing Bodies (P-Bodies)

First identified in yeast during the stationary growth phase or nutrient deprivation,[114] P-bodies comprise mRNAs in complex with translation repression proteins. Due to their composition, it has been suggested they play an active role in mRNA degradation, since the majority of proteins present in these RNA granules are involved in translation regulation (eIF4E, DDX6), mRNA surveillance (UPF1, SMG5) and mRNA decay (XRN1, DCP1).[115] However, it appears that the formation of P-bodies might be the consequence of, rather than the mechanism behind, mRNA degradation. The destiny and rate of degradation of different mRNAs within P-bodies varies to the extent that some of them appear to be protected from degradation, and the presence of P-bodies is not necessary for RNA decay to occur.[116] An alternative (but not contradictory) scenario contemplates these RNA granules as simple storage units of repressed mRNA and deactivated enzymes involved in mRNA decay processes that undergo LLPS due to the accumulation of mRNA decay factors on polysome-free transcripts.[96] The formation and maintenance of P-bodies depends on the presence of translationally repressed mRNA[117] but also on the concentration of certain proteins, such as the RGG-rich Lsm4[118] and DDX6,[119] which, with their low complexity domain and RNA-binding ability, are implicated in LLPS. *De novo* P-body formation also increases as a consequence of specific types of cellular stress, such as osmotic stress[120] or glucose starvation.[121]

3.5. XIST Granules

A newly discovered example of RNA-mediated crowding is represented by *XIST* noncoding RNA that drives X chromosome inactivation (XCI)[22,23] (see section XIST: A Recently Discovered Case of RNA-Mediated Biological Condensation). During XCI, *XIST* RNA (also acts as a scaffold by recruiting, on its multivalent repetitive elements, multiple ubiquitous RBPs (PTPB1, MATR3, TDP-43, and CELF1) that eventually lead to the condensation and consequent inactivation, of one of the X chromosomes in females.[122,123]

4. RNA-DRIVEN PATHOLOGICAL CROWDING

A delicately balanced and highly coordinated interplay between proteins and nucleic acids, occurring by means of molecular crowding, ensures spatiotemporal gene regulation at transcriptional and translational levels, guaranteeing functional cellular development and maintenance. During the formation of macromolecular condensates, the global RNA metabolism undergoes a complete revolution where splicing, stability, localization and translation are redefined by novel interactions with RBPs, or by the lack of them.[124] At the same time, RNA critically affects the behavior of RBPs within the droplets, promoting and regulating their structure and function.[62] While the formation of such highly crowded compartments is vital for numerous essential cellular pathways and events, such as translation control and stress response, their reorganization or dispersal are imperative. Molecules inside the droplets must be able to freely escape and interchange with others from the outside, to enable the physicochemical equilibrium necessary to maintain biological function. Considering the level of precision required for physiological coacervate formation and regulation, it is easy to imagine how alterations in such a delicate equilibrium may influence tremendously the stoichiometry of RNP formation or the ability of a given RBP to recognize its RNA binding partners. RNA granule dysfunction and, in general, impairments in RNA metabolism have been associated with pathological conditions such as neurodegeneration and cancer, where translation and mRNA stability are highly interconnected with the fate and the health of the cell.

4.1. Neurodegeneration

Age-driven loss of neuronal functions is a hallmark of many diverse neurodegenerative diseases, incurable and debilitating conditions whose progress inevitably leads to a gradual but irreversible loss of neurons, affecting both cognitive and physical functions.[125] Despite the fact some of these diseases can have a familiar origin and be hereditary, many forms are sporadic, lacking any specific etiology. Dysregulation in coacervate dynamics can lead to alterations in the precisely regulated RBP stoichiometry and have a colossal impact on neuronal function, regulation and synaptic communication.[126] These events could, therefore, be a common causative mechanism behind neurodegeneration. Subtle changes in RNA granule

https://doi.org/10.1021/acs.chemrev.3c00575
Chem. Rev. XXXX, XXX, XXX−XXX

composition or constituent levels could render the coacervates stiffer, limiting their fluidity and altering the liquid properties of the droplets, with the consequence of trapping essential biomacromolecules inside. These changes in RNA granule dynamics are often the result of disturbed RBP functions that may undergo aberrant liquid-to-solid phase transition (LSPT), which can lead to the accumulation of neurotoxic protein−RNA inclusions.[127]

Many RBPs are highly prone to LLPS and, in instances of alteration of their expression levels or mutations affecting their structural stability, they can become highly aggregation prone and undergo LSPT.[61] This phenomenon appears to be particularly associated with SGs. For instance, the accumulation of mutated TDP-43, FUS and SOD1 within SGs is a pathological feature of ALS and rare forms of frontotemporal lobar degeneration (FTLD);[128,129] huntingtin (HTT) and prion protein (PrP) are found to be associated with SGs in Huntington's disease and prion disease;[130,131] TIA1, TTP, and GBP, highly conserved RBPs with primary roles as nucleators of SGs, are found in condensates in Alzheimer's disease and other tauopathies.[132] Despite differences in composition and function, LSPT of RBPs is a common pathological feature among diverse neurodegenerative diseases.

Mutations in RBP genes do not necessarily directly alter the propensity of the proteins to aberrantly self-assemble but they might affect their ability to correctly process their cognate RNAs. Since every step of RNA life requires the action of RBPs, events altering their performance will directly affect RNA metabolism. Increasing evidence suggests alteration in RNA processing may be among the main factors contributing to disease pathogenesis, rather than being only a consequence.[124,133] For example, the protein TDP-43 alone can influence the global RNA expression of more than 600 genes, many of which are neuronal genes.[134] It is therefore highly likely that depletion of this RBP or alteration in its ability to bind RNA would have catastrophic consequences on gene expression, contributing to the pathogenesis of neurodegenerative diseases. RBP inability to bind RNA can also indirectly influence a protein tendency to phase separate. For instance, despite the lack of direct structural relevance, the mutation K181E on TDP-43 indirectly renders the protein more prone to aggregate since it strongly impairs the protein's ability to interact and process target RNAs, reducing the stabilizing contribution of RNA to function as a chaperone.[135]

Multiple links between dysregulation in granule dynamics and neurodegenerative disease have been reported. For example, the presence of a pathological number of CAG repeats in the gene coding for the protein HTT generates a mutated HTT that cannot properly fulfill its role in mRNA transport in neurons via transport granules. For this reason, in Huntington's disease, HTT coprecipitates with AGO2, protein of the P-bodies, and coaggregates with the SG protein TIA-1.[136,137] Another similar case is presented by CAG expansion in ATXN2: the mutant protein impairs SG and P-body assembly and affects granule physiology.[138]

Mutations in RBPs are known to be causative factors in the neurodegenerative disease ALS. As previously mentioned, mutations that affect the phase transition propensity or localization of RBPs, such as TDP-43 and FUS, are commonly found in ALS patients. Recent studies have identified mutations in TIA-1, a primary SG-nucleating protein. These mutations have been observed to slow down SG disassembly and mobility. Additionally, they are involved in the aggregation of wild-type TDP-43, though TIA-1 has not been found in the resulting inclusions.[139] Alterations in the eIF2α-independent SG formation pathway have also been implicated in ALS pathogenesis.[140] Components such as Angiogenin, tiRNAs, and ultimately SGs are part of a cytoprotective regulatory program enhancing cell survival under stress.[141] Diminished Angiogenin activity due to point mutations has been linked to both familial and sporadic ALS cases. Conversely, Angiogenin administration or transfection with tiRNA analogs has shown neuroprotective effects.[142−144]

A significant contributor to ALS pathology is the presence of hexanucleotide repeat expansion in the noncoding region of the C9ORF72 gene.[145] This mutation is thought to coaggregate with essential RBPs such as hnRNP A1, hnRNP A2/B1, HuR, and FUS, leading to neural toxicity.[146,147] It was also suggested that these repeats may disrupt tiRNA function, which is vital for translation regulation and SG formation.[144] tiRNAs typically have a guanosine-rich motif at their 5′ end, forming an intermolecular G-quadruplex structure crucial for SG biology.[144,148,149] The G-quadruplex formation by C9ORF72 repeats could impede tiRNAs, affecting SG formation and motor neuron viability.[144]

Furthermore, coacervate RBPs sequestered into GC-rich repeats are associated with Fragile X syndrome.[25,150] In Alzheimer's disease (AD), RNA influences the condensation state of associated proteins. For example, a soluble phosphorylated version of tau, an axonal microtubule-binding protein that preferentially binds to tRNAs, can undergo phase transitions over time with other AD and FTLD-related mutants.[151,152]

Although less studied in this context, neurodegeneration also correlates with P-body dysfunction. Knocking down P-body-associated RBPs of the RNA silencing pathway results in neuronal loss, impaired nerve regeneration and motor dysfunction.[153] In addition, it has recently been suggested that the filtering of mRNAs to be sent to P-bodies occurs in a context-dependent manner and that mitochondrial-related mRNAs, normally excluded from P-bodies, are instead particularly enriched under stress conditions.[121] This suggests that mitochondrial dysfunction might be associated with P-body malfunction in the context of mutants of the protein TIA-1.[154] P-bodies are implicated also in microRNA (miRNA) expression and control, so potential P-body dysfunction could influence miRNA and mRNA stability. Since miRNAs are necessary for managing localized translation at synapses, alterations in their expression levels are, by extension, associated with synaptic defects and loss, as occurs in ALS.[155] This hints at the fact that, in neurodegenerative diseases, P-bodies dysfunction might alter miRNA processing, decay, or storage. Changes in miRNA profile have also been connected to AD. The expression of the β-secretase BACE1, partially responsible for the release of the Aβ peptide by cleavage of the amyloid precursor protein (APP), is regulated by the miRNA miR-107, whose levels are decreased in the temporal cortex of AD patients.[156] Also the synthesis of APP itself, and so the generation of Aβ amyloid plaques, is miRNA-driven[157] and low levels of specific miRNAs are associated with the expression levels of the protein tau, which forms the intracellular tangles found in patients suffering from AD and other tauopathies.[158] Tau suppression is also miRNA-driven, and retention of highly crowded miRNAs within P-bodies leads to the LSPT of these coacervates, which also correlates with the sequestration of important RBPs, such as TIA-1 and of its binding partners.[159]

https://doi.org/10.1021/acs.chemrev.3c00575
Chem. Rev. XXXX, XXX, XXX−XXX

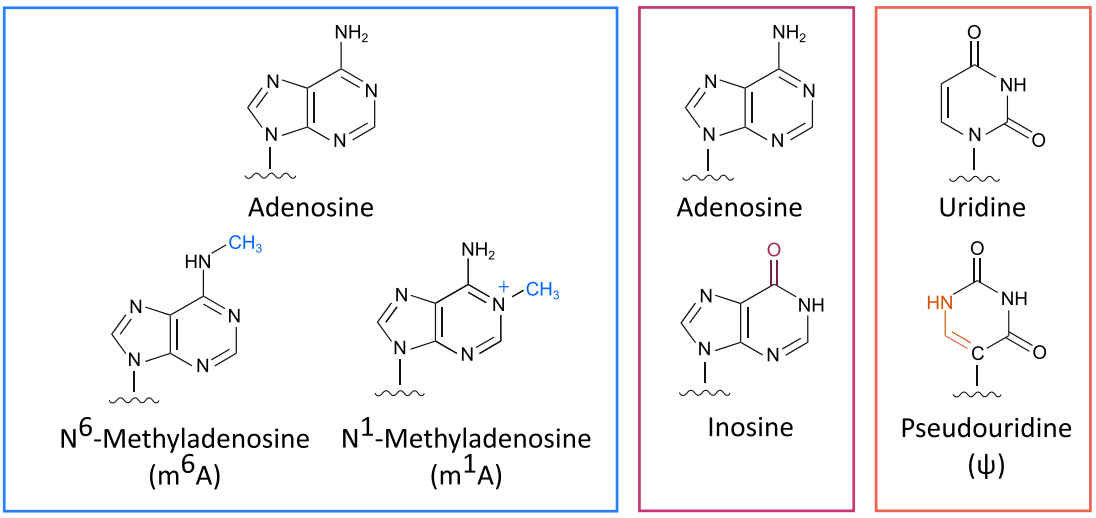

Figure 3. *RNA modifications discussed in this Review.* Example of the most frequent RNA modifications in the cell. The unmodified and modified chemical structures of the bases or of the ribose sugar are reported. RNA chemical modifications alter the ability of RNA molecules to participate in intermolecular interactions, impacting its multivalency and biophysical features. Multivalent weak interactions of RNAs and proteins promote their phase separation into biomolecular condensates. The study of RNA modifications and how they influence the formation and the characteristics of cellular condensates is gaining significant momentum.

4.2. Cancer

Cells carrying modifications in genes regulating growth and differentiation constitute the main structure of cancerous tumors. Cancer cells acquire mutations that can affect condensate-mediated cellular processes including transcription, chromatin structure and proliferative signaling, and that can affect the physiological regulation of molecular compartmentalization and crowding. Cancer, or uncontrolled cell proliferation, is caused by the activation of oncogenes and the inactivation of tumor suppressor genes.[160] When activated, oncogenes induce cell proliferation, survival and proliferative replication signaling. This activation is frequently achieved by the formation of clusters of enhancers occupied by highly crowded transcriptional components driving high gene expression.[161] These clusters promote the formation of liquid coacervates of clustered DNA, transcription factors and regulatory elements.[162] Within these liquid droplets, hundreds of RNA polymerase II molecules affect the transcription of the target genes; therefore, cancerous mutations in the elements involved in these condensates are able to alter the functional levels of specific master regulatory transcription factors and/or of the RNA polymerase II itself, while also affecting the dynamics of the granules.[161] Disrupted condensation in cancer cells can also affect tumor suppressors such as SPOP and PML. Mutations in SPOP, an E3 ligase implicated in many solid tumors, prevent the protein from condensating and reducing its enzymatic activity.[163] PML is compartmentalized in nuclear bodies with a variety of proteins, including DNA repair factors and p53, a protein that controls cell division and death and whose mutations highly correlate with tumor progression. Loss-of-function mutations on the PML gene have been shown to be associated with increase rate of tumor formation and poor prognosis.[164]

While the mechanisms by which RNA granules affect cancer development and growth have not yet been completely elucidated, these coacervates strongly influence the post-transcriptional pathways of the RNAs and proteins they contain, affecting many features of carcinogenesis and metastasis. As previously mentioned, changes in the concentration levels of any of the condensate constituents may alter the function of the condensate. In cancer cells, for example, the coacervate concentration of the oncogenic protein MYC is reported to be 50-fold higher than in noncancer cells, and this significant increment in MYC presence within the liquid droplets alters the behavior of the transcriptional condensates of the whole cell.[165] From the RNA side, a wide range of ncRNA, one of the main components of several RNA granules, are found post-transcriptionally modified,[166] under-expressed (e.g., *LET, MEG3, DRAIC, NKILA, PCAT*) or overexpressed (e.g., *MALAT1, lncRNA-ATB, lncTCF7, SRA, CCAT2, ZEB2-AS1, UCA1, SCHLAP1*).[167] In particular, the cancer-associated overexpression of the nuclear speckle lncRNA *MALAT1* influences many cellular physiological functions and alters condensate behavior.[168]

The link between RNA granules and cancer is made stronger by the cellular response to stress. Stress induces the formation of certain RNA granules or changes their size and composition, and cancer cells are particularly successful at adapting to stress and surviving.[169]

Among the numerous correlation points between cancer and RNA granules is *NEAT1* level in paraspeckles and tumor progression or poor prognosis, however the direction of such correlation is ambiguous. In fact, certain cohort studies report an upregulation of *NEAT1* in cancer samples while others report the opposite.[170,171] Also *NEAT1* knocked-out cancer mouse models reveal contradictory results.[172,173] It is worth noting that, in all animal models considered, p53 induces upregulation of *NEAT1* expression and paraspeckle enlargement.

Another connection between cancer and RNA phase separation is demonstrated by the roles played by SGs. The kinase mammalian target of rapamycin (mTOR) controls cell growth and mRNA translation in response to the presence of growth factor and to insulin signaling and it is widely implicated in cancer.[174] One way in which mTOR operates is by interacting with raptor in an association that is mediated by the protein astrin. Under oxidative or osmotic stress, astrin sequesters raptor inside SGs, inhibiting mTOR activation.[175] Altered mTOR activity determines important changes in translation, particularly in relation to eIF4F complex assembly. The expression of eIF4F

https://doi.org/10.1021/acs.chemrev.3c00575
Chem. Rev. XXXX, XXX, XXX−XXX

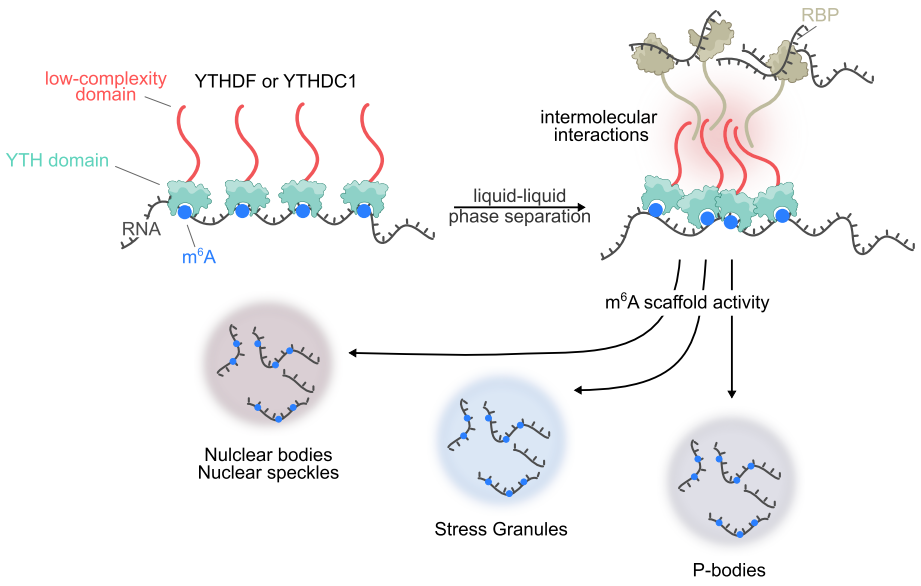

Figure 4. *m^6A and phase separation.* m^6A readers contain a low complexity region (disordered domain). It has been proposed that m^6A-modified RNAs can act as scaffolds to recruit multiple low complexity domain-containing readers in proximity, facilitating intermolecular interactions that ultimately trigger condensate formations. m^6A RNAs together with their readers participate in the formation of phase-separated compartments: stress granules (SG), P-bodies, and Nuclear bodies/speckles.

has been found upregulated in around 30% of all cancers, a phenomenon associated with poor prognosis since higher levels of eIF4F, an oncogene itself, determine enhanced cell proliferation and resistance to cell death.[176] Another effect of the incremented expression of eIF4F is on the regulation of a subset of mRNAs that encode for transcription factors, cell cycle and apoptosis regulators, kinases, cytokines and growth factors. It is not known whether these mRNA phase separate with their protein binding partners but solid evidence supports the presence of eIF4E in both SGs and P-bodies.[177]

There is another important protein family that localizes in SG and/or P-bodies and whose phase separation is associated with cancer: the cold shock domain (CSD) protein family, in particular LIN28. In cancer patients, LIN28 mediates the down-regulation of miRNAs of the let-7 family, which have tumor suppressor activity. As a consequence of the down-regulation of these miRNAs, their mRNA targets, which instead codify for pro-proliferative, oncogenic and antiapoptotic factors, are up-regulated.[178]

Other examples of SG/P-body-associated proteins that participate in carcinogenesis are the RNA-dependent helicase Ded1/DDX3, which functions both as an activator and repressor of translation;[179] eIF5A, involved in mRNA metabolism and SG assembly;[180] and the Argonaute proteins, a group of multifunctional proteins that are down-regulated in cancer cells.[181]

5. MODIFICATIONS INFLUENCING RNA-MEDIATED CELLULAR CROWDING

RNA molecules not only contain the canonical residues A, C, G and U, but they are also largely formed by modified ribonucleotides. To date, over 150 different types of modifications have been identified[77] and more are likely to be discovered. Despite being initially identified in rRNAs and tRNAs,[182] RNA modifications, following the advancements in sequencing and mass spectrometry, have been detected in mRNAs and lncRNAs. Indeed, eukaryotic mRNAs are not only modified at the extremities with a 5′ 7-methylguanosine cap and a 3′ poly(A) tail, but they are also internally modified; the most abundant RNA modification within the RNA body is the N6-methyladenosine (m^6A) consisting of an addition of a $-CH_3$ methyl group to the sixth nitrogen atom of an adenosine purine ring[183,184] (Figure 3).

Chemical modifications can greatly impact the resulting RNA molecules by altering their physical properties, such as charge, secondary structure and ultimately interactions with other molecules, including proteins. For instance, inosine—deriving from deamination of adenosine—is predicted to mimic guanine not only when interacting with RNA but also in the interaction with protein chains.[185] Chemical modifications play a key role in fine-tuning gene expression by modulating several aspects of RNA metabolism such as splicing, localization, translation, and degradation. More recently, RNA modifications have emerged as determinants in cellular compartmentalization by influencing the formation of MLOs. Considering that their formation depends on the properties of nucleotides and amino acids, along with their interaction capabilities, it is evident that modifications in their characteristics, stemming from chemical alterations in both RNAs and proteins, will significantly affect RNA−protein pairing and ultimately MLO generation.[74]

RNA chemical modifications are introduced by specific enzymes known as "writers", which catalyze the addition of chemical groups to specific nucleotides. For instance, addition of the methyl group in the m^6A modification is performed by the m^6A methyltransferase complex, including the proteins METTL3 —responsible for the catalytic activity—, METTL14 WTAP and KIAA1429.[186−188] RNA chemical modifications can be "read" and "erased" by specific proteins, thereby modulating their impact on gene expression. The "reader" proteins recognize and bind to modified nucleotides, leading to downstream effects on RNA metabolism. The YTH domain-containing family of proteins, such as YTHDC1 and YTHDF1, can bind to m^6A modifications and modulate mRNA splicing, stability, and translation.[189,190] Conversely, "eraser" proteins remove the modifications and restore the unmodified state of the nucleotide. FTO and ALKBH5 are two well-known m^6A eraser proteins that remove the methyl group of the m^6A

https://doi.org/10.1021/acs.chemrev.3c00575
Chem. Rev. XXXX, XXX, XXX−XXX

modification from RNA.[191,192] The interplay among writers, readers, and erasers is essential for maintaining a dynamic epitranscriptome. The next paragraphs offer an overview of the chemical modifications most commonly found in RNA granules.

5.1. Effect of m^{6}A in Biomolecular Condensate Formation

A connection between the m^{6}A RNA modification and phase separation was established when researchers unveiled that (i) the three m^{6}A readers, namely YTHDF1, YTHDF2, and YTHDF3, comprise a low complexity region (disordered domain) and thus have the capability to undergo phase separation;[13,193−196] (ii) m^{6}A modified RNAs are enriched in SG compartments[196,197] (Figure 4). The m^{6}A reader YTHDF2 was shown to form droplets with liquid properties *in vitro*, through a process of LLPS.[13,193] YTHDF2 phase separation was enhanced by the presence of poly methylated RNAs and the effect was strictly dependent on the number of methylated sites,[13] suggesting that the m^{6}A multivalency is crucial in this phenomenon. Therefore, m^{6}A-modified RNAs can act as scaffolds to recruit multiple low complexity domain-containing readers in proximity, facilitating intermolecular interactions that ultimately trigger condensate formation (Figure 4). Under stress conditions, the three readers YTHDF1, YTHDF2, and YTHDF3 were found in SGs with liquid-like properties.[13,196] While m^{6}A is not necessary for SG formation, localization of YTHDF2 in these condensates largely depends on the presence of m^{6}A-modified RNAs,[13] suggesting a role for methylated RNAs as scaffolds also in cells. The fact that the number of methylations is key in promoting reader-mediated phase separation reminds of the length-dependent formation of RNA foci arising from repeated RNAs.[11] The quantity of intermolecular interactions seems to be a critical parameter in determining the ability of RNA to phase separate or to induce condensation. Polymethylated RNAs are enriched in SGs, and they are translationally repressed compared to less modified RNAs.[13] This study revealed how m^{6}A can control the localization and thus the fate of cytoplasmic mRNAs through enhancing and modulating the formation of biomolecular condensates. Under stress conditions, the localization of YTHDF2 shifts from P-bodies to SGs,[13] possibly transferring mRNAs between the two compartments. In response to arsenite stress, YTHDF3 recognizes m^{6}A sites located at the 5′ end of mRNAs and repositions them in SGs[197] (Figure 4). The regulation of SGs by YTHDF does not solely depend on its low complexity region but also on the RNA-binding domain.[196] This observation indicates that the ability to interact with m^{6}A modified RNAs is an essential requirement for YTHDF's functions in condensate formation. A proposed model suggests that, in physiological conditions, G3BP1, key protein in SG assembly, and YTHDF1 form small clusters, which do not colocalize. However, under stress, YTHDF1 clusters increase in number, and they start to coalesce with the G3BP1 ones, yet remaining at the periphery of the newly formed granules.[196] Since YTHDF1 interacts with ribosomal proteins, the localization of YTHDF1 in SGs has potential implications for poststress recovery, specifically in the context of mRNA translation reinitiation.

Although these studies have emphasized the significance of m^{6}A as a crucial factor determining mRNA partitioning in SGs,[13,196,197] recent analysis challenges the notion that m^{6}A facilitates the enrichment of multimodified RNAs in these condensates.[16] Surprisingly, in the absence of METTL3, the accumulation of tested m^{6}A-modified mRNAs does not exhibit significant variation. In an attempt to assess the contribution of m^{6}A to mRNA enrichment into SGs, computational analysis was employed, leading the authors to conclude that m^{6}A can only account for approximately 6% of m^{6}A-mRNA localization in SGs.[16] Notably, the length of mRNAs, rather than m^{6}A modification, remains the primary factor influencing their enrichment in SGs. Although YTHDF proteins were implicated in recruiting mRNAs to SGs,[13] the authors determined that their effect is minimal. However, m^{6}A may facilitate the enrichment of multiple m^{6}A-edited mRNAs that are normally less susceptible to be recruited within SGs.[16] If on the one hand the role of m^{6}A is unclear, on the other hand YTHDF readers with their intrinsically disordered domains actively contribute to granules assembly. The role of m^{6}A readers in phase separation is not restricted to SGs, but other studies shed light on their contribution in nuclear speckles and nuclear bodies, with important consequences in cancer progression.[198,199] The lncRNA *MALAT1*, a key biomarker for cancer metastasis, is found specifically enriched in nuclear speckles where it is involved in the regulation of gene expression. *MALAT1* contains highly m^{6}A-modified RNA motifs encompassing the most conserved regions.[183,200,201] As for m^{6}A-modified RNAs that act as scaffold for the recruitment of readers undergoing phase separation, MALAT1 works as a platform to the nuclear reader YTHDC1[199] (Figure 4). As a result, YTHDC1 forms nuclear foci that highly colocalize with nuclear speckles[199] (Figure 4). APEX2-mediated proximity labeling coupled with quantitative SILAC proteomic analysis, in the presence of wild type *MALAT1* or *MALAT1* lacking a m^{6}A enriched motif, revealed that this modification is crucial in the regulation of nuclear speckles composition.[199] The recognition of YTHDC1 and its interaction with m^{6}A RNA is key for the maintenance of nuclear speckles and their function. The recognition of m^{6}A by YTHDC1 has an important biological implication as it controls the metastatic behavior of cancer cells.[199] Another study demonstrated that YTHDC1, which contains two intrinsically disordered regions, can undergo phase separation both *in vitro* and in cells where it leads to the formation of nuclear condensates, exhibiting liquid-like properties.[198] These condensates, partially colocalizing with nuclear speckles and superenhancer assemblies, protect m^{6}A-modified mRNAs from degradation and are important in controlling myeloid leukemic differentiation.[198] As demonstrated for the YTHDF proteins, both the intrinsically disordered region and the YTH domain, responsible for m^{6}A recognition, are required for proper phase separation,[198] suggesting a crucial role of methylated RNAs in controlling condensate formation.

Proteins involved in m^{6}A regulation can undergo phase separation beyond m^{6}A-readers. For instance, the writer METTL3, despite lacking intrinsically disordered regions, has been found to undergo phase separation within the nuclei.[202] This process relies on multiple factors, including METTL3 self-interaction, interaction with METTL14, and the presence of nascent RNAs, which collectively contribute to the sufficient multivalency required for phase separation. Interestingly, while METTL3 colocalizes with nuclear speckles, it tends to be predominantly distributed at the periphery of the assembly.[202] This suggests a distinct spatial organization within the phase-separated state. Phase separation may serve to regulate the methyltransferase activity, as the protein WTAP specifically interacts with the METTL3−METTL14 complex in the assembly state.[202]

https://doi.org/10.1021/acs.chemrev.3c00575
Chem. Rev. XXXX, XXX, XXX−XXX

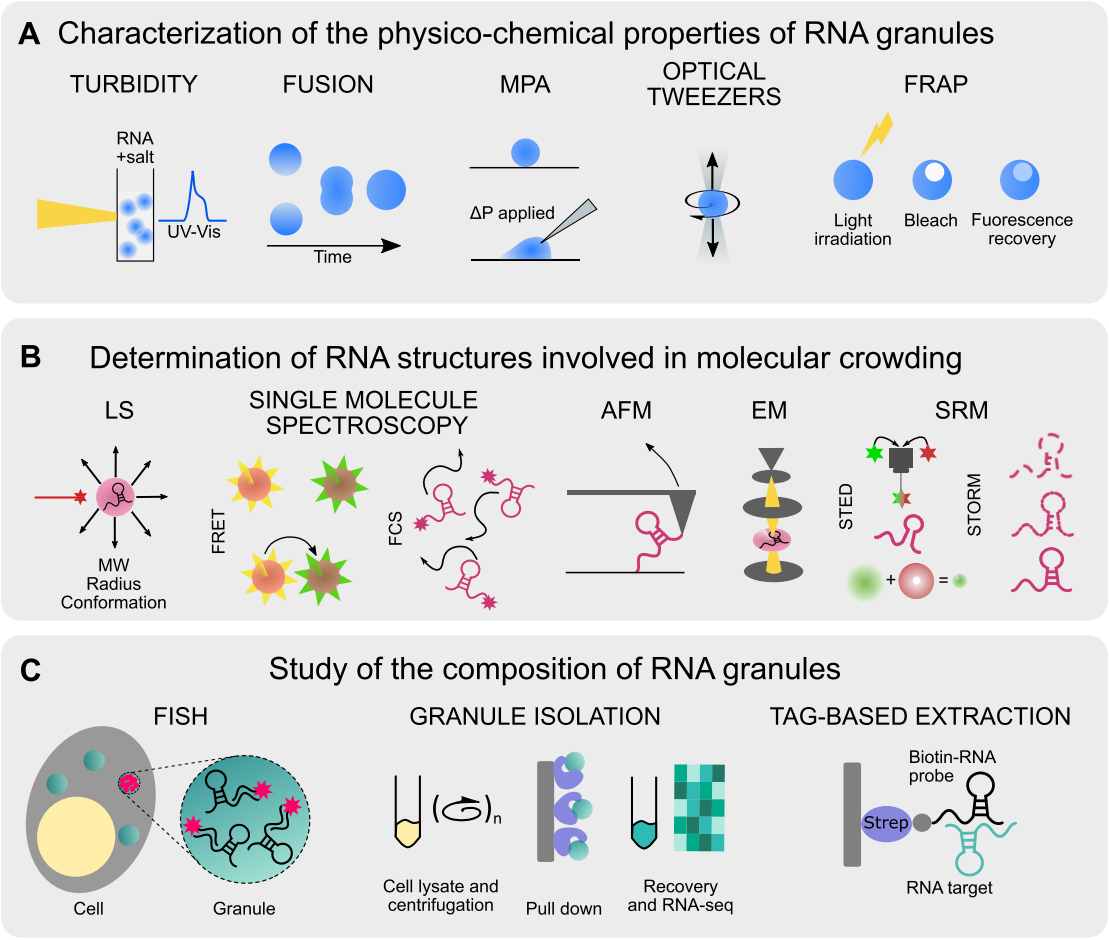

Figure 5. Summary of the experimental approaches to isolate and characterize RNA granules. (A) Methods for the characterization of the physicochemical properties of RNA granules. These techniques include: the analysis of the variation of the solution turbidity upon granule formation (turbidity); the observation of fusion events (fusion); the measurement of the viscoelastic properties of granules with micropipette aspiration (MPA); the determination of condensation occurrence and interfacial tension with optical tweezers; and the estimation of the dynamics of RNA within droplets with fluorescence recovery after photobleaching (FRAP). (B) Methods to determine the RNA structures within RNA granules. These approaches include: the analysis of particle size and shape by different applications of light scattering (LS); the observation of the dynamic nature of RNA granules with single molecule spectroscopy, with techniques such as Förster-resonance energy transfer (FRET) and fluorescence correlation spectroscopy (FCS); the characterization of structural aspects of intermolecular and intramolecular interactions with atomic force microscopy (AFM) and electron microscopy (EM); and the determination of RNA structural fine details with techniques that go beyond the diffraction limit of light, such as stimulated emission depletion microscopy (STED) and stochastic optical reconstruction microscopy (STORM). (C) Methods to study the composition of RNA granules, which include: the determination of their nature and cellular sublocalization with fluorescence *in situ* hybridization (FISH); the identification of the RNA sequences present in certain organelles with granule isolation protocols followed by RNA-seq; and the isolation of specific RNAs involved in condensate formation with tag-based extraction approaches.

5.2. Effect of m^{1}A in SGs

High-resolution mass spectrometry following SG isolation revealed an enrichment of N1-methyladenosine (m^{1}A)-modified RNAs upon heat shock.[14] m^{1}A motifs were found enriched, through bioinformatic analysis, also in mRNAs known to be partitioning in SGs.[14,81] TRMT6/61a, methyltransferase catalyzing the addition of a methyl group in N1 nitrogen, not only interacts with free mRNAs of stressed cells but it also localizes in SGs.[14,203] Unlike m^{6}A, which has been suggested to serve as a scaffold in granule assembly, m^{1}A motifs were not observed to be repeated along SG-enriched RNAs; instead, a single motif is present. In fact, the proposed function of m^{1}A in SGs is not that of a scaffold but rather the recovery of mRNA translation once the stress condition has subsided. A m^{1}A-modified 5′ UTR facilitated rapid translation reinitiation of a reporter gene when compared to the unmodified 5′ UTR.[14] Considering the m^{1}A can have a dramatic effect on RNA structure[204] and that it is found enriched in 5′ UTRs,[205] this modification could play a crucial role in mRNA rescue and translation restoration.

5.3. A-to-I Editing and Condensate Formation

Adenosine-to-inosine (A-to-I) editing is strongly linked to the membrane-less compartments named paraspeckles. mRNAs, containing edited Alu dsRNA in their 3′ UTRs, are recognized by the protein p54^{nrb} (NONO), which forms a nuclear complex that hinders the export of edited mRNA to the cytoplasm.[206,207] NONO is highly enriched in paraspeckles, also containing the proteins PSF and PSP1α and the long noncoding RNA *NEAT1*.[207−210] The retention in the nucleus of edited RNAs depends on paraspeckles, and therefore on *NEAT1*, which is essential for the integrity of this nuclear compartment.[101]

ADAR1 has been demonstrated to target an Alu region within *NEAT1*, which is near the binding region of the RNA-binding protein AUF1, thereby impairing AUF1's ability to interact with

https://doi.org/10.1021/acs.chemrev.3c00575
Chem. Rev. XXXX, XXX, XXX−XXX

NEAT1.[211] Given the crucial role of NEAT1 in preserving paraspeckle architectural integrity, it is likely that modifications impacting its ability to interact with RBP might result ultimately in a change in paraspeckle composition and activity. Predictions of the A-to-I effect on RNA structure revealed that that A-to-I editing could change the ability of *NEAT1* to interact with proteins important in phase separation, possibly altering paraspeckle structure.[212]

In addition to paraspeckle, there appears to be a connection between ADAR1 and A-to-I editing with SGs. The deaminases ADAR1 negatively regulates the formation of SGs, for instance by preventing PKR activation through the modification of endogenous dsRNAs.[15,213] In addition, ADAR1 can also prevent SG formation independently of its function in A-to-I editing. Indeed, by acting as an RBP for dsRNAs, ADAR1 competes with other proteins or RNAs for the interaction with free mRNAs and thus reshapes the composition of RNP complexes, ultimately affecting SGs formation.[15]

6. METHODS TO STUDY RNA CROWDING

The importance of digging deeper into the function and biological role of cellular coacervates is clearer than ever. Although the past decade has seen substantial progress in the identification of numerous RNA granules and in the definition of their features, many questions remain and researchers are investing a tremendous amount of effort into developing the most appropriate tools to answer them. The techniques currently available to the scientific community to investigate biological condensates can be divided into four categories: (1) methods to characterize physicochemical properties of RNA-granules (Figure 5A); (2) methods for determining RNA structures involved in molecular crowding (Figure 5B); (3) methods to study RNA-granule composition (Figure 5C).

RNA-mediated crowding is governed by an array of factors, from molecular interactions and concentration gradients to the prevailing environmental conditions. Experimental techniques, while critical to our understanding, often confront constraints when it comes to capturing molecular-level events or time frames pertinent to phase separation processes. This is where computational methods step in, adeptly bridging these gaps, offering a complementary lens through which to investigate dynamics and interactions that might otherwise elude the laboratory measurements (Figure 5D). Accordingly, while the focus of this Review is not on computational studies of RNA–protein phase separation, we would like to highlight the paramount importance that these strategies have complementing wet-lab data. The strength of computational methods lies in their proficiency at managing complex multicomponent systems. They enable us to glean insights into how varied biomolecules interact, segregate, and self-assemble to give rise to functional condensates. Thus, theoretical frameworks act as a potent supplement to wet lab techniques, giving the possibility to model and dissect the drivers behind RNA-mediated crowding, ultimately fostering a deeper comprehension of the underpinning thermodynamics and kinetics. By facilitating the fusion of wet lab data with simulations, theoretical frameworks and computational methods present a holistic portrayal of biomolecular phase separation.[34] This symbiotic relationship not only helps in validating theoretical models but also steers the interpretation of wet lab results, providing a more nuanced understanding of the convoluted processes involved. Readers interested in computational approaches to study biomolecular condensates can be referred to more in-depth reviews (*Theoretical and Data-Driven Approaches for Biomolecular Condensates*[214] *Computational approaches to predict protein-protein interactions in crowded cellular environments* by G. Grassmann published in this issue).

6.1. Methods to Characterize the Physicochemical Properties of RNA-Granules

The physical properties of RNA granules are highly related to their biological functions. Hence, the rheology features used to describe these coacervates, such as component concentration, diffusivity, viscosity, elasticity and interfacial tension, can reveal their involvement in different physiological pathways and potentially connect them with pathological cascades.

One of the essential features for LLPS and biological condensation is the increased local concentration of one or more scaffold macromolecules, which enables the differential recruitment of multiple clients. Under specific conditions, when an RNA molecule dissolved in solution reaches its saturation concentration (C_{sat}), it undergoes phase separation according to its partition coefficient (K), which is the ratio of its concentration in the dense phase (C_{den}) to the concentration in its dilute phase ($K = C_{den}/C_{sat}$).[215] The concentration of the RNA within the granules is strictly connected to its diffusivity (D), which is usually high in the dilute phase and decreases gradually in the dense phase. However, the many RNAs and proteins present within the same coacervate can display very different D values, to allow them to fulfill distinct biological functions. Therefore, measuring the D coefficient of the various components of a granule can be crucial to uncovering their molecular role. The fluidity of an RNA granule can also be described by its viscosity (η), which defines its resistance to flow and is usually negatively correlated to D.[37] Liquid-like condensates display low η, while gel-like or solid-like granules have high η. Whereas D can define the microscopic behavior of a molecule in a granule, η reflects its macroscopic features.

A phase-separated droplet with distinctive size, density and boundaries is also characterized by its ability to return to its original shape after deformation caused by mechanical loading, defined as elasticity (E). In RNA biology, however, it would be more precise to talk about apparent E, since RNA granules are more akin to liquid-like material than solids. Apparent E intrinsically reflects the stiffness (k) of the granule and it correlates with other physical properties such as shape and size but also its interface conditions. The interfacial boundary of phase-separated coacervate is maintained by the forces in place: molecules in the dense phase can attract equally adjacent molecules in all directions, with a resulting net force of 0. Molecules at the surface are, instead, strongly attracted by similar molecules in the dense phase while establishing weak interactions with different molecules from the dilute phase. This results in the surface molecules experiencing a net force toward the interior of the droplet, which pushes them toward the dense phase to minimize the surface area. The spherical shape of the droplets is a direct consequence of this force balance, since the interfacial tension in LLPS is equivalent to the interfacial energy required to increment the surface area per unit. Since the direction of interfacial tension is tangential to the surface, the spherical shape of the droplets minimizes the surface area.[216] Size and distribution of biological condensates is also dictated by surface tension because this determines fusion propensity and Ostwald ripening: when larger droplets grow by absorbing components from smaller ones.[18] Moreover, interfacial tension is what enables different granules to remain immiscible, each

https://doi.org/10.1021/acs.chemrev.3c00575
Chem. Rev. XXXX, XXX, XXX−XXX

performing its functional role without necessarily fusing with others, as in the case of rRNA production and processing in the nucleus[5] and in the case of the organization of liquid condensate-coated membrane organelles, such as synaptic vesicle reservoirs in presynaptic terminal.[217]

To study the rheology of RNA coacervates *in vitro* and in cell, classic methods are being backed up by recently emerged techniques, the majority of which are based on microscopy approaches. In both cases, *in vitro* approaches often imply the use of synthetic RNA while live imaging relies on tagging the molecule of interest with a fluorescent probe (Figure 5A).

6.1.1. Turbidity Assay and Salt Resistance Assay. When molecules are mixed under certain conditions, the most obvious parameter to observe when some of the parameters are changed is an increment in turbidity, or cloudiness of the solution. Changes in solution turbidity can correlate with the formation of RNA or protein granules and are detectable with a turbidity meter, nephelometer, or spectrophotometer by setting the instruments at a fixed wavelength far from the region of absorbance of the molecule under examination.[218] The turbidity of a solution can be used to determine the saturation limit of a molecule placed in solution to phase separate but imaging is always necessary to confirm the liquid-like properties of coacervates. The investigation should be directed toward the spherical morphology, fusion upon contact and deformation under shear forces. If the interest is in defining the liquid-like, gel-like, or solid-like nature of a condensate, the effect of salt is usually evaluated, since ionic strength can greatly influence η and E of a granule.[219] Due to the weak nature of the established intermolecular interactions, liquid-like droplets are particularly sensitive to the chemical changes in their environment and might dissolve if salt content is increased. The same cannot be said for gel-like or solid-like coacervates, which show a higher resistance to dissolution. Hence, this assay is usually employed to define the material properties of biological condensates and might be combined with turbidity assays to determine the effect of the environmental parameters on LLPS.[37]

6.1.2. Fusion Assay. Thanks to their liquid-like nature and their fluidity, phase-separated granules formed both *in vitro* and in cell can fuse upon encountering each other before shrinking back into a spherical shape. The rate by which fusion occurs and the time needed to recover the spherical shape correlate with the ratio between the shear strain γ (i.e., a measure of the deformation of the material) and η. Observing and recording fusion events over time can give information on many rheology parameters.[220] Two different *in vitro*-prepared coacervates can be labeled with different fluorescent molecules and the diffusion of one droplet inside the other can be observed. Rate of fusion and recovery can be calculated by plotting the fusion relaxation time against the length scale of the two coalescing liquid condensates.[17] Conventionally, fusion events are observed with a live video recording, after depositing the condensates on a glass surface[17] which, however, might create bias by opposing fusion with friction, altering the recovery time. Other technical limitations are represented by the high number of droplets needed to calculate a statistically significant number of events and by the high speed of the fusion between droplets with low η and/or high surface tension. Many of these limitations can be overcome with complementary techniques such as the use of optical tweezers, which will be discussed later.

6.1.3. Micropipette Aspiration Assay. Maintaining a different range of interfacial tension values among different MLOs is one way by which the cell layers multiphase condensates, as occurs in the compartmentalization of nucleoli.[5] High η and low surface tension are mechanical characteristics that render biological coacervates ideal for analysis by micropipette aspiration (MPA).[221] In the past, this technique has been applied to study whole cells or liposomal vesicles, due to the difficulty of applying it to liquid-like condensates. However, recent investigations report that MPA can be achieved also on liquids, as long as they display a $\eta > 2\%$ of their surface tension values.[222] MPA is an approachable and affordable way to measure the viscoelastic properties of granules via the use of a micropipette and of suction/aspiration pressure (ΔP), which is usually applied using a syringe pump or a fluid filled reservoir. The controlled aspiration avoids physical damage and prevents overconstructive manipulations. Usually, MPA is performed with a micromanipulator on a bright field microscope. When ΔP is applied to the surface of the droplet, a deformation of the coacervate is generated and interfacial tension and droplet radius can be measured when the sucked droplets reach a stable state and the deformation stops.

The most frequently used MPA is the single MPA which, as described above, enables the observation of morphological changes and the measurement of viscoelasticity and surface tension.[223] The addition of an opposite micropipette in a dual MPA enables the characterization of interactions between droplets and their associated biophysical parameters.[224]

6.1.4. Optical Tweezers. Optical tweezers belong to the group of single-molecule techniques that in recent years have provided a better understanding of multiple biomolecular processes, enabling the observation and recording of the contribution of individual components to overall events.[225] This methodology has been applied to the reconstruction of RNA structure, function and condensation.[226−228] The basic functional principle is ascribable to the momentum exchange between light and matter that generates optical forces.[229] Optical tweezers are created by a laser beam focused to its diffraction limits, creating a gradient of light intensities that renders it possible to hold particles in three dimensions. Implementing this technique with fluorescence can provide real-time information on condensate rheology and can be used to study individual granules. To study rheology, there are two different configurations: in the first, two μm-sized beads are trapped inside the coacervate, one for causing oscillatory movement and the other to measure the consequent deformation; in the second, the fluctuations caused by the thermal energy of a bead trapped inside a condensate can be measured as a function of time.[230] Fusion events and relative exerted force, a direct indicator of the material properties of the droplet, can also be observed with optical tweezers.[231] In this case, two droplets are trapped by two laser beams: one droplet is kept fixed and the other is moved toward the first. The fusion event is recorded and the force produced is measured and used to extract the relaxation time.[232] Optical tweezers can also be used to measure interfacial tension of coacervates: in this case, both beams are concentrated within the same droplet, where two beads are placed. One beam is fixed on a bead while the other, set on the second bead, moves away, stretching the condensate and oscillating at several predefined frequencies. Viscoelasticity properties and surface tension are then calculated.

6.1.5. Fluorescence Recovery after Photobleaching (FRAP). FRAP enables the estimation of the dynamics of two- or three-dimensional movements of a fluorescently labeled molecule and can be performed both *in vitro* and in cell. A small region of the droplets is irradiated with light until the

https://doi.org/10.1021/acs.chemrev.3c00575
Chem. Rev. XXXX, XXX, XXX−XXX

fluorophore is destroyed and the region is bleached. Since photobleaching is irreversible, the observed signal of fluorescence recovery is attributable to the exchange of bleached fluorophores with the unbleached ones present in the surrounding area.[233] Passive transport processes, such as Brownian motions, create a net transfer of molecules out and into the region of interest until equilibrium. The measure of how rapidly (or how slowly) the initial fluorescent is recovered, in full or partially, is correlated with the fluidity of the droplet.[234] The recovered fluorescence is defined as mobile fraction while the portion of loss fluorescence, if present, is defined as immobile fraction. Liquid-like condensates have a generally faster D and higher recovery rate than gel-like or solid-like granules and therefore show higher recovery fractions.[235] D can be calculated from the recovery curve and η can be derived from it using the Stokes−Einstein equation.[236] The fluidity of different components of a coacervate can differ, so it is recommended to select multiple regions within a droplet to be analyzed. Also, the presence of the fluorescent tag can vary the dynamic parameters of the granule, therefore dilution of the fluorescent molecules with unlabeled ones can mitigate undesired effects. The impact of the fluorescent tag can be also limited by complementing confocal microscopy imaging with bright field or differential interference contrast microscopy to measure fusion, wetting and droplet deformation. A pertinent example of FRAP application to study RNA motion can be found in the early studies by Braga et al.[237]

6.2. Methods for Determining RNA Structures Involved in Molecular Crowding

A number of techniques can be employed to investigate structural features of RNA involved in biological condensates (Figure 5B). Light scattering allows for the examination of molecular interactions and aggregation behavior, offering insights into RNA-promoted crowding. Single molecule spectroscopy provides a detailed view of individual RNA dynamics and conformational changes influencing crowding. Atomic force microscopy (AFM) reveals the physical characteristics and topography of RNA molecules, enabling a thorough understanding of their crowding potential. Electron microscopy (EM) provides high-resolution images, allowing for an intricate exploration of RNA structures contributing to crowding. Finally, super-resolution microscopy (SRM) transcends the diffraction limit of light, presenting a detailed view of molecular structures, and thus, can clarify how RNA contributes to molecular crowding at the nanoscale.

We note that the methods described in this section regard mostly the application of biophysical techniques to identify the structure of the RNA components in the context of the granule. Other classical techniques are available to characterize in more detail the structure of isolated RNA molecules at the atomic level (nuclear magnetic resonance NMR,[238] X-ray crystallography[239]) and at the secondary and tertiary structure levels (circular dichroism,[240] infrared spectroscopy[241]). More modern methods rely instead on enzymatic or chemical probing to routinely and efficiently determine the secondary structure of individual RNAs, distinguishing between single and double-stranded regions[242]. This is the case of techniques such as selective 2′-hydroxyl acylation analyzed by primer extension (SHAPE),[243] and PARIS, based on reversible psoralen cross-linking for RNA duplexes mapping.[244]

6.2.1. Light Scattering. Nondisruptive techniques such as static light scattering (SLS), dynamic light scattering (DLS), or small angle scattering (SAS) can be employed to analyze particle size and shape, including hydrodynamic radius, to determine the oligomeric state of a polymer and to assess the solubility limit of a phase-separated molecule in solution.[245] In the simplest SLS configuration, a laser beam passes through the solution under examination and a detector measures the photons scattered by the particles at different angles around the sample. The result is a mean intensity of the scattering, mainly determined by molecular weight, size, concentration, refractive index and interacting forces of the analyzed particles.[246] Changes in granule dimensions or states can be measured by applying a temperature ramp or salt titration to the sample. DLS, instead, measures the fluctuations in intensity of the scattered light at a fixed angle in a time-resolved manner, providing information on diffusion rates and particle size.[247,248] Considering the type of information extracted, DLS has been more frequently used for studying size and features of coacervates made of either proteins or RNAs.[218,249]

In addition to information on size and molecular weight, the SAS technology, more appropriate for particles of 1−100 nm, can offer important details on conformational transitions and biomolecular interactions.[250,251] Irrespective of the type of SAS, be it small-angle X-ray scattering (SAXS) or small-angle neutron scattering (SANS), electrons or neutrons of a solution are scattered by a laser beam at a low angle and radially averaged to determine a scattering curve, derived from the scattering intensity as a function of the scattering angle.[252] The obtained intensity arises from the differences between the signal of the solvent and the one of the electron/nuclear spin densities of the particles under examination. In SAXS, when a beam meets an electron, an oscillating electric field is applied. This causes an acceleration of the electrons resulting in the emission of secondary electromagnetic waves of identical frequency.[253] In SANS experiments instead, the scattering results from the quantum-mechanical effect of the wave functions derived from the interaction between the incoming neutrons and the nuclei of the sample.

Scattering technologies have found ample application in the biophysics of proteins and their phase separation and phase transition but they are still only applied in a limited manner to RNA biology. However, an increasing number of research works are exploiting scattering techniques for determining RNA folding,[254] thermodynamic and structural features of RNA,[255] RNA−protein interaction mechanisms[256] and effects of RNA on the structure of other biomacromolecules.[257]

6.2.2. Single Molecule Spectroscopy. The dynamic nature of biological condensates and the heterogeneity associated with each component present in the phase-separated droplet render the direct observation of diffusional and conformational variations challenging. The presence of a fluorescent probe to function as a detector of a single type of molecule within the crowded environment enables the tracking and analysis of the RNA of interest at a subnm scale.[258] Fluorescence fluctuation of a chemically modified RNA can be measured with a confocal fluorescence microscope equipped with high-sensitivity photon counting detectors. The demixing process *in vitro*[259] and in live cells[259] can be investigated with single-molecule approaches such as Förster-resonance energy transfer (FRET) and fluorescence correlation spectroscopy (FCS).

Förster energy transfer refers to the phenomenon in which an excited donor fluorophore transfers energy to an acceptor fluorophore via the nonradioactive process of resonance. The

https://doi.org/10.1021/acs.chemrev.3c00575
Chem. Rev. XXXX, XXX, XXX−XXX

transfer is highly dependent on the distance between them and is mediated by dipole−dipole interactions.[260] FRET enables the measurement of the distance between donor and acceptor and has found application in the investigation of inter- and intramolecular interactions and conformational changes of macromolecules. The distance between the two fluorophores is derived from the ratio between donor and acceptor fluorescence emissions upon donor excitation[261] and enables the calculation of the efficiency of the energy transfer. Alternatively, the transfer energy can also be calculated from the difference between the change in fluorescence lifetime of the donor alone, compared to its lifetime in the presence of the acceptor.[262] Single-molecule FRET (smFRET) has recently acquired particular relevance for the study of conformational changes and molecular proximity in RNA biology and in the study of phase separation. In smFRET, a single pair of donor and acceptor is excited[258] and therefore requires bright fluorophores with stable emissions. The main advantage of extending FRET to single molecules is that conformational changes can be observed one molecule at a time, resulting in the determination of the whole conformational ensemble.

FCS is a powerful technique used for quantitative analysis of molecular diffusion. The results are derived by observing fluctuations in the fluorescence intensity of labeled molecules within very small focal volumes, typically in the femtoliter range.[263] FCS has proven valuable in determining diffusion coefficients and fluorophore concentrations for labeled molecules both in controlled *in vitro* conditions and within living cells. Additionally, FCS enables the monitoring of conformational fluctuations, the investigation of the thermodynamics and kinetics of molecular interactions, and the analysis of both intermolecular and intramolecular dynamics.[37] When applying FCS to study MLOs and *in vitro* phase-separated bodies, several technical limitations must be taken into consideration. In particular, these limitations can be ascribed to differences in refractive indexes between the molecules on the surface of the droplet and the ones present in the dense phases, differences that can introduce artifacts in the quantification of the focal volume. In addition, the effects of η, molecular weight heterogeneity, and quinary interactions can render the measurement of diffusion coefficients challenging. Despite these technical limitations, FCS serves as a valuable tool for analyzing molecular diffusion through the measurement of fluorescence intensity fluctuations and has found widespread use in the investigation of various biological systems, including MLOs and phase-separated bodies.[264] It has been used thus far, among other applications, to determine the composition of RNPs,[265] to analyze the diffusion and hybridization rates of different oligonucleotide populations,[266] and to measure mRNA dynamics in living neurons.[267]

6.2.3. Atomic Force Microscopy (AFM). Structural aspects of intermolecular and intramolecular interactions within or between RNA granules under near-physiological conditions,[268] as well as many rheology features,[269] can be investigated using AFM, with a relatively simple experimental setup and sample preparation. At its core, AFM analyses rely on measuring the forces of interaction between a scanning probe and the specimen under investigation. The specimen of interest is positioned on a stage that can be precisely controlled to move up and down using piezoceramics. This controlled movement brings the specimen into contact with the probe or separates them. The scanning probe itself is mounted on a cantilever with a known spring coefficient. By measuring the degree of bending of the cantilever, the interaction forces acting on the probe can be determined.[270] The bending of the cantilever is detected by a laser beam which is reflected by the cantilever and directed onto a photodiode for detection and analysis. Commercial AFM systems are widely accessible and serve as a starting point for many studies. Notably, the emergence of high-speed AFM[271] and the integration of AFM with fluorescence microscopy have revolutionized the single-molecule field.[272] These cutting-edge technologies enable the capture of dynamic processes in exceptional detail and provide deeper insight into the behavior of individual molecules. Numerous recent research studies have leveraged AFM to investigate the formation, structure, and heterogeneity of biological condensates within *in vitro* LLPS systems, by employing high-speed AFM to capture the dynamic surface movements exhibited by biological condensates.[273−275] In the specific case of RNA, AFM was able to unveil condensation leading to complex quaternary structures such as nanorings[276] and to investigate the dynamic behavior of RNA nanoparticles.[277]

6.2.4. Electron Microscopy (EM). EM captures images with a spatial resolution as low as 0.8 Å by exploiting a beam of accelerated electrons illuminating a fixed and contrast-stained sample.[278] The resulting micrographs originate from deflecting electrons through electro-magnetic fields generated by atoms within the specimen. Transmission electron microscopy (TEM) employs fixed specimens stained with heavy metal salts such as uranyl acetate, tungsten, or molybdenum salts. These heavy metals bind preferentially to the surfaces of biological structures, providing the necessary contrast to visualize organelles and their substructural features. TEM is one of the most commonly used techniques to study MLOs and to investigate macromolecular assemblies formed *in vitro*, including RNA hydrogels[279] and protein fibrils.[280] To determine the localization and spatial distribution of specific components using TEM, samples can be immuno-conjugated with colloidal gold particles coated with specific antibodies,[278] as applied in the study of the composition and localization of the CRM1 nucleolar bodies.[281] While conventional TEM achieves high contrast with negative staining, different cellular components may react differently to staining agents, resulting in uneven labeling. To address this limitation, a modified form of TEM called electron spectroscopic imaging exploits the differential energy loss of naturally abundant elements to discern nucleic acids and proteins within subcellular structures.[282] For example, the relatively uniform distribution of proteins and nucleic acids within Ddx4-containing organelles was demonstrated with the use of electron spectroscopic imaging applied to HeLa cells.[55]

Combined use of light microscopy and EM is a common approach to gain comprehensive insights into the structural and dynamic properties of cellular bodies.[283−285] Recent advancements in specimen positioning on mounting grids, instrumental enhancements, and software tools for data correlation across different platforms have facilitated the development of correlated light and EM (CLEM) techniques. CLEM enables researchers to acquire both types of images from a single sample, providing a more complete understanding of cellular structures. The CLEM process involves initially examining a cellular sample using light microscopy and subsequently preparing it for EM imaging. By employing a shared positional reference, it becomes possible to directly correlate the information obtained from light microscopy, which offers broader context, with the high-resolution ultrastructural details obtained from EM.[286] CLEM has been successfully applied to visualize the intricate ultra-

https://doi.org/10.1021/acs.chemrev.3c00575
Chem. Rev. XXXX, XXX, XXX−XXX

structure of nucleolar subcompartments[287,288] and to track the localization of specific proteins within cytoplasmic aggregates.[289]

6.2.5. Super-Resolution Microscopy (SRM). SRM includes a series of microscopy techniques that overcomes the diffraction barrier of light (around 200 nm) by 5−20-times and enables the visualization of structures with enhanced special resolution. It merges optical inputs with mathematical analysis to generate images of the sample under examination by employing advanced computational algorithms and specialized fluorophores. Readers can refer to the 2022 work by Liu et al. for a comprehensive review on SRM applied to cell biology.[290] SRM techniques can be grouped into two categories, according to the main approach they employ: the first group, comprising stimulated emission depletion microscopy (STED), uses patterned illumination to manipulate fluorescence behavior and related variations; the second group, which includes stochastic optical reconstruction microscopy (STORM), achieves super-resolution images by localizing individual emitting molecules.

STED uses distinctly shaped beams to achieve super-resolution imaging.[291] By applying a STED beam, the emission of fluorescent molecules outside the core of the excitation region is suppressed, resulting in a sharpened effective point spread function (PSF).[292] To accomplish this, the depletion beam is shaped like a doughnut, with a certain intensity at the periphery and zero intensity at the center of the excitation spot. By scanning these sharpened PSFs across the sample, high-resolution super-resolved images can be obtained. The advantages of STED direct image acquisition can be applied to *in vivo* imaging[293] and the possibility of 3D-sectioning renders this technique particularly suited for whole cell and tissue imaging.[294] STED can offer valuable insights into the spatial organization and dynamics of RNA molecules. It enables the direct visualization of labeled RNA with improved resolution and detail, allowing for a comprehensive examination of the spatial organization, distribution, and colocalization of condensed RNA structures with other cellular components in both cellular and *in vitro* systems. Moreover, STED microscopy is well-suited for characterizing the morphology and shape of RNA condensates, as well as for investigating their dynamics by capturing the processes of formation, dissolution, and rearrangement of RNA coacervates.

STORM stands out as a super-resolution method, offering the highest spatial resolution for imaging subcellular structures with XY and axial resolutions ranging from 10 to 20 nm and 10 to 75 nm, respectively.[295] The working principle is based on a sequential, sparse activation of photoswitchable fluorophores, in order to precisely determine their individual positions with subnanometer accuracy. Multiple images of the same observation volume with different sets of individual fluorophores activated through repetitive illumination are acquired to generate a super-resolved image.[296] Morphology and core composition of SGs have been resolved using 2D and 3D STORM[297] but STORM can be also used to precisely map the position of individual RNA molecules in cells,[298] to investigate protein−RNA interactions and their spatial organization by combining dual-color labeling,[299] and to study RNA granules and their assembly.[300] Of particular relevance, STORM was fundamental in modeling PRC2−*XIST* interaction and dynamics[301] (see section XIST: A Recently Discovered Case of RNA-Mediated Biological Condensation).

6.3. Methods to Study RNA Granule Composition

Specific techniques can be exploited to determine the composition of RNA granules (Figure 5C). In this section, we focus on the general principles to determine the RNA component of coacervates. The interactions that RNA establishes with other macromolecules and with proteins in particular, influence and determine granules' nature. For the specific study of RNA−protein interactions, we recommend referring to other reviews focusing on these aspects to gain a better knowledge of the interplay between RNA and proteins in biological granules formation and function.[302,303]

Fluorescence *in situ* hybridization (FISH) allows for the specific detection and localization of RNA molecules within their biological context, providing insights into how their spatial distribution might contribute to crowding. Coacervate isolation enables the study of phase-separated structures often implicated in crowding, and how RNA molecules contribute to their formation and stability. Tag-based extraction allows for the selective isolation and subsequent analysis of RNA, which can shed light on the molecular interactions and structural attributes that make them effective promoters of crowding.

6.3.1. Fluorescence *In Situ* Hybridization (FISH). Because it is low throughput and often requires prior knowledge of the system under investigation, FISH is a technique mostly used in earlier studies. However, it remains an informative method to investigate the spatial organization, abundance, and localization of specific RNA in a whole-cell context. FISH's working principle is based on the thermodynamic annealing of two complementary strands of nucleic acids that, under proper conditions, form a duplex called a hybrid.[304] Fluorescently labeled probes are designed to hybridize to their target RNA sequence, which can then be visualized using a fluorescence microscope. Exploiting, at the same time, fluorescent protein markers for different MLOs, it is possible to screen the presence of target RNAs in different cellular compartments and to define the partial composition of the condensates under exam (colocalization studies).

Initially, *in situ* hybridization (ISH) with RNA probes was performed solely to detect complementary DNA sequences and the visualization required autoradiography.[305] The first examples of fluorescent RNA probes (FISH) to visualize DNA were seen around 10 years later,[306] while the tracking of RNA molecules by means of RNA probes was first performed on Actin mRNA in a culture of skeletal muscle.[307] Since then, FISH has been used for multiple applications and has been developed into a single molecule tool (smFISH) with a sensitivity high enough to resolve individual mRNA transcripts.[308] Many versions of FISH exist today, but the core of the technique always relies on the common steps of sample preparation (prehybridization), hybridization and washing. The most delicate and complex phase, which precedes these steps, is probably the design of the RNA probe, which must take into account GC content, secondary structure propensities, length and pairing (specificity).[309] Because of their accessibility and stability, chemically synthesized or PCR-made probes are currently preferred to *in vitro*-transcribed ones. In the most modern application within the field of RNA condensation, FISH has been deployed, among other uses, to detect the phenomenon of RNA microsatellite repeat-driven LLPS to regulate oncogene transcription,[310] to track the chemical modulation of RNA LLPS,[311] and to localize a target RNA within the outer shell of ribonucleoprotein coacervates.[312] Quantitative information can also be extracted by analyzing fluorescence intensity in condensed RNA regions,

https://doi.org/10.1021/acs.chemrev.3c00575
Chem. Rev. XXXX, XXX, XXX−XXX

while combining FISH with time-lapse imaging can enable the observation of dynamic changes in RNA granules over time.

6.3.2. Granule Isolation. For an unbiased, large-scale analysis of the content of RNA coacervates, the ideal approach consists of extracting all macromolecules found within their boundaries. MLOs or other liquid-separated compartments can be purified under certain conditions or from specific tissues/cell types and sent for RNA sequencing to gain insights into the spatiotemporal location and abundance of RNAs and how they change over time. The experimental approaches used to isolate MLOs are similar to the ones employed in the purification of membrane-bound organelles. The nucleolus was one of the first condensates to have ever been isolated and extensively studied in its components via density gradient fractionation.[313] Since then, extraction of the nucleolus has become a routine procedure. When smaller, more dynamic coacervates are under examination, further methodologies must be implemented to unveil their content. One way to do so is via fluorescence activated cell sorting (FACS),[154] by labeling a protein marker specific for a certain MLO with a fluorescent tag and by sorting only the fluorescent cells with a cytofluorometer. After density gradient centrifugation, RNA can then be extracted from the marker-positive granules and sent for sequencing.

Differential centrifugation, based on size and density of the particles under study, is probably the most commonly used way to isolate coacervates. Other methods include: (i) immunoprecipitation, which can be used when a protein bound to the RNA of interest is known and which employs antibodies targeting a protein of interest to pull down the whole organelle, followed by a gentle centrifugation or filtration to separate them from the rest of the cellular components;[314] (ii) microdissection, which involves physically separating the organelles from the surrounding cellular material but which requires micromanipulation tools such as microcapillaries;[315] (iii) biochemical fractionation, which enables the isolation of the MLOs according to their biochemical properties and which requires cellular lysis followed by a chromatographic or centrifugation-based technique to separate the organelle based on their solubility, size or affinity to specific molecules.[316] The selection of one method over another often depends on the properties of the coacervate of interest and on the goals of the study.

6.3.3. Tag-Based Extraction. The concept of using affinity tags to identify the interactome of specific macromolecules goes back to the production and purification of proteins. The idea behind this is simple: a biological or chemical molecule with high affinity toward the tag captures the tagged one, which remains detained after multiple rounds of washing. By applying a buffer with specific pH or a high concentration of a competitor of the tag, the labeled molecule is released.[317] This principle, still commonly used in protein purification protocols, finds a better application in the study of molecular condensates when expanded to its high-throughput variations. While remaining one of the main tools to isolate and identify proteins, the exploration of RNA affinity tags has been limited to few applications, such as antisense probe pulldown. Compounds such as biotin and fluorescent dyes can be incorporated to *in vitro*-synthesized RNA, while the detection of *in vivo*-generated RNAs can be achieved by hybridizing them with synthetic DNA or RNA oligonucleotides that carry tags. However, the isolation of RNA complexes in live cells might be more fruitful if a native, in cell-produced RNA with specific recognition motifs or structures can be used as a bait.[318] When selecting target ligands for RNA affinity tags, several factors must be taken into account, including cost and availability of the affinity resin, practical aspects of how to elute the bond RNA under native conditions, the best protocols to follow to avoid the coelution of nonspecifically bound contaminants, and minimization of background noise.

Single point mutations or expansions in key transcripts are frequently associated with changes in the ability of that RNA to function as a scaffold or a client in the formation of phase-separated droplets, a phenomenon that can be linked to disease.[319,320] The RNA affinity tags offer potential applications for the specific isolation and characterization of RNAs that contain such mutations. In cells where the presence of the wild-type gene is essential for growth, these tags can be exclusively added to the mutant RNA. The use of RNA tags in this context has been applied to protocols for affinity purification using Sephadex or streptavidin-agarose in which the tagged mutant RNAs could be selectively isolated from the corresponding wild-type RNA, enabling the study of the subunit composition and function of these lethal mutants.[321] RNA tags can also be employed for the rapid and specific isolation of specific precursor or product forms of RNA, for isolation of RNA species from crude cellular RNA extract, and for tagging specific positions within macromolecular complexes.[321]

7. NEAT1: AN ARCHETYPICAL CASE OF RNA-MEDIATED BIOLOGICAL CONDENSATION

Paraspeckles were initially identified in 2002 as nuclear bodies that contain a group of RBPs known as the DBHS (Drosophila Behavior and Human Splicing) family, which includes PSPC1, SFPQ, and NONO.[209,322] In 2009, four research groups nearly simultaneously reported that a ncRNA, *NEAT1* (Nuclear Enriched Abundant Transcript 1) or MEN ϵ/β (Multiple Endocrine Neoplasia Transcripts Epsilon and Beta), localizes specifically to paraspeckles.[82,98,323] Importantly, the depletion of *NEAT1* using antisense-oligonucleotides led to the disassembly of paraspeckle components, suggesting that *NEAT1* functions as a structural component of paraspeckles (Figure 6).

NEAT1, now renamed as Nuclear Paraspeckle Assembly Transcript 1, is a gene conserved in mammalian species, including humans and mice. Two distinct isoforms, *NEAT1_1* (3.7 kb) and *NEAT1_2* (22.7 kb), are generated through alternative 3′ end processing of RNA polymerase II transcripts[20,98,323] (Figure 6A). This process involves conventional polyadenylation and cleavage of a tRNA-like structure by RNaseP, respectively.[20,97] Both *NEAT1* isoforms localize to paraspeckles, but only the longer isoform, *NEAT1_2*, is essential for paraspeckle formation whereas the shorter isoform, *NEAT1_1*, is dispensable (Figure 6A,B).[20,323]

De novo paraspeckles form in close proximity to the *NEAT1* gene locus, however the tethering of paraspeckle protein components at a specific genomic locus does not trigger the formation of paraspeckles.[324] This suggests that ongoing transcription of *NEAT1* is required for paraspeckle formation. Indeed, transcriptional inhibition by Actinomycin D or DRB swiftly results in the disappearance of paraspeckles, leading to the relocation of paraspeckle proteins to the perinucleolar cap.[20,209] It is worth noting that conventional RNA purification protocols using acid guanidinium thiocyanate-phenol-chloroform reagents, such as TRIzol (Thermo Fisher Scientific), are inefficient in extracting *NEAT1_2*, a feature termed "semi-extractability".[325] To enhance *NEAT1_2* extraction, extensive needle shearing or heating of the cell lysate in the RNA extraction reagent is required. This suggests that *NEAT1_2*

https://doi.org/10.1021/acs.chemrev.3c00575
Chem. Rev. XXXX, XXX, XXX−XXX

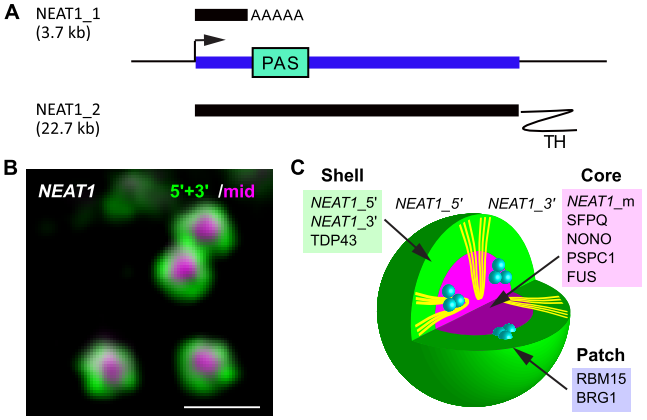

Figure 6. *NEAT1_2, an architectural lncRNA, is an essential component of paraspeckles.* (A) *NEAT1_1* (3.7 kb) and *NEAT1_2* (22.7 kb) represent two distinct isoforms, synthesized through alternative 3′ end processing. *NEAT1_2* features a 3′ triple helix structure (TH). PAS indicates the polyadenylation signal. (B) Structured illumination microscopy revealing the structure of mouse paraspeckles. *NEAT1* FISH probe-stained paraspeckles are shown (green signals show the 5′ and 3′ regions of *NEAT1_2* distribution, while magenta signals show the middle region of *NEAT1_2*). Scale bar equals 500 nm. (C) A schematic illustration depicting the core−shell arrangement of paraspeckle components. Figure in panel B is taken from ref 326 with permission (license 5675280613706 from https://s100.copyright.com/). Copyright 2016 Elsevier.

associates with a substantial amount of proteins and forms a unique molecular milieu distinct from the conventional RNP complex.

7.1. Protein Components of Paraspeckles and Their Fine Structure

Following the initial identification of DBHS family RBPs within paraspeckles, genome-wide subcellular localization studies using EGFP-fusion proteins, as well as proteomic analyses, have identified over 60 paraspeckle proteins (PSPs), the majority of which are RBPs.[20,327] Subsequent RNAi-mediated knockdown analyses have determined the essential PSPs needed for paraspeckle formation, each of which uniquely influences this process. NONO, SFPQ, and RBM14 are necessary for the stable expression of both *NEAT1_1* and *NEAT1_2*, and depletion of these PSPs results in a loss of *NEAT1_1/2* expression and the concomitant disappearance of paraspeckles.[20] FUS, DAZAP1, HNRNPH3, and BRG1 do not significantly affect *NEAT1_2* expression; however, the RNP complex containing *NEAT1_1/2* diffuses into the nucleoplasm upon their loss, suggesting these PSPs are vital for the assembly of *NEAT1* RNP.[20] Notably, BRG1 and BRM1 are components of SWI/SNF (switch/sucrose non-fermentable) chromatin-remodeling complexes, but their ATPase activities are not essential for paraspeckle assembly, indicating they primarily provide a structural platform for the assembly of *NEAT1* RNPs.[328]

Unlike round liquid droplets with variable size formed by phase separation of polymer mixtures, paraspeckles form a spheroidal or cylindrical structure with a defined diameter of around 300 nm.[209,329] Each paraspeckle sphere houses approximately 50 *NEAT1_2* molecules, which are folded in a U shape and radially arranged in a regular manner.[329,330] Both the 5′ and 3′ ends of *NEAT1_2* are located in the paraspeckle's outer shell, with the lncRNA's middle region situated in the interior, creating a distinctive core−shell structure (Figure 6C).[330] PSPs are also localized to specific positions along the radially arranged *NEAT1_2:* SFPQ and NONO are localized in the core region of paraspeckles, RBM14 and BRG1 form small patches throughout paraspeckles, whereas TDP-43 is located in the shell. The shell regions also contain the short isoform *NEAT1_1* and various AG-rich RNAs, although the physiological significance of these RNAs' localization remains to be investigated.

7.2. Functional Domains of NEAT1_2 Revealed by Mutational Studies

The organized arrangement of *NEAT1_2* within paraspeckles suggests the existence of functional domains that associate with specific PSP components. Indeed, systematic analyses of a series of *NEAT1_2* deletion mutants, created by CRISPR/Cas9 genome editing technology in a haploid HAP1 cell line, revealed that *NEAT1_2* contains three functional domains: the 5′ and 3′ domains necessary for *NEAT1_2* stabilization, the domains required for *NEAT1* isoform switching, and the domains needed for paraspeckle assembly, respectively (Figure 7A).[331]

The 3′ stabilization domain forms a triple helix structure, commonly found in stable nuclear RNAs, including *MALAT1* and *PAN* RNA from Kaposi Sarcoma Virus, which protects the transcripts from exonuclease degradation.[97,332] The first 1 kilobase of the 5′ region also contributes to the stabilization of *NEAT1_1/2*, although to a lesser extent compared to the triple helix structure. This region also contains *cis*-acting DNA elements necessary for the proper expression of *NEAT1*, and deletion of this region leads to a reduction in *NEAT1* expression.[331]

The isoform switching domains are located around the polyadenylation signal, which is required for the production of the short, polyadenylated isoform, *NEAT1_1*. As with conventional polyadenylated mRNAs, the 3′ processing of *NEAT1_1* is regulated by the cleavage and polyadenylation specificity factor (CPSF) complex, which recognizes the polyadenylation signals and triggers the cleavage and subsequent polyadenylation by poly-A polymerase. The isoform switching domain associates with HNRNPK, which functionally counteracts with CPSF, resulting in RNA polymerase II readthrough and the production of the architectural isoform, *NEAT1_2*.[20]

Deletion of the middle region of *NEAT1_2* results in the formation of small, dispersed paraspeckles lacking the characteristic core−shell structures, suggesting that this region serves to assemble *NEAT1* RNPs to build paraspeckles.[331] Notably, an artificial *NEAT1_2*, termed mini-*NEAT1*, comprising the 5′ and 3′ stabilization domains and the assembly domain, can induce the formation of paraspeckles with a core−shell structure, implying that these two elements are sufficient to create the ordered structure. The assembly region consists of three redundant subdomains that possess binding sites for NONO and SFPQ, and forced recruitment of NONO using an artificial MS2 stem loop and MS2 coat protein fused to these proteins can replace the function of the assembly domain of mini-*NEAT1*. NONO has been shown to dimerize via a domain called the NOPS domain and forms higher-order polymers via a coiled-coil domain.[333] The tethering of mutant NONO lacking either the NOPS domain or the coiled-coil domain fails to replace the function of the assembly domain of *NEAT1_2*, suggesting that the dimerization of NONO and subsequent polymerization is essential for the assembly of *NEAT1* RNP to form paraspeckles.[331]

https://doi.org/10.1021/acs.chemrev.3c00575
Chem. Rev. XXXX, XXX, XXX−XXX

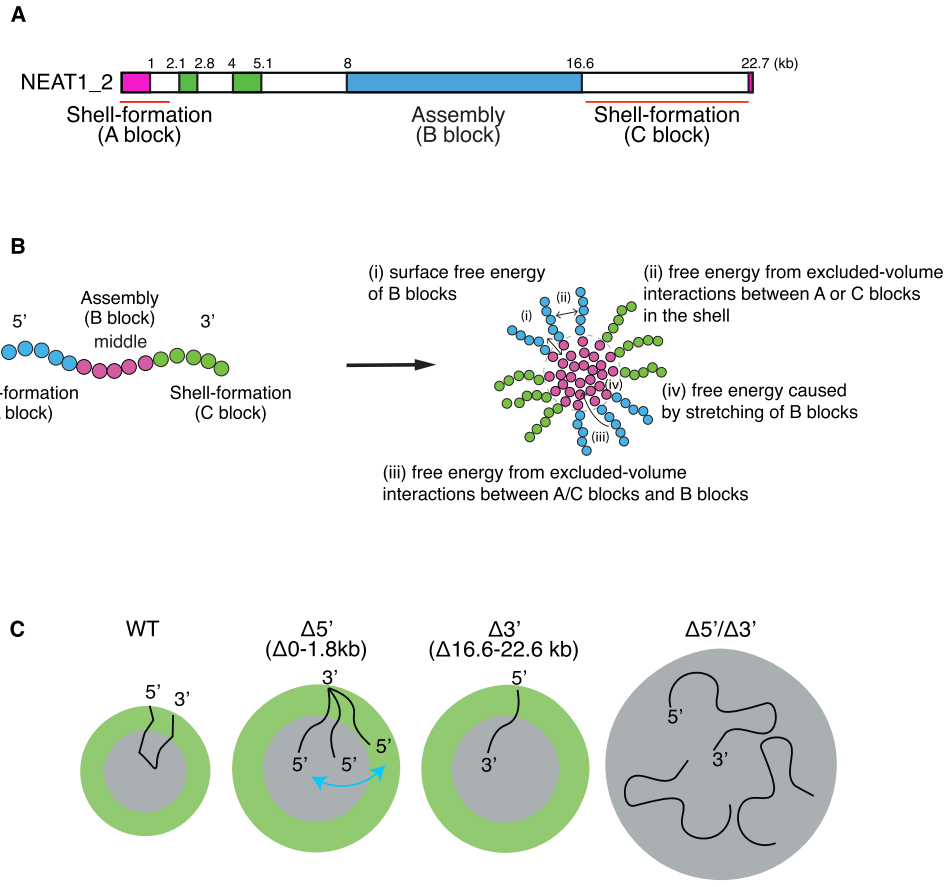

Figure 7. *Functional domain of NEAT1_2 and the block copolymer model of paraspeckles.* (A) Schematics show the functional domain of the human *NEAT1_2*. Pink and green rectangles indicate *NEAT1_2* stabilization domains and *NEAT1* isoform switching domains, respectively. Blue rectangle, which functions as B block, is required for paraspeckle assembly through interaction with PSPs. A and C block domains, which are required for shell formation, are shown as red lines. (B) The amphipathic ABC triblock copolymer model for paraspeckles with the four types of free energy (i–iv) shown. (C) Displays the localization of *NEAT1_2* within paraspeckles and the size of paraspeckles in *NEAT1* mutants lacking either or both of the 5 and 3′domains.

7.3. Role of IDRs of PSPs during the Formations of Paraspeckles

While the components of paraspeckles are arranged into characteristic core–shell structures, they can fuse to form elongated structures with distinct diameter. This flexible nature is commonly observed in MLOs, and the underlying molecular mechanisms used to build these structures differ from those that create more defined submicron-scale molecular machines of similar sizes, such as proteasomes or nuclear pores, in which each component binds to a specific partner through highly specific molecular interactions. The roles of IDRs in the formation of nonmembranous organelles have attracted significant attention since the discovery that IDRs of their components undergo phase transitions to form hydrogels or liquid droplets *in vitro*.[334] Interestingly, all the RBPs required for the stabilization of *NEAT1* or assembly of *NEAT1* RNPs contain distinct IDRs.[335]

The IDRs of PSPs are particularly enriched in polar and noncharged amino acids, specifically glycine (G), glutamine (Q), serine (S), and tyrosine (Y), which are hallmarks of prion-like domains (PrLD) commonly found in proteins that exhibit prion-like properties in yeast cells.[23] Disassembly of paraspeckles in FUS/RBM14-depleted mutant cells can be rescued by full-length FUS/RBM14, but not with mutant molecules lacking the PrLD,[335] suggesting that these PrLDs play essential roles during paraspeckle formation. The PrLDs of FUS and RBM14 undergo phase transition *in vitro*, forming hydrogels that exhibit X-ray diffraction corresponding to ∼4.6 and 10 Å, reminiscent of the X-ray diffraction of amyloid fibrils.[335] The function of PrLD to induce paraspeckle formation is impaired when Y residues are mutated to S, suggesting that π–cation or π–π interactions mediate the multivalent weak interactions essential for the assembly of *NEAT1*. Given that all essential PSPs exhibit RNA-binding properties, association of the PSPs with *NEAT1_2* may increase their local concentration at the transcription site of this transcript, enabling multivalent weak interactions between IDRs to undergo phase transitions and form higher-order assemblies of *NEAT1* RNPs. The recruitment and polymerization of NONO and SFPQ along the assembly domain of *NEAT1_2* may be particularly important in triggering the assembly process by providing a molecular milieu enriched in their IDRs.

Considering that the IDRs of FUS or RBM14 alone can localize to paraspeckles when exogenously expressed, the molecular milieu enriched in IDRs of NONO and SFPQ may further recruit other RBPs with distinct IDRs that exhibit preferential affinity, and undergo phase transition to form flexible paraspeckles. It should be noted that not all RBPs with distinct IDRs are enriched in paraspeckles, implying there is a certain specificity between each IDR. How each IDR exhibits specific affinity to other IDRs is not fully understood and currently represents an active area of research.

https://doi.org/10.1021/acs.chemrev.3c00575
Chem. Rev. XXXX, XXX, XXX–XXX

7.4. The Block Copolymer Model of Paraspeckles

Unlike typical spherical droplets formed by LLPS, paraspeckles can adopt both cylindrical and spherical shapes, each with a highly ordered internal structure.[209,329,330] Moreover, paraspeckles demonstrate a defined minimum diameter, contrasting with the variable sizes of spherical liquid droplets formed by LLPS. Recent research suggests that the formation of paraspeckles is similar to micellization or local phase separation seen in block copolymers, which are composed of two or more chemically distinct polymer blocks.[336] In this context, *NEAT1_2*, a central component of paraspeckles, can be considered as a block copolymer due to its distinct regions associating with unique sets of RNA binding proteins, imparting different properties to each region. In the simplest block copolymer models, AB block copolymers composed of two distinct polymer blocks (e.g., the A block is hydrophilic, and the B block is hydrophobic) self-assemble to form spheres and cylinders with distinct diameters, evoking the formation of both spherical and elongated paraspeckles. This model has been further expanded into an ABC triblock copolymer model,[337] which can elucidate the complex organization of a series of mutant *NEAT1_2* molecules within paraspeckles (Figure 7B).[338]

In the triblock copolymer model, hydrophilic A and C blocks correspond to the 5′ and 3′ terminal regions of *NEAT1_2*, respectively, while the middle region of *NEAT1_2* corresponds to hydrophobic B blocks.[338] This analogy is strengthened by the middle region of *NEAT1_2*, the assembly domain, which associates with NONO to form an oligomer primarily via hydrophobic interactions.[339] Like micellization in block copolymers, the assembly process of paraspeckles aims to minimize the total free energy. This goal is achieved by considering four types of free energy in the triblock copolymer model: (i) surface free energy of B blocks, (ii) free energy from excluded-volume interactions between A or C blocks in the shell, (iii) free energy from excluded-volume interactions between A/C blocks and B blocks, and (iv) free energy caused by stretching of B blocks.

The formation of paraspeckles under standard conditions can be understood as follows.[338] Paraspeckles adopt a spherical shape to minimize the surface area of the core, reducing (i). The number of *NEAT1_2* molecules that can be incorporated into each paraspeckle sphere is limited because (ii) results in repulsive interactions between A/C blocks (i.e., A/C blocks preferentially interact with the solvent in the shell rather than with each other), thereby creating paraspeckle spheres of a constant size. To minimize (iii), hydrophilic A/C blocks are excluded from the hydrophobic core composed of B blocks, resulting in the formation of a characteristic core−shell structure with the 5′ and 3′ terminals of *NEAT1_2* located in the shell and the middle region in the core. (iv) constrains the diameter of the core to a constant length, explaining the formation of elongated, sausage-like paraspeckles with a fixed diameter.

The triblock copolymer model can also rationalize the behavior of mutant *NEAT1_2* and the organization of the molecular condensates they create.[338] First, a reduction in the length of A or C blocks decreases the energetic cost to enter the core region, prompting the redistribution of these components into the core of the micelles. Consistently, deletion of either the 5′ or the 3′ terminal region of *NEAT1_2* leads to the redistribution of either end into the core of the paraspeckle (Figure 7C). Second, the model predicts that the absence of hydrophilic A/C blocks eliminates the repulsive interactions that limit the number of copolymers entering each micelle, leading to the formation of larger condensates. Indeed, a mutant *NEAT1_2* lacking both 5′ and 3′ terminal regions induces the formation of large, round paraspeckles, resembling liquid droplets formed by LLPS (Figure 7C). These droplets can coalesce to form larger droplets with a shape solely regulated by surface tension. Third, the model suggests that the internal organization of *NEAT1_2* within paraspeckles is primarily determined by its transcriptional levels. As the number of *NEAT1_2* molecules within a paraspeckle increases, the 5′ and 3′ terminal regions tend to redistribute toward the core or even display a random distribution within the paraspeckles. This phenomenon may be attributed to the fact that an increase in *NEAT1_2* production significantly affects the repulsive interactions between the A blocks as well as between the C blocks. These interactions tend to have a more pronounced effect than the repulsive interactions between the A/C blocks and B blocks in the core. This hypothesis aligns with observed behavior in experiments where *NEAT1_2* expression, enhanced by the proteasome inhibitor MG132, resulted in the random localization of a mutant *NEAT1_2* lacking a short stretch of the 5′ terminal region within paraspeckles. While these models effectively explain the behavior of paraspeckles, the precise molecular entities that confer hydrophobic and hydrophilic properties to each region remain to be elucidated.

In summary, the block copolymer model accounts for the unique dynamics of the micellization process of paraspeckle assembly, which differs from the condensates formed purely by LLPS. This model provides insights into the morphological changes in paraspeckles due to alterations in the *NEAT1_2* molecule. However, further analysis is necessary to investigate the precise molecular basis that provides the properties of each region of *NEAT1_2*, which represent the “hydrophilic” and “hydrophobic” nature of the block copolymer in the theoretical model.

8. XIST: A RECENTLY DISCOVERED CASE OF RNA-MEDIATED BIOLOGICAL CONDENSATION

The formation of the inactive X chromosome (Xi) by the lncRNA *XIST* through X-Chromosome Inactivation (XCI) has been a predominant model system for understanding how chromatin-associated lncRNAs can induce changes in chromosome structure and gene regulation and establish nuclear compartments.[340,341] XCI occurs in the epiblast cells of implanting female blastocysts and induces the transition from two active X chromosomes (Xa) to one Xa and one Xi. This developmental process is recapitulated in female embryonic stem cells (ESCs) when differentiated in culture.[342] In the following text, we distinguish between *Xist* for experiments conducted in mice and *XIST* when addressing properties conserved in humans. Upon XCI onset, Xist becomes upregulated on one of the two active Xa’s and Xist RNA then transfers across the entirety of the X chromosome from which it is expressed, using the local 3D chromatin architecture to guide its spread.[343,344] Xist spreading initiates a cascade of epigenetic changes, transcriptional silencing, and chromatin rearrangement that results in formation of the Xist-coated Xi.[345] The Xi is heritably maintained for the lifetime of the cell and throughout all subsequent cell divisions.[346,347]

https://doi.org/10.1021/acs.chemrev.3c00575
Chem. Rev. XXXX, XXX, XXX−XXX

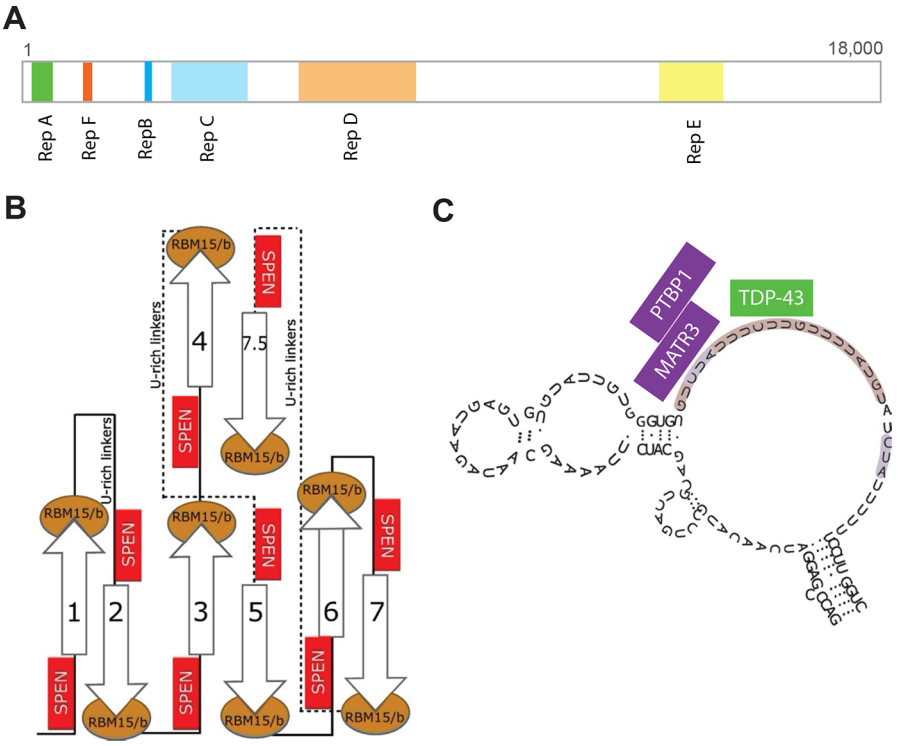

Figure 8. *Xist* tandem repeats and secondary structures of the A- and E-repeats. (A) tandem repeats A-F localization and approximate length is shown. (B) A-repeats, containing 7.5 copies of a repeat unit, are shown as oriented numbered arrows (1−7.5). SPEN and RBM15/15b (displayed as RBM15/b) binding sites are shown in red and orange, respectively. Solid and dashed lines represent RNA nucleotides on different planes. (C) One of the suggested structures of the E-repeat is shown. Binding sites for MATR3, PTBP1, and TDP-43 are shown (in purple and green respectively).

8.1. XIST RNA: A Modular Scaffold for Diverse Protein Interaction

A fundamental question has been how *XIST* (or other gene- and chromatin-regulatory lncRNAs) functionally compartmentalize the nucleus. Xist is a long RNA close to 18 kb in length.[348−350] It harbors 6 repetitive elements termed A−F[122,351] (Figure 8A). Each repeat element is composed of smaller tandem repeats and current data indicate that they confer the various functions of Xist through the recruitment of diverse interacting proteins.[352] Thus, *Xist* RNA acts as a scaffold that integrates many interaction partners through discrete domains and individual RNA−protein interaction modules carry out the distinct functions of the RNA. As shown in mouse, the A-repeat is a region of *Xist* RNA that is essential for *Xist*-mediated gene silencing[353] through binding of the transcriptional repressor SPEN/SHARP[354−356] (Figure 8B). SPEN activates the histone deacetylase HDAC3 and likely other complexes on chromatin through its SPOC domain to force eviction of RNA polymerase II, thereby initiating (and maintaining) gene silencing,[354,357] while contributing to upregulation of *Xist* with other transcription factors and chromatin remodeling complexes.[358] Consequently, the deletion of the A-repeat or of SPEN/SHARP leads to a nearly complete lack of gene silencing.[353,357] Intriguingly, as discussed below in detail, the large IDR of SPEN/SHARP is essential for the integration of many SPEN molecules into the *Xist* assembly and for gene silencing on the Xi.[22,359] The A-repeat of *Xist* also recruits the SPEN/SHARP-like proteins RBM15 and its homologue RBM15b (Figure 8B), which interacts with the METTL3/14 complex that in turn confers the m^{6}A modification on the *Xist* RNA.[360] In contrast to the deletion of SPEN/SHARP, the deletion of RBM15/15b yields a limited defect in gene silencing by *Xist*.[361] Heterochromatinization of the Xi is regulated through the B- and C-proximal repeats, which recruit various repressive epigenetic modifiers, including the Polycomb repressive complexes PRC1 and PRC2 and the structural regulator Smchd1 (structural maintenance of chromosomes flexible hinge domain containing 1) via binding of hnRNP-K.[355,362,363] HnRNPK binds directly to the B-/C-proximal repeats of *Xist*; yet, how this protein can recruit various repressive chromatin regulators is currently unknown. Without these regions of *Xist* RNA or the proteins this repeat sequence recruits, repressive chromatin marks including histone H2AK119ub, H3K27me3, H4K20me1, DNA methylation and many of the 3D chromatin organization changes characteristic of the Xi are not correctly established and a subset of genes on the Xi lacks silencing.[364,365] The RBPs CIZ1, PTBP1, MATRIN3, TDP-43 and CELF1 assemble on the multivalent E-repeat element and are required for faithful XCI establishment, including continued gene silencing and *Xist* localization[123] (Figure 8C).

CIZ1 appears to function separately from the other E-repeat binding proteins and in addition to controlling *Xist* localization regulates *Xist* transcription and stability of the RNA.[123,366−368] Deletion of PTBP1, MATRIN3, TDP-43, and CELF1 (or the E-repeat) does not disrupt the initial *Xist* spreading or XCI-initiation but interferes with the maintenance of silencing and *Xist* sequestration in the X-territory, indicating that these proteins shape the Xi to enable the maintenance of gene silencing, in line with early evidence showing no major defects in the maintenance of XCI in the absence of *Xist*.[369] PTBP1, MATRIN3, TDP-43, and CELF1 are well-characterized RNA-processing factors that form higher-order assemblies, particularly when concentrated by RNAs containing multivalent protein binding sites such as *Xist* RNA.[123,367,370] Moreover,

https://doi.org/10.1021/acs.chemrev.3c00575
Chem. Rev. XXXX, XXX, XXX−XXX

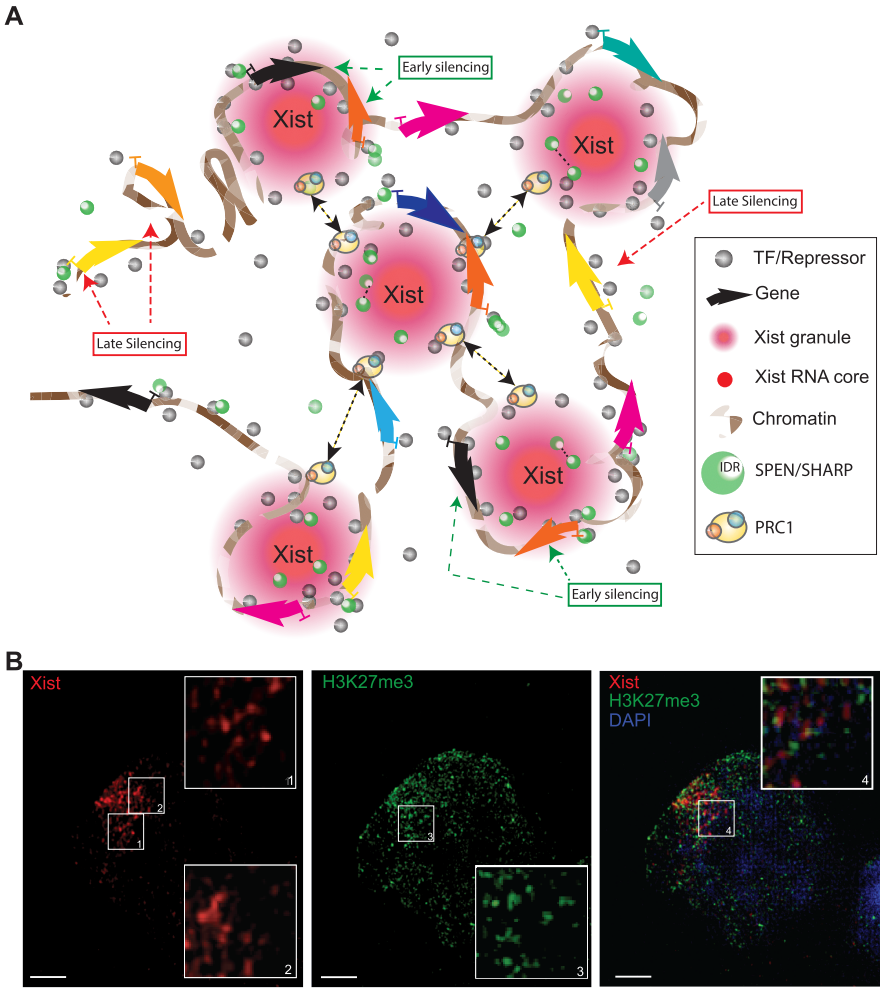

Figure 9. *The functional and structural role of XIST RNA granules-*. (A) In mouse it has been shown that *Xist* condensates in the Xi generate gradients of repressive proteins that silence *Xist*-proximal and distant genes on the whole X chromosome. Two *Xist* RNA molecules (red solid center) form discrete granules (red spheres) localizing in close proximity to open chromatin channels (interchromatin space). These interactions likely happen through direct contacts with matrix proteins. *Xist* granules generate, by means of phase separation, the accumulation of repressive proteins within the condensates and in the intracondensate territory. In particular, SPEN (SHARP) (green circles) accumulates on the Xi via its IDR (smaller dot inside a larger green circle; dashed black line indicates propensity to interact). Local high-concentration availability of repressors is used to silence the genes that are not in close proximity to the *Xist* condensates (concentration gradient and sink effect). This effect is dependent on PRC1-mediated chromatin compaction by PRC1 multimerization (black dashed arrows, indicating contraction; PRC1 complex, yellow, orange, light-blue circles). This model explains how a limited number of *Xist* molecules or granules can silence a large chromosome such as the X chromosome. According to this model, genes (large arrows) in close proximity to *Xist* condensates are silenced early (green boxes), whereas distant genes are silenced late (red boxes). The key indicates all participants in the model. Dark and light shades of brown represent compact and less-compact chromatin regions, respectively. TF, transcription factor. (B) Discrete granules formed by *Xist* RNA molecules in the nucleus. Granules distribution is visualized using double staining where *Xist* is highlighted in red and the histone marker H3K27me3 is shown in green. Cells are also counterstained with DAPI, which appears blue. The preparation of cells for IF and super-resolution imaging was carried out following a previously published method.[383] Imaging was conducted using a confocal microscope LSM 900 equipped with Airyscan 2, and the resulting images were processed using ImageJ, adhering to previously described procedures.[383] The figure includes numbered squares, indicating an area approximately 3× magnified compared to the original image's background. This magnification focuses on regions around the *Xist* RNA-enriched domain within a cell. A scale-bar representing approximately 1 μm is also included. Note that only one z-stack is presented in the image.

these proteins harbor multiple RNA binding domains that allow for the simultaneous engagement of distinct repeat motifs within the E-repeat on or between individual RNA transcripts. When bound to *Xist*, these factors engage in self-aggregation (homotypic) and with other proteins/RNA (heterotypic interactions) that induce the formation of a heteromeric higher-order *Xist*–protein network.[123,367] At a critical concentration threshold, these self-aggregation properties and multivalent RNA–protein and protein–protein interactions induce liquid–liquid demixing *in vitro* for PTBP1 and CELF1,[123] and for PTBP1[371] and TDP-43.[372] Thus, it is likely that by binding and concentrating PTBP1, CELF1, MATRIN3 and TDP-43, *Xist* establishes a protein condensate within the Xi, which in turn contributes to the sequestration of *Xist* within a defined nuclear territory. Together, studies of the function of each repeat highlight that *Xist* exploits extensive RNA–protein and protein–protein interactions to build a repressive chromatin compartment across an entire chromosome and that higher-order protein–protein interactions are critical for the formation of a functional compartment.

https://doi.org/10.1021/acs.chemrev.3c00575
Chem. Rev. XXXX, XXX, XXX–XXX

8.2. Protein Crowding Induced by XIST RNA

Original studies using diffraction-limited microscopes, revealed that *Xist*-interacting proteins concentrate within the Xi-territory, suggesting that *Xist* induces the accumulation of interacting proteins at a high concentration within a territory spatially proximal to its transcription locus,[22,373] to establish an intrachromosomal silencing compartment.[22,374,375] However, SRM experiments determined that *Xist* RNA forms about 50−100 granules within the Xi territory to mediate XCI.[22,301,368,376,377] In this text, the term "*Xist* granule" refers to SRM imaging data, while "*Xist* foci" is used to indicate diffraction-limited studies in which *Xist* condensates partially or completely overlapping with the Xi. Careful measurements of *Xist* granules through live cell super-resolution microscopy and single particle tracking revealed that they are not diffusible, remaining spatially constrained to particular chromosomal locations.[22] The tethering to chromatin and the nuclear matrix[345] with high affinity, likely including proteins such as hnRNP-U (also known as SAF-A),[378] confines *Xist* granules locally and limits movement to the motion of bound chromatin. Moreover, it was shown that each *Xist* granule contains two *Xist* RNA molecules.[22,368] The application of super-resolution microscopy to *Xist*-effector proteins showed that these "static" *Xist* granules concentrate the proteins known to bind the RNA directly and indirectly in their vicinity. Thus, rather than concentrating proteins equally across the entire Xi territory, *Xist*-interacting proteins are most highly concentrated around the *Xist* granules (Figure 9A,B). Markaki et al. quantified the number of SPEN/SHARP molecules around each *Xist* granule and demonstrated that at least 35 SPEN/SHARP molecules are present.[22] The authors suggested that many other *Xist* interacting proteins may be also present in high copy number relative to *Xist* within each *Xist* granule.[22] FRAP combined with mathematical modeling was exploited to define spatiotemporal dynamics of *Xist* and its effector proteins and showed that CIZ1 and *Xist* molecules form a stable core of *Xist*-granules with long residence time.[22,379] All other tested *Xist*-interacting proteins have a much shorter residence time in the Xi-territory, sometimes nearing that of transcription factors.[22,375] Imaging studies indicate that the proteins with short residence times aggregate around the slowly exchanging *Xist*-CIZ1 core.[22,375] In *Xist* granules, this arrangement of proteins induces the formation of supra-molecular protein complexes (SMACs) that are protein accumulations or crowding granules located around the two stably confined *Xist* RNA molecules. *Xist*-associated SMACs are persistent yet highly dynamic structures with high protein content.[22]

Two studies examined further how *Xist*-interacting proteins can accumulate in *Xist* granules superstoichiometrically relative to the two constituent *Xist* molecules, by exploring how the SPEN/SHARP protein accumulates in each *Xist* granule.[22] They found that the accumulation of SPEN molecules in SMACs is driven by the interactions established by its IDRs. Without these, SPEN/SHARP does not accumulate in *Xist*-SMACs.[22,359] Intriguingly, a large number of *Xist*-effector proteins contains IDRs and they are often found in MLOs such as paraspeckles and/or SGs.[23] The lack of SPEN/SHARP's accumulation in *Xist*-SMACs in the absence of its IDR enabled both research teams to assess the functional importance of the SPEN/SHARP protein accumulation in SMACs for gene silencing. In the absence of the IDR, gene silencing does not take place.[22,359] Intriguingly, the Guttman lab showed that the replacement of the SPEN IDR with that of the FUS protein rescues both protein accumulation and gene silencing.[359] Together, these findings indicate that weak IDR-mediated intermolecular interactions are required for the formation of *Xist*-SMACs and for the gene regulatory function of Xist (Figure 9A). In addition, the *Xist* E-repeat instance has demonstrated that this multivalent RNA sequence additionally plays a key role in nucleating weak protein−protein interactions between associated proteins.[123] Thus, high effective concentrations and weak, multivalent interactions between proteins appear to provide the functionality of *Xist*. A detailed mechanistic understanding of how selective inclusion of proteins into *Xist*-SMACs is achieved is largely lacking, yet, direct binding of proteins to the *Xist* RNA may dictate the molecular makeup of proteins within the *Xist*-SMAC compartment and thereby the function of *Xist*.

The accumulation of proteins creates local concentration gradients of these proteins around each *Xist* hub, resulting in an increased presence of transcriptional repressors, RBPs and other *Xist*-interactors within the Xi-compartment[22] (Figure 9A,B). In addition to *Xist* RNA, other RNA molecules, such as transcripts arising from transposable elements, may participate in the formation of the Xi.[380] The rapid binding and dissociation possibly enables *Xist* effector proteins to probe and regulate targets beyond the locations where the two *Xist* molecules of a given *Xist* granule are confined.[22] Thus, *Xist* establishes the Xi compartment by inducing macromolecular crowding of heterochromatinization proteins, rather than through stoichiometric interaction of individual *Xist* protein complexes with target genes and *cis*-regulatory elements. In turn, the limited set of 50−100 *Xist* granules is sufficient to induce the inactivation of the ∼1000 genes on the X-chromosome that are subject to XCI. The comprehensive understanding of how *Xist*-seeded SMACs control gene silencing and maintain the silent Xi would involve the determination of all the involved components and of their stoichiometry within each *Xist*-granule and across the Xi, as well as further biophysical characterization of the interactions. There is little doubt that, as a model system for lncRNA-seeded nuclear compartmentalization, studies of Xist will continue to provide critical insights in this emerging field of RNA-mediated nuclear compartmentalization.

The repeat-driven multivalent nature of *Xist* and the many weak intermolecular (and possibly intramolecular) interactions among *Xist*-binding proteins suggest that *Xist* granules may undergo phase separation.[381] Indeed, PTBP1, one of the interactors of the *Xist* E-repeat, can undergo liquid−liquid demixing *in vitro* when incubated at high concentrations with the RNA.[26,123] The addition of CELF1 to these *in vitro* reactions lowers the concentration of each factor required for condensate formation.[123] Whether phase separation occurs for the Xi, in the context of the *Xist* granule, and whether such phase separation would be functionally important, is currently under investigation. Protein recruitment and exchange with its surroundings by phase separation can sustain the recruitment of silencing proteins at high-concentration, as hypothesized by the Cerase and Tartaglia laboratories[23,382] and experimentally shown by the Plath and the Guttman groups.[22,359]

8.3. XIST RNA Structures Guide Protein Recruitment and Functional Modularity

RNA structures are essential for protein recruitment[7] and might act as seeds for nucleation.[359,384] Functional and structural studies have shown that secondary structures of the *XIST* RNA are fundamental for its biological function.[351,385] However, there is not a single structure (or an ensemble of structures) that is

https://doi.org/10.1021/acs.chemrev.3c00575
Chem. Rev. XXXX, XXX, XXX−XXX

universally accepted in the field. Pioneer experiments by the Jaenisch lab suggested that the A-repeat, a region of *Xist* that is necessary for silencing[353] and interacts with SPEN/SHARP and RBM15/15b, is likely to assume a double stem and loop structure.[353] The authors also showed, using mutagenesis analysis, that the secondary structure of the A-repeat is essential for the silencing ability of *Xist* RNA.[353] Work from the Sattler group subsequently showed that each A-repeat can assume a single stem-loop structure, rather than a double stem loop one,[386,387] that this structure is repeated several times, and that it is essential for its biological function.[353,387] Subsequently, work from the Chang lab suggested that an ensemble of structures, functionally similar to the one suggested by the Sattler group, is more likely to be found *in vivo*, rather than a fixed, single structure,[244] as originally suggested by several groups.[353,388,389] Notably, the structures proposed by the Sattler and the Chang groups are compatible with the recruitment of multiple proteins,[244] working as a multimerization platform for protein recruitment and potentially as a seed for aggregation and SMAC formation[23,382] (Figure 8B). Long-range interactions between *Xist* repeats are also possible in the context of the *Xist* granules.

The *Xist* E-repeat has been reported to be loosely structured, i.e., it displays double stranded RNA segments intertwined with single stranded RNA segments.[351,385] The single stranded RNA segments are important for interactions with MATR3 and PTBP1, two proteins necessary for the supra-stoichiometric recruitment of protein repressors by *Xist*,[123,390] and TDP-43, a protein associated with cellular aggregation[123,391] (Figure 8C). There is relatively little structural information regarding the other repeats of *Xist*; therefore, these will not be discussed here.

8.4. Types of Interactions in the XIST Granule

XIST RNA, like any other RNA, is capable of interacting with other nucleic acids and proteins through a series of weak noncovalent interactions. RNA molecules can interact with themselves (homotypic interaction) or other RNAs (heterotypic interactions) through partial complementary base pairing (Figure 10). Complementary base pairing (i.e., A/U, C/G) allows the formation of 2 and 3 hydrogen bonds, respectively, leading to a pairing of enthalpy energy in the range of 10−20 kcal/mol in water[392] (Figure 10A). It is not known yet whether *XIST* molecules are kept together through complementary RNA:RNA interactions or through protein−RNA:protein−protein interactions (Figure 10A). RNA:RNA interactions can also be mediated by weak noncovalent interactions between the aromatic rings of nucleotides (π stacking, $\pi-\pi$ stacking) (Figure 10B) or between the ribose and the aromatic rings of nucleotides (lone pair$-\pi$).[393,394] The energy of π stacking and lone-pair interactions is usually below 10 kJ/mol in water solutions.[395] Nevertheless, $\pi-\pi$ stacking interactions help the RNA to assume secondary structures, which in turn is important in shaping protein binding interfaces and stabilizing protein−RNA complexes. Together, these interactions can influence the conformational dynamics and functional properties of protein−RNA interactions.[396]

Xist RNA interacts through direct binding with ∼50 proteins, sustaining interactions with hundreds of nuclear proteins.[397] In particular, repetitive regions of *Xist* RNA,[351] support most of the direct RNA−protein interactions,[397,398] even though direct interactions often occur in nonpaired regions of *Xist* RNA. *Xist* RNA can interact with proteins through weak electrostatic forces[399] (Figure 10C−F). These interactions are also essential for the folding of specific RNA segments (i.e., the *Xist* A-repeat,

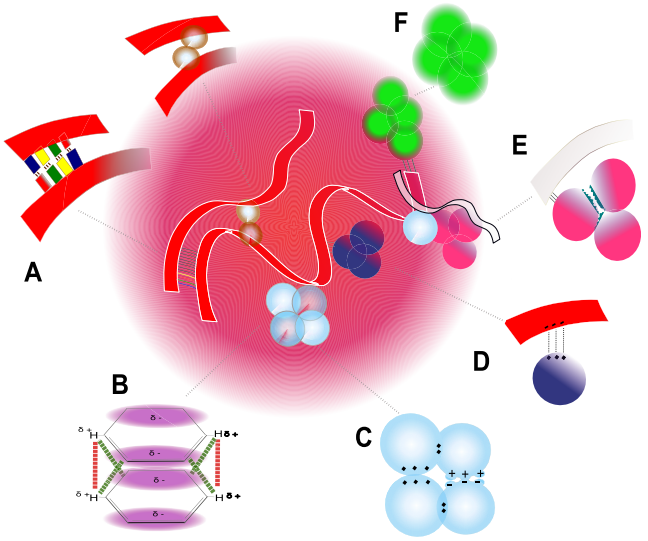

Figure 10. *Selected functional, weak interactions likely to be present in XIST granules.* Red ribbons: *Xist* RNA, 2 molecules of full length *Xist* RNA per *Xist* granule; gray ribbons: unrelated RNA or *Xist* fragments (not detectable by single-molecule RNA-FISH; filled gradient circles: proteins; same-color protein: homotypic interactions; different-color proteins: heterotypic interactions; hexagons: nucleotides; purple ovals: dipole moments; ±: net positive or negative charge; δ: dipole; red and green lines represent repulsive or attractive forces, respectively. (A) left, RNA−RNA base pairing. Partial complementarity is shown (blue−red, green−yellow represent the 4 nucleotides, i.e., AUCG). The *Xist* RNA molecule can potentially self-pair through its repeats. Right, *Xist*−*Xist* interaction through RNA−protein and protein−protein interactions. (B) π-stacking: dipole−dipole interaction between the aromatic ring of two stacked nucleotides or protein aromatic rings; red and green lines represent repulsive or attractive forces, respectively (RNA/RNA is shown, but similar interaction can occur between aromatic groups of proteins). (C) Protein dipole−dipole or ionic interactions are shown. (D) RNA−protein dipole−ion interactions are shown. Proteins kept together by van der Waals interactions are shown in the center (van der Waal radii are larger than covalent or ionic interactions). (E) Protein binding to RNA through the formation of hydrogen bonding. Proteins interacting with the RNA might interact between themselves through IDR-mediated interactions (jagged darker shading on circles). (F) RNA−protein interaction is mediated by hydrophobic bonds (shown by darker shading). Protein−protein interactions are mediated by small force interactions (see text and recommend reviews for more details).

see previous paragraph) into non-random ensembles of 2D and 3D structures.[399] The energy stored in this type of interaction varies largely depending on the chemical nature of the solvent, the type, hydration or chelation of the ions[400] and the interactions of the RNA with its surrounding (solvent, proteins, etc.) and with itself.[399] Other types of RNA−protein, protein−proteins interactions likely occurring in the *Xist* granules are described in other sections of this chapter.

8.5. Are XIST Granules Phase-Separated?

Xist RNA granules exhibit characteristics consistent with phase separation.[22,23,123,359,382,390] For example:

i) They appear as discrete punctate structures within the nucleus, suggesting the formation of distinct liquid-like compartments.[23,382]

ii) They exhibit liquid-like behavior and rapid exchange of their components, although they do not undergo fusion or fission,[22,379,390] possibly because of the tight interactions

https://doi.org/10.1021/acs.chemrev.3c00575
Chem. Rev. XXXX, XXX, XXX−XXX

that *Xist* RNA establishes with the nuclear matrix[378] and the nuclear envelope.[401,402]

iii) *Xist* behavior is consistent with the properties of phase-separated droplets. In particular, the Plath and Guttman laboratories have shown that the IDRs of SPEN/SHARP are necessary for the supra-stoichiometric recruitment of these proteins into the *Xist* granule.[22,359] However, based on the data available at the moment, it is not possible to completely exclude IDR-independent multimerization of *Xist*-interacting proteins[403,404] in the formation of *Xist*-mediated SMACs within the *Xist* granules.

iv) *Xist* RNA granules can be biochemically fractionated from cellular extracts.[405] This possibility to be fractionated suggests that *Xist* RNA granules represent condensed phase-separated entities. However, this type of purification enables the recovery of only the most stable interactions (core), such as the proteins interacting directly with *Xist*, potentially affecting its reported biochemical composition.[297]

v) *Xist* RNA granules recruit various RBPs and chromatin modifiers that contain IDRs and potentially contribute to XCI through phase separation.[397] These proteins and their interactions with *Xist* RNA may contribute to the formation and regulation of the phase-separated granules[23,382] It is possible that alterations in the concentration or valency of RBPs, RNA modifications, or ionic strength might affect the integrity and dynamics of *Xist* RNA granules. Importantly, *Xist* granules, but not the whole Xi chromosome, seems to behave like a phase-separated entity.[406]

It is important to stress the concept that the Xi is a functional nuclear compartment but not a physical nuclear compartment, meaning that RNA, proteins and can freely diffuse to the Xi, which can exchange with its surroundings. Finally, while these lines of evidence collectively suggest that *Xist* RNA granules exhibit properties consistent with phase separation, it is worth noticing that alternative biochemical contributions, such as stoichiometric rearrangements, polymerization and self-aggregation, are possible. Further studies will be necessary to better understand the nature and regulation of *Xist* RNA granules and their role in XCI.

9. CONCLUSIONS AND PERSPECTIVES

Our understanding of cellular biology has been significantly reshaped by the realization of the crucial role played by RNA-mediated crowding, and the subsequent formation and dynamics of ribonucleoprotein assemblies. The discovery and consequent investigation into these phenomena have revealed far-reaching effects, the full extent of which we are still in the process of deciphering.

First and foremost, the emphasis on RNA-mediated crowding and its essential contribution to the formation of membrane-less organelles may lead to a paradigm shift in our understanding of various cellular processes (see section RNA as the Crowding Agent of the Cell).[4] These unique organelles, devoid of a traditional lipid bilayer, are involved in a plethora of critical biological functions, notably gene expression and the finely tuned regulation of RNA metabolism.[40] As we delve deeper into these processes, the formation of biomolecular condensates, especially through LLPS, emerges as a cornerstone of the spatiotemporal organization of cellular constituents. A recent study[407] indicates that molecular connectivity, referring to the number of weak attractive interactions within these condensates, significantly influences their stability. Such profound insights suggest that the composition of highly multicomponent condensates can be anticipated based on the critical parameters (like temperature, pH, and salt concentration) of their constituent biomolecules. Further atomistic exploration[408] emphasizes the importance of configurational entropy, valency, and protein compactness in condensate formation. Such comprehensive knowledge could remarkably widen our lens to perceive the intricate mechanisms governing cellular behavior (see section RNA-Driven Physiological Crowding).[57] This enhanced insight could unlock new possibilities for cell function manipulation, representing a substantial stride forward in the fields of synthetic biology and regenerative medicine. It could potentially allow us to program cells to execute desired functions, a possibility with numerous biomedical and biotechnological applications.[409]

Moreover, the ability of RNA to independently drive phase separation and the formation of RNA granules, particularly via percolation,[34,35] is a testament to its importance in cellular organization and function. If we were able to control or direct this process, we might create specific granules with designed properties, gaining greater control over cellular processes (see section Chemical Forces of RNA-Mediated Crowding in the Cell). The principles of RNA crowding could thus act as a crucial factor in the engineering of cellular systems, paving the way for exciting explorations into RNA function and structure (see section Physico-chemical Determinants of RNA-Mediated Interactions). These developments may also have implications for therapeutic strategies, potentially heralding new classes of RNA-targeted therapies.

Our growing understanding of RNA-mediated crowding could also present new opportunities for disease diagnosis and treatment. Dysregulation of LLPS and consequent aberrations in membraneless organelle formation have been implicated in a variety of diseases, including neurodegenerative disorders such as ALS and FTD, as well as various forms of cancer (see section RNA-Driven Pathological Crowding). By elucidating the molecular mechanics of RNA crowding, we could potentially identify novel biomarkers for early disease detection, or devise therapeutic interventions that target the underlying mechanisms of these disorders. Indeed, the intricate balance of physiological coacervate formation and regulation requires a high degree of precision. When considering this delicate process, one might easily imagine the far-reaching effects that any deviations from this equilibrium could have on the cell.[135,410] For instance, slight alterations could drastically affect the stoichiometry of RNP formation or the ability of a specific RBP to recognize its RNA partners. One might consider that these altered interactions could cause a ripple effect throughout the cell's activities, resulting in cascades of changes that could potentially lead to the onset of pathological conditions. As we have seen, disturbances in RNA metabolism and RNA granule function are already known to be linked with diseases like neurodegeneration and cancer. However, it is possible that our understanding is only scratching the surface, and the impact of these disturbances might be more extensive and complex than currently comprehended.[135,410]

In the nervous system, for example, a disruption in coacervate dynamics could lead to massive alterations in the carefully balanced stoichiometry of RBPs.[126] We might speculate that these changes could have a profound impact on neuronal function, possibly even impacting synaptic communication and

https://doi.org/10.1021/acs.chemrev.3c00575
Chem. Rev. XXXX, XXX, XXX−XXX

regulatory processes. Might these alterations be a common underlying mechanism in various forms of neurodegeneration?

Moreover, could minor changes in the composition or constituent levels of RNA granules induce a stiffer state of coacervates, trapping crucial biomacromolecules inside and leading to a cascade of functional impairments in the cell?[127] Given that many RBPs have a predisposition to undergo LLPS,[411] any variations in their expression levels of structural stability could render them aggregation-prone and trigger a deleterious LSPT.[61] Could this LSPT of RBPs then be a common pathological denominator across diverse neurodegenerative diseases?

When considering cancer, which is driven by uncontrolled cell proliferation due to the activation of oncogenes and the silencing of tumor suppressor genes,[160] the implications become even more intriguing. Oncogenes often promote cell survival and proliferation by driving high gene expression through densely crowded clusters of enhancers.[161] These clusters can lead to the formation of liquid coacervates, creating a crowded environment conducive to active transcription.[162] Could disruptions in these highly crowded cellular microenvironments, triggered by cancerous mutations, then lead to a significant alteration in transcriptional activity, effectively pushing the cell into a cancerous state?[161]

These questions and hypotheses, built on our understanding of RNA-mediated crowding and its central role in cellular function, underscore the importance of ongoing research in this area. The knowledge gained will not only elucidate these molecular dynamics in health and disease but also pave the way for novel therapeutic approaches.

On another level, gaining insights into the chemical modifications of RNA molecules could open an entirely new sphere of therapeutic opportunities (see section Modifications Influencing RNA-Mediated Cellular Crowding). Given that these modifications play a profound role in gene expression regulation, manipulating them could offer a means of altering disease progression. This knowledge could also contribute significantly to our understanding of epigenetics, and the role these modifications play in cellular differentiation and disease development. Specifically, RNA modifications such as m^{6}A can act as recognition sites and facilitate the recruitment of specific mRNAs into condensates, e.g., SGs, although this is still under debate. Several studies have demonstrated that modified RNAs can function as scaffolds, promoting the recruitment and organization of proteins possessing disordered regions. Additionally, condensates themselves can serve as sites for RNA modification, as for instance the 2′-*O*-methylation occurring in Cajal bodies[412] or as in the case of paraspeckles that act as storage for the modified RNA. RNA modification has the potential to control phase separation by affecting the interactions with RBPs and other RNA molecules or by reshaping RNA structure. Thus, as a source of multivalency,[9,13] RNA modifications could regulate the formation and properties of condensate by changing the network of multiple interactions required for phase separation; understanding these molecular mechanisms will shed light on the intricate interplay between RNA regulation and cellular compartmentalization.

Assigning a function to a specific RNA modification in condensate formation poses a significant challenge in the field. It is crucial to study the localization of the modified RNA with respect to the condensate and also delete the specific modified RNA site and assess its impact on RNA localization within the condensate and on their function.[63] Of note, phase separation and thus formation of condensates relies on the multiple and transient interactions between proteins and RNA molecules. It is unlikely that a single type of interaction, such as the one between m^{6}A and YTHDF, solely determines the recruitment of RNAs into SGss. Instead, it is the cumulative effect of multiple interactions that plays a significant role in this phenomenon.[16]

It is yet to be determined whether RNA modifications can contribute to protein-independent RNA phase separation and what is the impact on assembly formed in nonphysiological conditions. It is now well-known that also RNA can undergo phase separation as for the case of RNAs containing G-quadruplex.[413,414] The G-quadruplexes formed by the GGGGCC repetition in the *C9ORF72* gene promotes granule assembly via phase separation.[66] To date, it is still unknown whether RNA modifications can modulate the involvement of G-quadruplex in liquid−liquid phase separation. In this context, tiRNAs are among the RNAs that assume a G-quadruplex structure within cells, and this structural conformation is crucial for SG formation. Indeed, disruption of this structure, e.g., destabilizing ionic conditions leads to a diminished capacity for translation inhibition.[415] tRNAs are highly modified RNAs and so are the derivative tiRNAs.[416] Endogenous modified G-quadruplex tiRNAs are more efficient than their synthetic counterparts in translation inhibition,[417] suggesting that G-quadruplex structures require the proper combination of modified nucleobases to exert their function. In addition, G-quadruplexes can recruit factors involved in the RNA modification, namely writers, readers and erasers, which can in turn change the chemical and physical properties of the modified RNAs.[63,418,419] The recruitment of METTL1 in regions forming G-quadruplex results in the m^{7}G addition within the RNA. This modification hampers the G-quadruplex formation and allows the correct processing of the RNA producing tumor suppressor miRNAs.[420]

The role of RNA modifications in contributing to *XIST* stability and, possibly, phase separation is an active and evolving area of research (see section XIST: A Recently Discovered Case of RNA-Mediated Biological Condensation). Current evidence suggests that RNA modifications can impact the stability, localization, and function of *XIST* RNA, and potentially influence its ability to phase separate and form foci. m^{6}A is a prevalent RNA modification that has been implicated in various cellular processes, both physiological and aberrant.[421,422] *XIST* RNA carries the m^{6}A modification,[360] and the presence of m^{6}A marks on the RNA has been associated with its stability. Specifically, by knocking-out METTL3, the enzyme responsible for m^{6}A methylation, it has been discovered that this modification stimulates XIST RNA degradation, potentially affecting its accumulation and the formation of *XIST* RNA foci. Besides m^{6}A, *XIST* RNA has also been reported to undergo other modifications, including pseudouridylation[423,424] It is possible that *XIST* RNA also carries other types of RNA modifications yet to be discovered. The impact of these modifications on *XIST* RNA is not yet understood, and further investigations are required to determine their specific roles. RNA modifications can serve as binding sites for specific proteins known as “modification readers”.[425] These proteins recognize and interact with modified RNA molecules, influencing their stability, localization, or function. Some RNA-binding proteins known to interact with *XIST* RNA, such as YTHDC1 and YTHDF2, have been implicated in m^{6}A modification recognition and *XIST*-mediated gene silencing.[360] RNA modifications may modulate interactions between *XIST*

https://doi.org/10.1021/acs.chemrev.3c00575
Chem. Rev. XXXX, XXX, XXX−XXX

RNA and other RBPs not directly interacting with *XIST* RNA, influencing *XIST* RNA's ability to recruit factors involved in phase separation. Finally, the Sattler group showed that m^{6}A can modulate the structure and function of *XIST*. In particular, they recently investigated changes downstream to the m^{6}A modification of the A-repeat of *XIST*.[426] In brief, using a combination of NMR, isothermal titration calorimetry (ICT) and crystallographic approaches, Jones et al. showed that the presence of a modified A in the AUGC tetraloop ((m^{6}A)UCG) does not significantly affect the A-repeat structure. However, this modification can be promptly recognized by YTHDC1. The interaction of YTHDC1 with the A-repeat stem and loop partially melts the stem, exposing the C5-G10 residues, which are paired in the absence of YTHDC1 binding. Jones et al. also suggested that this interaction might fine-tune the association with other proteins such as SPEN/SHARP,[426] which is critical for the silencing of X-linked genes by *XIST*.[354]

At present, further research is needed to uncover the effect of other RNA modifications and importantly their interplay in the context of phase separation. Future studies should aim at understanding whether RNA modifications are required for the formation of condensate, or essential for determining the RNAs which are recruited or excluded from these compartments. From a technical perspective, the implications of RNA-mediated crowding also extend to the evolution of innovative experimental techniques. As our comprehension of RNA's structural features and their role in biological condensates broadens, so will the range and sophistication of methodologies used to investigate them (see section Methods to Study RNA Crowding). The demand for greater precision and depth of investigation could catalyze the development of new techniques that enable us to probe the intricacies of RNA biology in unprecedented detail.

At the edges of laboratory experimentation, various algorithms have been developed to estimate biophysical parameters related to RNA-mediated crowding, including rates of protein aggregation, protein−RNA binding, and RNA-condensate binding.[427−429] By harnessing the capabilities of computational methods, it becomes feasible to simulate and predict how molecules behave in a range of cellular scenarios.[430] These predictive models play a pivotal role in unraveling the processes by which proteins and nucleic acids come together to form membraneless organelles and condensates. For instance, the *cat*RAPID algorithm,[428] which utilizes RNA and protein biophysical parameters, can help identify RNAs that act as scaffolds for granule formation and predict which RNAs are abundant in granules formed by RBPs.[7,25] However, it is essential to recognize that current models of biomolecular condensates have limitations due to the scarcity of experimental data and reliance on properties of a specific set of proteins, such as those employed in *cat*GRANULE[427] and PScore.[431] In the future, the integration of molecular dynamics simulations and mean-field models will provide both detailed and simplified insights into how biomolecules behave in crowded cellular environments. For more information on this topic, please refer to the review titled *Computational approaches to predict protein-protein interactions in crowded cellular environments* by G. Grassmann, published in this issue and other works.[432] These approaches will shed light on critical molecular interactions, transitional states, and dynamic behaviors, which might be challenging to directly observe using traditional wet lab techniques.[433]

The combination of theoretical frameworks and computational methodologies paves the way for the strategic design of biomolecular condensates with tailored properties or functionalities.[7] By modifying molecular parameters within simulations, it is possible to predict the impacts of mutations, binding affinities, or other alterations on the behavior of biomolecular condensates.[60]

Finally, it is important to consider that the exploration of RNA-mediated crowding is not limited to understanding natural biological systems. The principles uncovered could also be employed in synthetic systems, such as the development of biomaterials with specific properties controlled by RNA molecules. This could have numerous applications in materials science, nanotechnology, and bioengineering.

In conclusion, the role of RNA-mediated crowding in cellular functions and disease processes is a vast frontier teeming with scientific promise. As our understanding of this fascinating aspect of cellular biology deepens, we can anticipate groundbreaking discoveries that could significantly impact a wide array of fields, from molecular biology to biotechnology and medicine. While we have already begun to chart this terrain, the journey is far from over. The road to comprehensive understanding promises to be a transformative one, ripe with challenges, discoveries, and the potential for remarkable scientific advancement. The realm of RNA-mediated crowding encompasses not only chemical modifications and their implications for human pathology but also countless other areas that are waiting to be unearthed. As we continue to delve into this fascinating field, we may uncover a plethora of novel phenomena and intricate mechanisms at play. For instance, the influence of RNA-mediated crowding on cellular signaling pathways, gene regulation networks, and protein synthesis processes remains largely unexplored. Additionally, the impact of RNA-mediated crowding on cellular stress responses, viral replication, and neurodegenerative disorders presents a vast terrain of research possibilities. Furthermore, understanding the interplay between RNA molecules and cellular structures in the context of RNA granules, such as SGs and P-bodies, holds tremendous potential in unraveling the complexities of cellular organization and function. The exploration of these uncharted territories promises to provide valuable insights into fundamental biological processes, paving the way for innovative therapeutic strategies and deepening our understanding of molecular crowding in the field of RNA biology.

AUTHOR INFORMATION

Corresponding Author

Gian Gaetano Tartaglia − *RNA Systems Biology Lab, Center for Human Technologies, Istituto Italiano di Tecnologia, 16152 Genova, Italy; Catalan Institution for Research and Advanced Studies, ICREA, 08010 Barcelona, Spain;* orcid.org/0000-0001-7524-6310; Email: gian.tartaglia@iit.it

Authors

Elsa Zacco − *RNA Systems Biology Lab, Center for Human Technologies, Istituto Italiano di Tecnologia, 16152 Genova, Italy*

Laura Broglia − *RNA Systems Biology Lab, Center for Human Technologies, Istituto Italiano di Tecnologia, 16152 Genova, Italy*

https://doi.org/10.1021/acs.chemrev.3c00575
Chem. Rev. XXXX, XXX, XXX−XXX

Misuzu Kurihara − *RNA Biology Laboratory, Faculty of Pharmaceutical Sciences, Hokkaido University, Sapporo 060-0812, Japan*

Michele Monti − *RNA Systems Biology Lab, Center for Human Technologies, Istituto Italiano di Tecnologia, 16152 Genova, Italy*

Stefano Gustincich − *Central RNA Lab, Center for Human Technologies, Istituto Italiano di Tecnologia, 16152 Genova, Italy*

Annalisa Pastore − *UK Dementia Research Institute at the Maurice Wohl Institute of King's College London, London SE5 9RT, U.K.;* orcid.org/0000-0002-3047-654X

Kathrin Plath − *Department of Biological Chemistry, David Geffen School of Medicine at the University of California Los Angeles, Los Angeles, California 90095, United States*

Shinichi Nagakawa − *RNA Biology Laboratory, Faculty of Pharmaceutical Sciences, Hokkaido University, Sapporo 060-0812, Japan*

Andrea Cerase − *Blizard Institute, Barts and The London School of Medicine and Dentistry, Queen Mary University of London, London E1 4NS, U.K.; Unit of Cell and developmental Biology, Department of Biology, Università di Pisa, 56123 Pisa, Italy*

Natalia Sanchez de Groot − *Unitat de Bioquímica, Departament de Bioquímica i Biologia Molecular, Universitat Autònoma de Barcelona, 08193 Barcelona, Spain*

Complete contact information is available at: https://pubs.acs.org/10.1021/acs.chemrev.3c00575

Author Contributions

EZ wrote multiple sections of the Review and helped revise and edit the whole chapter. LB cowrote sections about RNA chemical modifications and phase separation and revised the manuscript. MK and SN wrote the NEAT section. MM, SG, and AP inspired and discussed the Review with GGT. KP and AC wrote the XIST section. NSG wrote multiple sections, focusing on RNA as the crowding agent of the cell. GGT conceived the Review, organized the contributions of all authors, and wrote the manuscript. CRediT: **Elsa Zacco** writing-original draft, writing-review & editing; **Laura Broglia** methodology, writing-original draft; **Misuzu Kurihara** methodology, writing-original draft; **Michele Monti** formal analysis; **Stefano Gustincich** funding acquisition, writing-original draft; **Annalisa Pastore** resources, writing-review & editing; **Kathrin Plath** funding acquisition, resources, writing-original draft; **Shinichi Nakagawa** funding acquisition, resources, writing-original draft; **Andrea Cerase** funding acquisition, resources, writing-original draft; **Natalia Sanchez de Groot** funding acquisition, supervision, writing-original draft; **Gian Gaetano Tartaglia** conceptualization, funding acquisition, methodology, project administration, supervision, writing-original draft, writing-review & editing.

Notes

The authors declare no competing financial interest.

Biographies

Elsa Zacco (EZ) graduated in Molecular Biotechnologies from the University of Milano-Bicocca and University of Birmingham (2010). She joined a Doctorate program at the Freie Universität Berlin (DE), working across chemistry, molecular biology, and cell biology to develop delivery systems for vaccine and gene therapy applications, and received her Doctoral degree in Natural Sciences, specialty Medicinal Chemistry (2011−2015). EZ was then awarded a Newton International Fellowship by the Royal Society for a postdoctoral position at the Dementia Research Institute within the King's College London (UK), during which she specialized in the investigation of protein aggregation and the role that RNA may play in it (2016−2018). She received the MINDED Fellowship from the Marie Skłodowska-Curie action and she moved to the Italian Institute of Technology in Genova (IT) to continue developing her expertise in understanding the structural and functional interplay between proteins and RNA in disease (2019−present). EZ is currently an experienced Marie Curie researcher.

Laura Broglia (LB) studied Biotechnology (2010−2013) and Molecular & Industrial Biotechnology (2013−2015) at the Alma Mater Studiorum - University of Bologna. She then joined the International Max Planck Research School for Infectious Diseases and Immunology (Berlin) and obtained her Ph.D. in Microbiology - Molecular Biology under the supervision of Prof. Emmanuelle Charpentier at the Max Planck Unit for the Science of Pathogens (2016−2020). During her Ph.D. studies, LB investigated the role of RNA degradation and processing on the post-transcriptional regulation of gene expression. Supported by an EMBO fellowship, she joined Gian Gaetano Tartaglia's lab at the Italian Institute of Technology, studying the function of regulatory RNA regions in protein assemblies and condensation (2021−2022). LB is currently a Marie Skłodowska-Curie postdoctoral fellow studying the regulation of RNA binding proteins undergoing phase separation.

Misuzu Kurihara (MK) is an assistant professor at the Faculty of Pharmaceutical Sciences at Hokkaido University. She received her Ph.D. degree (2015), studying transcriptional regulation of a tissue specific gene at Hokkaido University. In the period 2015−2020, she conducted postdoctoral research on transcriptional regulation by the PML body at the National Institute for Basic Biology in Japan. Her research is supported by Grants-in-aid for Scientific Research from MEXT and PRESTO, JST.

Michele Monti (MM) initiated his career in Rome as a Theoretical Physicist. He earned his Ph.D. from AMOLF in 2018, specializing in the application of mathematical models to biological phenomena, with a focus on the behavior of biological clocks. As a postdoc at the Centre for Genomic Regulation in 2019, he explored the application of Neural Networks and machine learning algorithms to decipher complex datasets. Since 2020, MM has been at the Italian Institute of Technology, where he conducts research on phase separation and phase transitions using theoretical approaches.

Stefano Gustincich (SG), after his training in Biology, obtained his Ph.D. degree in Molecular Genetics & Biotechnology at SISSA, Trieste. In 1993, he was awarded a long-term EMBO fellowship to join the Department of Neurobiology of Harvard Medical School, Boston (USA) where in 1998 he was appointed Instructor in Neurobiology. In 2003, he was granted the "Career Developmental Award" by "The Giovanni Armenise-Harvard Foundation" to establish the Laboratory of Neurogenomics at SISSA where he later became Full Professor in Applied Biology. In 2011, he was awarded the National Prize for Innovation in Biotechnology. He is currently tenured at the Istituto Italiano di Tecnologia, Genova where he has been the Associate Director for the LIFETECH research domain and the Director of the Department of Neurobiology and Brain Technologies. He is currently the Scientific Director of the Center for Personalized, Predictive and Preventive Medicine at Aosta, Italy. His research interests concern the biology of long noncoding RNAs and transposable elements in the brain. SG is the cofounder of TranSINE Therapeutics, an RNA therapeutics company located at Cambridge, UK.

Annalisa Pastore (AP), starting her career at the University of Oxford, swiftly moved through the ranks at the European Molecular Biology

Laboratory. She contributed significantly to the Protein Data Bank while at the National Institute for Medical Research. Her sabbatical at the French National Institute for Agricultural Research led to several patents. AP worked at King's College London from 2013 to 2018, studying neurodegeneration and protein aggregation diseases. In 2018, she became the first woman appointed full professor at Scuola Normale Superiore di Pisa's Science faculty. In 2022, she was appointed research director for life sciences, chemistry, and soft matter science at the European Synchrotron Radiation Facility.

Kathrin Plath (KP) earned her doctorate degree in cell biology from Humboldt University in Berlin (Germany), performed her postdoctoral studies at UCSF and the Whitehead Institute at MIT, and then joined the faculty at the University of California Los Angeles. KP's lab uses differentiation and reprogramming processes from and to the pluripotent state as powerful in vitro models for studying the molecular mechanisms underlying cell fate changes and cellular specification with a particular emphasis on enhancer selection, genome organization, and the role of long-noncoding RNAs. In the context of lncRNA biology, KP particularly focuses on the exploration of the function of the lncRNA XIST, which mediates X-inactivation and has revealed the molecular crowding induced by *Xist*. She serves on the editorial board of Cell, Science, Cell Stem Cell and other journals, and has served on the Board of Directors of the International Society for Stem Cell Research. KP has been selected as a HHMI Faculty Scholar. She is currently funded by the NIH and CIRM.

Shinichi Nakagawa (SN) studied developmental biology at Kyoto University, Japan, where he earned his Ph.D. in 1998. Following his graduation, he embarked on postdoctoral research at the Department of Anatomy, Cambridge University, UK, with a focus on axon guidance and neural development from 1998 to 2000. He subsequently took on the role of Assistant Professor at the Graduate School of Biostudies, Kyoto University, where he explored retinal histogenesis and stem cell biology. In 2002, SN joined the RIKEN Center for Developmental Biology as a Researcher, furthering his studies in the same area. By 2005, he transitioned to the Nakagawa Initiative Research Unit at RIKEN, where he initiated his intensive research into the functional analyses of long noncoding RNAs. His dedication to this field continued as he served as an Associate Chief Scientist Researcher at RIKEN's RNA Biology Laboratory from 2010 to 2016. Later, he moved to the Faculty of Pharmaceutical Sciences at Hokkaido University, where he now leads as a Professor in the RNA Biology Laboratory. His research has been primarily supported by Grants-in-aid for Scientific Research from MEXT.

Andrea Cerase (AC) achieved his M.Sc. degree in Molecular Biology from the University of Naples Federico II. AC became part of Prof. Maurizio D'Esposito's group at the Institute of Genetics and Biophysics (IGB-National Council of Research, CNR) in Naples, where he pursued his Ph.D. His doctoral research focused on unraveling the epigenetic mechanism responsible for silencing the SPRY3 gene in humans. AC joined the Brockdorff lab at the University of Oxford. Here, his research centered on the epigenetics of X chromosome inactivation, with a keen focus on understanding the intricate relationship between *Xist*and Polycomb Repressive Complexes. In 2013, AC returned to Italy, joining Prof. Phil Avner's group at the EMBL-Rome as an EMBL fellow to investigate the initiation phase of mouse X inactivation, particularly focusing on the role of chromatin remodelers in regulating XIST and Tsix. In 2018, AC established his own laboratory at the Blizard Institute, Queen Mary University of London. In 2022, AC started his lab at the university of Pisa. The lab's primary research revolves around epigenetics, X chromosome inactivation, and long noncoding RNAs (lncRNAs). They are actively engaged in studying X chromosome inactivation and its reversal using both cell and animal models.

Natalia Sanchez de Groot (NSG) is a principal investigator at the Autonomous University of Barcelona. She spent five years working at the Laboratory of Molecular Biology (Cambridge, UK, 2010−2014), where she was awarded the MRC Centenary Early Career Award (2012). She is also a recipient of the Spanish L'OREAL-UNESCO for Women in Science (2021). Throughout her research career, she has utilized model microorganisms to comprehend the molecular basis that governs protein aggregation. Through these approaches, she established connections between protein aggregation and population variability, mathematically defined the effects of protein aggregation on cell well-being, and designed the AGGRESCAN prediction program.

Gian Gaetano Tartaglia (GGT) studied theoretical Physics (University of Rome Sapienza, Italy) and Biochemistry (University of Zurich, Switzerland). After postdoctoral studies in Cambridge, United Kingdom (Chemistry Department), he became PI at the Centre for Genomic Regulation (Barcelona, Spain). In 2013, GGT was awarded an European Research Council grant for studies on the role of coding and noncoding RNAs in regulation of amyloid genes. In 2014, he was tenured in Catalonia as ICREA professor of Life and Medical Sciences and in December 2018 became full professor of Biochemistry in the Department of Biology at University La Sapienza. In 2019, GGT started to work at the Italian Institute of Technology where he currently leads the "RNA Systems Biology Lab". In 2020, he was awarded an ERC grant for the study on the composition of phase-separated assemblies. Since September 2020, GGT is MAE (Member of Academia Europaea).

ACKNOWLEDGMENTS

The authors would like to thank the RNA Flagship at IIT. The research leading to this manuscript has been supported by the European Research Council (RIBOMYLOME_309545 and ASTRA_855923), EIC PATHFINDER (IVBM-4PAP_101098989) and PNRR (CN00000041, EPNRRCN3) to GGT. EZ received funding from the MINDED fellowship of the European Union's Horizon 2020 research and innovation program under the Marie Skłodowska-Curie grant agreement No. 754490. LB was supported by an EMBO postdoctoral fellowship (ALTF 1149-2021) and she is currently receiving funding by Marie Skłodowska-Curie postdoctoral fellowship (UNDERPIN_101063903). KP is supported by an Innovation Award from the BSCRC, the David Geffen School of Medicine and the Jonsson Comprehensive Cancer Center at UCLA, and the NIH (R01HD098387). AC is supported by a Rett Syndrome Research Trust (RSRT) grant, a Orphan Disease Center (ODC) grant, and internal funding from the University of Pisa. NSG is supported by RYC2019-026752-I and PID2020-117454RA-I00 funded by MCIN/AEI/10.13039/501100011033.

ABBREVIATIONS

A	Adenine
AD	Alzheimer's disease
AFM	Atomic force microscopy
APP	Amyloid precursor protein
ALS	Amyotrophic lateral sclerosis
Aβ	Amyloid β
C	Cytosine
CB	Cajal body
CLEM	Correlated light and EM
D	Diffusivity
DLS	Dynamic light scattering

https://doi.org/10.1021/acs.chemrev.3c00575
Chem. Rev. XXXX, XXX, XXX−XXX

DNA	Deoxyribonucleic acid
E	Elasticity
EM	Electron microscopy
FACS	Fluorescence associated cell sorting
FCS	Fluorescence correlation spectroscopy
FISH	Fluorescence *in situ* hybridization
FRAP	Fluorescence recovery after photobleaching
FRET	Föster-resonance energy transfer
FTLD	Frontotemporal lobar degeneration
FTD	Frontotemporal dementia
G	Guanine
HTT	Huntingtin
I	Inosine
IDR	Intrinsically disordered region
LCD	Low complexity domain
LLPS	Liquid−liquid phase separation
lnc	Long noncoding
LSPT	Liquid-to-solid phase transition
m^1A	N1-methyladenosine
m^6A	N6-methyladenosine
MLO	Membrane-less organelle
MPA	Micropipette aspiration
NB	Nuclear body
nc	Noncoding
NEAT1	Nuclear enriched abundant transcript 1
P	Pressure
P-body	Processing body
PrLD	Prion-like domain
PrP	Prion protein
PSK	Point spread function
PSP	Paraspeckle protein
RBP	RNA-binding protein
RNA	Ribonucleic acid
RNP	Ribonucleoprotein
SANS	Small angle neutron scattering
SAS	Small angle scattering
SAXS	Small angle X-ray scattering
SG	Stress granule
SLS	Static light scattering
SMAC	Supra-molecular protein complex
SRM	Super-resolution microscopy
STED	Stimulated emission depletion microscopy
STORM	Stochastic optical reconstruction microscopy
TEM	Transmission electron microscopy
U	Uracil
Xa	Active X chromosome
XCI	X chromosome inactivation
Xi	Inactive X chromosome
XIST	X inactive specific transcript
γ	Shear strain
η	Viscosity

REFERENCES

(1) Wiedner, H. J.; Giudice, J. It's Not Just a Phase: Function and Characteristics of RNA-Binding Proteins in Phase Separation. *Nat. Struct. Mol. Biol.* **2021**, *28* (6), 465−473.

(2) Nakano, S.-I.; Miyoshi, D.; Sugimoto, N. Effects of Molecular Crowding on the Structures, Interactions, and Functions of Nucleic Acids. *Chem. Rev.* **2014**, *114* (5), 2733−2758.

(3) Mitrea, D. M.; Kriwacki, R. W. Phase Separation in Biology; Functional Organization of a Higher Order. *Cell Commun. Signal.* **2016**, *14*, 1.

(4) Donau, C.; Späth, F.; Sosson, M.; Kriebisch, B. A. K.; Schnitter, F.; Tena-Solsona, M.; Kang, H.-S.; Salibi, E.; Sattler, M.; Mutschler, H.; Boekhoven, J. Active Coacervate Droplets as a Model for Membraneless Organelles and Protocells. *Nat. Commun.* **2020**, *11* (1), 5167.

(5) Feric, M.; Vaidya, N.; Harmon, T. S.; Mitrea, D. M.; Zhu, L.; Richardson, T. M.; Kriwacki, R. W.; Pappu, R. V.; Brangwynne, C. P. Coexisting Liquid Phases Underlie Nucleolar Subcompartments. *Cell* **2016**, *165* (7), 1686−1697.

(6) Alberti, S.; Gladfelter, A.; Mittag, T. Considerations and Challenges in Studying Liquid-Liquid Phase Separation and Biomolecular Condensates. *Cell* **2019**, *176* (3), 419−434.

(7) Sanchez de Groot, N.; Armaos, A.; Graña-Montes, R.; Alriquet, M.; Calloni, G.; Vabulas, R. M.; Tartaglia, G. G. RNA Structure Drives Interaction with Proteins. *Nat. Commun.* **2019**, *10* (1), 3246.

(8) Maharana, S.; Wang, J.; Papadopoulos, D. K.; Richter, D.; Pozniakovsky, A.; Poser, I.; Bickle, M.; Rizk, S.; Guillén-Boixet, J.; Franzmann, T. M.; Jahnel, M.; Marrone, L.; Chang, Y.-T.; Sterneckert, J.; Tomancak, P.; Hyman, A. A.; Alberti, S. RNA Buffers the Phase Separation Behavior of Prion-like RNA Binding Proteins. *Science* **2018**, *360* (6391), 918−921.

(9) Langdon, E. M.; Qiu, Y.; Ghanbari Niaki, A.; McLaughlin, G. A.; Weidmann, C. A.; Gerbich, T. M.; Smith, J. A.; Crutchley, J. M.; Termini, C. M.; Weeks, K. M.; Myong, S.; Gladfelter, A. S. mRNA Structure Determines Specificity of a polyQ-Driven Phase Separation. *Science* **2018**, *360* (6391), 922−927.

(10) Van Treeck, B.; Protter, D. S. W.; Matheny, T.; Khong, A.; Link, C. D.; Parker, R. RNA Self-Assembly Contributes to Stress Granule Formation and Defining the Stress Granule Transcriptome. *Proc. Natl. Acad. Sci. U. S. A.* **2018**, *115* (11), 2734−2739.

(11) Jain, A.; Vale, R. D. RNA Phase Transitions in Repeat Expansion Disorders. *Nature* **2017**, *546* (7657), 243−247.

(12) Boeynaems, S.; Holehouse, A. S.; Weinhardt, V.; Kovacs, D.; Van Lindt, J.; Larabell, C.; Van Den Bosch, L.; Das, R.; Tompa, P. S.; Pappu, R. V.; Gitler, A. D. Spontaneous Driving Forces Give Rise to Protein-RNA Condensates with Coexisting Phases and Complex Material Properties. *Proc. Natl. Acad. Sci. U. S. A.* **2019**, *116* (16), 7889−7898.

(13) Ries, R. J.; Zaccara, S.; Klein, P.; Olarerin-George, A.; Namkoong, S.; Pickering, B. F.; Patil, D. P.; Kwak, H.; Lee, J. H.; Jaffrey, S. R. m6A Enhances the Phase Separation Potential of mRNA. *Nature* **2019**, *571* (7765), 424−428.

(14) Alriquet, M.; Calloni, G.; Martínez-Limón, A.; Delli Ponti, R.; Hanspach, G.; Hengesbach, M.; Tartaglia, G. G.; Vabulas, R. M. The Protective Role of m1A during Stress-Induced Granulation. *J. Mol. Cell Biol.* **2021**, *12* (11), 870−880.

(15) Corbet, G. A.; Burke, J. M.; Parker, R. ADAR1 Limits Stress Granule Formation through Both Translation-Dependent and Translation-Independent Mechanisms. *J. Cell Sci.* **2021**, *134* (17), jcs258783 DOI: 10.1242/jcs.258783.

(16) Khong, A.; Matheny, T.; Huynh, T. N.; Babl, V.; Parker, R. Limited Effects of m6A Modification on mRNA Partitioning into Stress Granules. *Nat. Commun.* **2022**, *13* (1), 3735.

(17) Brangwynne, C. P.; Eckmann, C. R.; Courson, D. S.; Rybarska, A.; Hoege, C.; Gharakhani, J.; Jülicher, F.; Hyman, A. A. Germline P Granules Are Liquid Droplets That Localize by Controlled Dissolution/condensation. *Science* **2009**, *324* (5935), 1729−1732.

(18) Brangwynne, C. P. Phase Transitions and Size Scaling of Membrane-Less Organelles. *J. Cell Biol.* **2013**, *203* (6), 875−881.

(19) Ganser, L. R.; Myong, S. Methods to Study Phase-Separated Condensates and the Underlying Molecular Interactions. *Trends Biochem. Sci.* **2020**, *45* (11), 1004−1005.

(20) Naganuma, T.; Nakagawa, S.; Tanigawa, A.; Sasaki, Y. F.; Goshima, N.; Hirose, T. Alternative 3′-End Processing of Long Noncoding RNA Initiates Construction of Nuclear Paraspeckles. *EMBO J.* **2012**, *31* (20), 4020−4034.

(21) Hirose, T.; Virnicchi, G.; Tanigawa, A.; Naganuma, T.; Li, R.; Kimura, H.; Yokoi, T.; Nakagawa, S.; Bénard, M.; Fox, A. H.; Pierron, G. NEAT1 Long Noncoding RNA Regulates Transcription via Protein Sequestration within Subnuclear Bodies. *Mol. Biol. Cell* **2014**, *25* (1), 169−183.

(22) Markaki, Y.; Gan Chong, J.; Wang, Y.; Jacobson, E. C.; Luong, C.; Tan, S. Y. X.; Jachowicz, J. W.; Strehle, M.; Maestrini, D.; Banerjee, A.

https://doi.org/10.1021/acs.chemrev.3c00575
Chem. Rev. XXXX, XXX, XXX−XXX

K.; Mistry, B. A.; Dror, I.; Dossin, F.; Schöneberg, J.; Heard, E.; Guttman, M.; Chou, T.; Plath, K. Xist Nucleates Local Protein Gradients to Propagate Silencing across the X Chromosome. *Cell* **2021**, *184* (25), 6174−6192.e32.
(23) Cerase, A.; Armaos, A.; Neumayer, C.; Avner, P.; Guttman, M.; Tartaglia, G. G. Phase Separation Drives X-Chromosome Inactivation: A Hypothesis. *Nat. Struct. Mol. Biol.* **2019**, *26* (5), 331−334.
(24) Childs-Disney, J. L.; Yang, X.; Gibaut, Q. M. R.; Tong, Y.; Batey, R. T.; Disney, M. D. Targeting RNA Structures with Small Molecules. *Nat. Rev. Drug Discovery* **2022**, *21* (10), 736−762.
(25) Cid-Samper, F.; Gelabert-Baldrich, M.; Lang, B.; Lorenzo-Gotor, N.; Ponti, R. D.; Severijnen, L.-A. W. F. M.; Bolognesi, B.; Gelpi, E.; Hukema, R. K.; Botta-Orfila, T.; Tartaglia, G. G. An Integrative Study of Protein-RNA Condensates Identifies Scaffolding RNAs and Reveals Players in Fragile X-Associated Tremor/Ataxia Syndrome. *Cell Rep.* **2018**, *25* (12), 3422−3434.e7.
(26) Li, P.; Banjade, S.; Cheng, H.-C.; Kim, S.; Chen, B.; Guo, L.; Llaguno, M.; Hollingsworth, J. V.; King, D. S.; Banani, S. F.; Russo, P. S.; Jiang, Q.-X.; Nixon, B. T.; Rosen, M. K. Phase Transitions in the Assembly of Multivalent Signalling Proteins. *Nature* **2012**, *483* (7389), 336−340.
(27) Novotný, I.; Blažíková, M.; Staněk, D.; Herman, P.; Malinsky, J. In Vivo Kinetics of U4/U6·U5 Tri-snRNP Formation in Cajal Bodies. *Mol. Biol. Cell* **2011**, *22* (4), 513−523.
(28) Strulson, C. A.; Molden, R. C.; Keating, C. D.; Bevilacqua, P. C. RNA Catalysis through Compartmentalization. *Nat. Chem.* **2012**, *4* (11), 941−946.
(29) Boeynaems, S.; Alberti, S.; Fawzi, N. L.; Mittag, T.; Polymenidou, M.; Rousseau, F.; Schymkowitz, J.; Shorter, J.; Wolozin, B.; Van Den Bosch, L.; Tompa, P.; Fuxreiter, M. Protein Phase Separation: A New Phase in Cell Biology. *Trends Cell Biol.* **2018**, *28* (6), 420−435.
(30) Milovanovic, D.; Wu, Y.; Bian, X.; De Camilli, P. A Liquid Phase of Synapsin and Lipid Vesicles. *Science* **2018**, *361* (6402), 604−607.
(31) Zeng, M.; Shang, Y.; Araki, Y.; Guo, T.; Huganir, R. L.; Zhang, M. Phase Transition in Postsynaptic Densities Underlies Formation of Synaptic Complexes and Synaptic Plasticity. *Cell* **2016**, *166* (5), 1163−1175.e12.
(32) Saito, Y.; Kimura, W. Roles of Phase Separation for Cellular Redox Maintenance. *Front. Genet.* **2021**, *12*, 691946.
(33) Su, X.; Ditlev, J. A.; Hui, E.; Xing, W.; Banjade, S.; Okrut, J.; King, D. S.; Taunton, J.; Rosen, M. K.; Vale, R. D. Phase Separation of Signaling Molecules Promotes T Cell Receptor Signal Transduction. *Science* **2016**, *352* (6285), 595−599.
(34) Mittag, T.; Pappu, R. V. A Conceptual Framework for Understanding Phase Separation and Addressing Open Questions and Challenges. *Mol. Cell* **2022**, *82* (12), 2201−2214.
(35) Harmon, T. S.; Holehouse, A. S.; Rosen, M. K.; Pappu, R. V. Intrinsically Disordered Linkers Determine the Interplay between Phase Separation and Gelation in Multivalent Proteins. *Elife* **2017**, *6*, e30294 DOI: 10.7554/eLife.30294.
(36) Feng, Z.; Chen, X.; Wu, X.; Zhang, M. Formation of Biological Condensates via Phase Separation: Characteristics, Analytical Methods, and Physiological Implications. *J. Biol. Chem.* **2019**, *294* (40), 14823−14835.
(37) Wang, Z.; Lou, J.; Zhang, H. Essence Determines Phenomenon: Assaying the Material Properties of Biological Condensates. *J. Biol. Chem.* **2022**, *298* (4), 101782.
(38) Dolgin, E. What Lava Lamps and Vinaigrette Can Teach Us about Cell Biology. *Nature* **2018**, *555* (7696), 300−302.
(39) Shin, Y.; Brangwynne, C. P. Liquid Phase Condensation in Cell Physiology and Disease. *Science* **2017**, *357* (6357). DOI: 10.1126/science.aaf4382.
(40) Gomes, E.; Shorter, J. The Molecular Language of Membraneless Organelles. *J. Biol. Chem.* **2019**, *294* (18), 7115−7127.
(41) Bevilacqua, P. C.; Williams, A. M.; Chou, H.-L.; Assmann, S. M. RNA Multimerization as an Organizing Force for Liquid−liquid Phase Separation. *RNA* **2022**, *28* (1), 16−26.
(42) Bou-Nader, C.; Zhang, J. Structural Insights into RNA Dimerization: Motifs, Interfaces and Functions. *Molecules* **2020**, *25* (12), 2881.
(43) Varshney, D.; Spiegel, J.; Zyner, K.; Tannahill, D.; Balasubramanian, S. The Regulation and Functions of DNA and RNA G-Quadruplexes. *Nat. Rev. Mol. Cell Biol.* **2020**, *21* (8), 459−474.
(44) Williams, A. M.; Dickson, T. M.; Lagoa-Miguel, C. A.; Bevilacqua, P. C. Biological Solution Conditions and Flanking Sequence Modulate LLPS of RNA G-Quadruplex Structures. *RNA* **2022**, *28* (9), 1197−1209.
(45) Ulyanov, N. B.; James, T. L. RNA Structural Motifs That Entail Hydrogen Bonds Involving Sugar-Phosphate Backbone Atoms of RNA. *New J. Chem.* **2010**, *34* (5), 910−917.
(46) Skeparnias, I.; Zhang, J. Cooperativity and Interdependency between RNA Structure and RNA-RNA Interactions. *Noncoding RNA* **2021**, *7* (4), 81.
(47) Boo, S. H.; Kim, Y. K. The Emerging Role of RNA Modifications in the Regulation of mRNA Stability. *Exp. Mol. Med.* **2020**, *52* (3), 400−408.
(48) Fay, M. M.; Anderson, P. J. The Role of RNA in Biological Phase Separations. *J. Mol. Biol.* **2018**, *430* (23), 4685−4701.
(49) Schreiber, V.; Dantzer, F.; Ame, J.-C.; de Murcia, G. Poly(ADP-Ribose): Novel Functions for an Old Molecule. *Nat. Rev. Mol. Cell Biol.* **2006**, *7* (7), 517−528.
(50) Cremers, C. M.; Knoefler, D.; Gates, S.; Martin, N.; Dahl, J.-U.; Lempart, J.; Xie, L.; Chapman, M. R.; Galvan, V.; Southworth, D. R.; Jakob, U. Polyphosphate: A Conserved Modifier of Amyloidogenic Processes. *Mol. Cell* **2016**, *63* (5), 768−780.
(51) Dai, X.; Zhang, S.; Zaleta-Rivera, K. RNA: Interactions Drive Functionalities. *Mol. Biol. Rep.* **2020**, *47* (2), 1413−1434.
(52) Schmidt, H. B.; Görlich, D. Nup98 FG Domains from Diverse Species Spontaneously Phase-Separate into Particles with Nuclear Pore-like Permselectivity. *Elife* **2015**, *4*, e04251 DOI: 10.7554/eLife.04251.
(53) Aumiller, W. M., Jr; Keating, C. D. Phosphorylation-Mediated RNA/peptide Complex Coacervation as a Model for Intracellular Liquid Organelles. *Nat. Chem.* **2016**, *8* (2), 129−137.
(54) Parisien, M.; Wang, X.; Perdrizet, G., 2nd; Lamphear, C.; Fierke, C. A.; Maheshwari, K. C.; Wilde, M. J.; Sosnick, T. R.; Pan, T. Discovering RNA-Protein Interactome by Using Chemical Context Profiling of the RNA-Protein Interface. *Cell Rep.* **2013**, *3* (5), 1703−1713.
(55) Nott, T. J.; Petsalaki, E.; Farber, P.; Jervis, D.; Fussner, E.; Plochowietz, A.; Craggs, T. D.; Bazett-Jones, D. P.; Pawson, T.; Forman-Kay, J. D.; Baldwin, A. J. Phase Transition of a Disordered Nuage Protein Generates Environmentally Responsive Membraneless Organelles. *Mol. Cell* **2015**, *57* (5), 936−947.
(56) Guenther, E. L.; Cao, Q.; Trinh, H.; Lu, J.; Sawaya, M. R.; Cascio, D.; Boyer, D. R.; Rodriguez, J. A.; Hughes, M. P.; Eisenberg, D. S. Atomic Structures of TDP-43 LCD Segments and Insights into Reversible or Pathogenic Aggregation. *Nat. Struct. Mol. Biol.* **2018**, *25* (6), 463−471.
(57) Dignon, G. L.; Best, R. B.; Mittal, J. Biomolecular Phase Separation: From Molecular Driving Forces to Macroscopic Properties. *Annu. Rev. Phys. Chem.* **2020**, *71*, 53−75.
(58) Garcia-Jove Navarro, M.; Kashida, S.; Chouaib, R.; Souquere, S.; Pierron, G.; Weil, D.; Gueroui, Z. RNA Is a Critical Element for the Sizing and the Composition of Phase-Separated RNA-Protein Condensates. *Nat. Commun.* **2019**, *10* (1), 3230.
(59) Sanders, D. W.; Kedersha, N.; Lee, D. S. W.; Strom, A. R.; Drake, V.; Riback, J. A.; Bracha, D.; Eeftens, J. M.; Iwanicki, A.; Wang, A.; Wei, M.-T.; Whitney, G.; Lyons, S. M.; Anderson, P.; Jacobs, W. M.; Ivanov, P.; Brangwynne, C. P. Competing Protein-RNA Interaction Networks Control Multiphase Intracellular Organization. *Cell* **2020**, *181* (2), 306−324.e28.
(60) Gotor, N. L.; Armaos, A.; Calloni, G.; Torrent Burgas, M.; Vabulas, R. M.; De Groot, N. S.; Tartaglia, G. G. RNA-Binding and Prion Domains: The Yin and Yang of Phase Separation. *Nucleic Acids Res.* **2020**, *48* (17), 9491−9504.

https://doi.org/10.1021/acs.chemrev.3c00575
Chem. Rev. XXXX, XXX, XXX−XXX

(61) Armaos, A.; Zacco, E.; Sanchez de Groot, N.; Tartaglia, G. G. RNA-Protein Interactions: Central Players in Coordination of Regulatory Networks. *Bioessays* **2021**, *43* (2), No. e2000118.
(62) Vandelli, A.; Cid Samper, F.; Torrent Burgas, M.; Sanchez de Groot, N.; Tartaglia, G. G. The Interplay Between Disordered Regions in RNAs and Proteins Modulates Interactions Within Stress Granules and Processing Bodies. *J. Mol. Biol.* **2022**, *434* (1), 167159.
(63) Roden, C.; Gladfelter, A. S. RNA Contributions to the Form and Function of Biomolecular Condensates. *Nat. Rev. Mol. Cell Biol.* **2021**, *22* (3), 183−195.
(64) Sanchez-Burgos, I.; Herriott, L.; Collepardo-Guevara, R.; Espinosa, J. R. Surfactants or Scaffolds? RNAs of Varying Lengths Control the Thermodynamic Stability of Condensates Differently. *Biophys. J.* **2023**, *122*, 2973.
(65) Ma, Y.; Li, H.; Gong, Z.; Yang, S.; Wang, P.; Tang, C. Nucleobase Clustering Contributes to the Formation and Hollowing of Repeat-Expansion RNA Condensate. *J. Am. Chem. Soc.* **2022**, *144* (11), 4716−4720.
(66) Fay, M. M.; Anderson, P. J.; Ivanov, P. ALS/FTD-Associated C9ORF72 Repeat RNA Promotes Phase Transitions In Vitro and in Cells. *Cell Rep.* **2017**, *21* (12), 3573−3584.
(67) Guillén-Boixet, J.; Kopach, A.; Holehouse, A. S.; Wittmann, S.; Jahnel, M.; Schlüßler, R.; Kim, K.; Trussina, I. R. E. A.; Wang, J.; Mateju, D.; Poser, I.; Maharana, S.; Ruer-Gruß, M.; Richter, D.; Zhang, X.; Chang, Y.-T.; Guck, J.; Honigmann, A.; Mahamid, J.; Hyman, A. A.; Pappu, R. V.; Alberti, S.; Franzmann, T. M. RNA-Induced Conformational Switching and Clustering of G3BP Drive Stress Granule Assembly by Condensation. *Cell* **2020**, *181* (2), 346−361.e17.
(68) Razin, S. V.; Gavrilov, A. A. Non-Coding RNAs in Chromatin Folding and Nuclear Organization. *Cell. Mol. Life Sci.* **2021**, *78* (14), 5489−5504.
(69) Quiroz, F. G.; Chilkoti, A. Sequence Heuristics to Encode Phase Behaviour in Intrinsically Disordered Protein Polymers. *Nat. Mater.* **2015**, *14* (11), 1164−1171.
(70) Romero, P.; Obradovic, Z.; Li, X.; Garner, E. C.; Brown, C. J.; Dunker, A. K. Sequence Complexity of Disordered Protein. *Proteins* **2001**, *42* (1), 38−48.
(71) Ukmar-Godec, T.; Hutten, S.; Grieshop, M. P.; Rezaei-Ghaleh, N.; Cima-Omori, M.-S.; Biernat, J.; Mandelkow, E.; Söding, J.; Dormann, D.; Zweckstetter, M. Lysine/RNA-Interactions Drive and Regulate Biomolecular Condensation. *Nat. Commun.* **2019**, *10* (1), 2909.
(72) Ribeiro, D. M.; Zanzoni, A.; Cipriano, A.; Delli Ponti, R.; Spinelli, L.; Ballarino, M.; Bozzoni, I.; Tartaglia, G. G.; Brun, C. Protein Complex Scaffolding Predicted as a Prevalent Function of Long Non-Coding RNAs. *Nucleic Acids Res.* **2018**, *46* (2), 917−928.
(73) Hlevnjak, M.; Polyansky, A. A.; Zagrovic, B. Sequence Signatures of Direct Complementarity between mRNAs and Cognate Proteins on Multiple Levels. *Nucleic Acids Res.* **2012**, *40* (18), 8874−8882.
(74) Zagrovic, B.; Bartonek, L.; Polyansky, A. A. RNA-Protein Interactions in an Unstructured Context. *FEBS Lett.* **2018**, *592* (17), 2901−2916.
(75) Polyansky, A. A.; Zagrovic, B. Evidence of Direct Complementary Interactions between Messenger RNAs and Their Cognate Proteins. *Nucleic Acids Res.* **2013**, *41* (18), 8434−8443.
(76) Kuechler, E. R.; Huang, A.; Bui, J. M.; Mayor, T.; Gsponer, J. Comparison of Biomolecular Condensate Localization and Protein Phase Separation Predictors. *Biomolecules* **2023**, *13* (3), 527.
(77) Boccaletto, P.; Stefaniak, F.; Ray, A.; Cappannini, A.; Mukherjee, S.; Purta, E.; Kurkowska, M.; Shirvanizadeh, N.; Destefanis, E.; Groza, P.; Avşar, G.; Romitelli, A.; Pir, P.; Dassi, E.; Conticello, S. G.; Aguilo, F.; Bujnicki, J. M. MODOMICS: A Database of RNA Modification Pathways. *2021 Update. Nucleic Acids Res.* **2022**, *50* (D1), D231−D235.
(78) Choi, J.-M.; Holehouse, A. S.; Pappu, R. V. Physical Principles Underlying the Complex Biology of Intracellular Phase Transitions. *Annu. Rev. Biophys.* **2020**, *49*, 107−133.
(79) Boeynaems, S.; Bogaert, E.; Kovacs, D.; Konijnenberg, A.; Timmerman, E.; Volkov, A.; Guharoy, M.; De Decker, M.; Jaspers, T.; Ryan, V. H.; Janke, A. M.; Baatsen, P.; Vercruysse, T.; Kolaitis, R.-M.; Daelemans, D.; Taylor, J. P.; Kedersha, N.; Anderson, P.; Impens, F.; Sobott, F.; Schymkowitz, J.; Rousseau, F.; Fawzi, N. L.; Robberecht, W.; Van Damme, P.; Tompa, P.; Van Den Bosch, L. Phase Separation of C9orf72 Dipeptide Repeats Perturbs Stress Granule Dynamics. *Mol. Cell* **2017**, *65* (6), 1044−1055.e5.
(80) Gallivan, J. P.; Dougherty, D. A. Cation-Pi Interactions in Structural Biology. *Proc. Natl. Acad. Sci. U. S. A.* **1999**, *96* (17), 9459−9464.
(81) Khong, A.; Matheny, T.; Jain, S.; Mitchell, S. F.; Wheeler, J. R.; Parker, R. The Stress Granule Transcriptome Reveals Principles of mRNA Accumulation in Stress Granules. *Mol. Cell* **2017**, *68* (4), 808−820.e5.
(82) Clemson, C. M.; Hutchinson, J. N.; Sara, S. A.; Ensminger, A. W.; Fox, A. H.; Chess, A.; Lawrence, J. B. An Architectural Role for a Nuclear Noncoding RNA: NEAT1 RNA Is Essential for the Structure of Paraspeckles. *Mol. Cell* **2009**, *33* (6), 717−726.
(83) Li, R.; Harvey, A. R.; Hodgetts, S. I.; Fox, A. H. Functional Dissection of NEAT1 Using Genome Editing Reveals Substantial Localization of the NEAT1_1 Isoform Outside Paraspeckles. *RNA* **2017**, *23* (6), 872−881.
(84) Hafner, M.; Landthaler, M.; Burger, L.; Khorshid, M.; Hausser, J.; Berninger, P.; Rothballer, A.; Ascano, M.; Jungkamp, A.-C.; Munschauer, M.; Ulrich, A.; Wardle, G. S.; Dewell, S.; Zavolan, M.; Tuschl, T. PAR-CliP–a Method to Identify Transcriptome-Wide the Binding Sites of RNA Binding Proteins. *J. Vis. Exp.* **2010**, *2* (41), 2034 DOI: 10.3791/2034.
(85) Rhine, K.; Vidaurre, V.; Myong, S. RNA Droplets. *Annu. Rev. Biophys.* **2020**, *49*, 247−265.
(86) Kistler, K. E.; Trcek, T.; Hurd, T. R.; Chen, R.; Liang, F.-X.; Sall, J.; Kato, M.; Lehmann, R. Phase Transitioned Nuclear Oskar Promotes Cell Division of Drosophila Primordial Germ Cells. *Elife* **2018**, *7*, e37949 DOI: 10.7554/eLife.37949.
(87) Kim, Y.; Myong, S. RNA Remodeling Activity of DEAD Box Proteins Tuned by Protein Concentration, RNA Length, and ATP. *Mol. Cell* **2016**, *63* (5), 865−876.
(88) Tian, S.; Curnutte, H. A.; Trcek, T. RNA Granules: A View from the RNA Perspective. *Molecules* **2020**, *25* (14), 3130.
(89) Zhang, H.; Elbaum-Garfinkle, S.; Langdon, E. M.; Taylor, N.; Occhipinti, P.; Bridges, A. A.; Brangwynne, C. P.; Gladfelter, A. S. RNA Controls PolyQ Protein Phase Transitions. *Mol. Cell* **2015**, *60* (2), 220−230.
(90) Jolma, A.; Zhang, J.; Mondragón, E.; Morgunova, E.; Kivioja, T.; Laverty, K. U.; Yin, Y.; Zhu, F.; Bourenkov, G.; Morris, Q.; Hughes, T. R.; Maher, L. J., 3rd; Taipale, J. Binding Specificities of Human RNA-Binding Proteins toward Structured and Linear RNA Sequences. *Genome Res.* **2020**, *30* (7), 962−973.
(91) Kapral, T. H.; Farnhammer, F.; Zhao, W.; Lu, Z. J.; Zagrovic, B. Widespread Autogenous mRNA-Protein Interactions Detected by CLIP-Seq. *Nucleic Acids Res.* **2022**, *50* (17), 9984−9999.
(92) Zagrovic, B.; Adlhart, M.; Kapral, T. H. Coding From Binding? Molecular Interactions at the Heart of Translation. *Annu. Rev. Biophys.* **2023**, *52*, 69−89.
(93) Van Treeck, B.; Protter, D. S. W.; Matheny, T.; Khong, A.; Link, C. D.; Parker, R. RNA Self-Assembly Contributes to Stress Granule Formation and Defining the Stress Granule Transcriptome. *Proc. Natl. Acad. Sci. U. S. A.* **2018**, *115* (11), 2734−2739.
(94) Van Treeck, B.; Parker, R. Emerging Roles for Intermolecular RNA-RNA Interactions in RNP Assemblies. *Cell* **2018**, *174* (4), 791−802.
(95) Buchan, J. R.; Parker, R. Eukaryotic Stress Granules: The Ins and Outs of Translation. *Mol. Cell* **2009**, *36* (6), 932−941.
(96) Parker, R.; Sheth, U. P Bodies and the Control of mRNA Translation and Degradation. *Mol. Cell* **2007**, *25* (5), 635−646.
(97) Wilusz, J. E.; JnBaptiste, C. K.; Lu, L. Y.; Kuhn, C.-D.; Joshua-Tor, L.; Sharp, P. A. A Triple Helix Stabilizes the 3′ Ends of Long Noncoding RNAs That Lack poly(A) Tails. *Genes Dev.* **2012**, *26* (21), 2392−2407.
(98) Sunwoo, H.; Dinger, M. E.; Wilusz, J. E.; Amaral, P. P.; Mattick, J. S.; Spector, D. L. MEN Epsilon/beta Nuclear-Retained Non-Coding

RNAs Are up-Regulated upon Muscle Differentiation and Are Essential Components of Paraspeckles. *Genome Res.* **2009**, *19* (3), 347−359.
(99) Wang, Y.; Hu, S.-B.; Wang, M.-R.; Yao, R.-W.; Wu, D.; Yang, L.; Chen, L.-L. Genome-Wide Screening of NEAT1 Regulators Reveals Cross-Regulation between Paraspeckles and Mitochondria. *Nat. Cell Biol.* **2018**, *20* (10), 1145−1158.
(100) Visa, N.; Puvion-Dutilleul, F.; Bachellerie, J. P.; Puvion, E. Intranuclear Distribution of U1 and U2 snRNAs Visualized by High Resolution in Situ Hybridization: Revelation of a Novel Compartment Containing U1 but Not U2 snRNA in HeLa Cells. *Eur. J. Cell Biol.* **1993**, *60* (2), 308−321.
(101) Chen, L.-L.; Carmichael, G. G. Altered Nuclear Retention of mRNAs Containing Inverted Repeats in Human Embryonic Stem Cells: Functional Role of a Nuclear Noncoding RNA. *Mol. Cell* **2009**, *35* (4), 467−478.
(102) Prasanth, K. V.; Prasanth, S. G.; Xuan, Z.; Hearn, S.; Freier, S. M.; Bennett, C. F.; Zhang, M. Q.; Spector, D. L. Regulating Gene Expression through RNA Nuclear Retention. *Cell* **2005**, *123* (2), 249−263.
(103) Cho, E. J.; Kim, J. S. Crowding Effects on the Formation and Maintenance of Nuclear Bodies: Insights from Molecular-Dynamics Simulations of Simple Spherical Model Particles. *Biophys. J.* **2012**, *103* (3), 424−433.
(104) Kiss, T.; Fayet, E.; Jády, B. E.; Richard, P.; Weber, M. Biogenesis and Intranuclear Trafficking of Human Box C/D and H/ACA RNPs. *Cold Spring Harb. Symp. Quant. Biol.* **2006**, *71*, 407−417.
(105) Meier, U. T.; Blobel, G. NAP57, a Mammalian Nucleolar Protein with a Putative Homolog in Yeast and Bacteria. *J. Cell Biol.* **1994**, *127* (6), 1505−1514.
(106) Wang, Q.; Sawyer, I. A.; Sung, M.-H.; Sturgill, D.; Shevtsov, S. P.; Pegoraro, G.; Hakim, O.; Baek, S.; Hager, G. L.; Dundr, M. Cajal Bodies Are Linked to Genome Conformation. *Nat. Commun.* **2016**, *7*, 10966.
(107) Thomas, M. G.; Loschi, M.; Desbats, M. A.; Boccaccio, G. L. RNA Granules: The Good, the Bad and the Ugly. *Cell. Signal.* **2011**, *23* (2), 324−334.
(108) Yamasaki, S.; Ivanov, P.; Hu, G.-F.; Anderson, P. Angiogenin Cleaves tRNA and Promotes Stress-Induced Translational Repression. *J. Cell Biol.* **2009**, *185* (1), 35−42.
(109) Fu, H.; Feng, J.; Liu, Q.; Sun, F.; Tie, Y.; Zhu, J.; Xing, R.; Sun, Z.; Zheng, X. Stress Induces tRNA Cleavage by Angiogenin in Mammalian Cells. *FEBS Lett.* **2009**, *583* (2), 437−442.
(110) Saikia, M.; Krokowski, D.; Guan, B.-J.; Ivanov, P.; Parisien, M.; Hu, G.-F.; Anderson, P.; Pan, T.; Hatzoglou, M. Genome-Wide Identification and Quantitative Analysis of Cleaved tRNA Fragments Induced by Cellular Stress. *J. Biol. Chem.* **2012**, *287* (51), 42708−42725.
(111) Ivanov, P.; Emara, M. M.; Villen, J.; Gygi, S. P.; Anderson, P. Angiogenin-Induced tRNA Fragments Inhibit Translation Initiation. *Mol. Cell* **2011**, *43* (4), 613−623.
(112) Wallace, E. W. J.; Kear-Scott, J. L.; Pilipenko, E. V.; Schwartz, M. H.; Laskowski, P. R.; Rojek, A. E.; Katanski, C. D.; Riback, J. A.; Dion, M. F.; Franks, A. M.; Airoldi, E. M.; Pan, T.; Budnik, B. A.; Drummond, D. A. Reversible, Specific, Active Aggregates of Endogenous Proteins Assemble upon Heat Stress. *Cell* **2015**, *162* (6), 1286−1298.
(113) Omer, A.; Patel, D.; Lian, X. J.; Sadek, J.; Di Marco, S.; Pause, A.; Gorospe, M.; Gallouzi, I. E. Stress Granules Counteract Senescence by Sequestration of PAI-1. *EMBO Rep.* **2018**, *19* (5), e44722 DOI: 10.15252/embr.201744722.
(114) Sheth, U.; Parker, R. Decapping and Decay of Messenger RNA Occur in Cytoplasmic Processing Bodies. *Science* **2003**, *300* (5620), 805−808.
(115) Standart, N.; Weil, D. P-Bodies: Cytosolic Droplets for Coordinated mRNA Storage. *Trends Genet.* **2018**, *34* (8), 612−626.
(116) Eulalio, A.; Behm-Ansmant, I.; Schweizer, D.; Izaurralde, E. P-Body Formation Is a Consequence, Not the Cause, of RNA-Mediated Gene Silencing. *Mol. Cell. Biol.* **2007**, *27* (11), 3970−3981.
(117) Teixeira, D.; Sheth, U.; Valencia-Sanchez, M. A.; Brengues, M.; Parker, R. Processing Bodies Require RNA for Assembly and Contain Nontranslating mRNAs. *RNA* **2005**, *11* (4), 371−382.
(118) Arribas-Layton, M.; Dennis, J.; Bennett, E. J.; Damgaard, C. K.; Lykke-Andersen, J. The C-Terminal RGG Domain of Human Lsm4 Promotes Processing Body Formation Stimulated by Arginine Dimethylation. *Mol. Cell. Biol.* **2016**, *36* (17), 2226−2235.
(119) Kamenska, A.; Simpson, C.; Vindry, C.; Broomhead, H.; Bénard, M.; Ernoult-Lange, M.; Lee, B. P.; Harries, L. W.; Weil, D.; Standart, N. The DDX6−4E-T Interaction Mediates Translational Repression and P-Body Assembly. *Nucleic Acids Res.* **2016**, *44* (13), 6318−6334.
(120) Majumder, S.; Jain, A. Osmotic Stress Triggers Phase Separation. *Mol. Cell* **2020**, *79* (6), 876−877.
(121) Wang, C.; Schmich, F.; Srivatsa, S.; Weidner, J.; Beerenwinkel, N.; Spang, A. Context-Dependent Deposition and Regulation of mRNAs in P-Bodies. *Elife* **2018**, *7*, e29815 DOI: 10.7554/eLife.29815.
(122) Brockdorff, N. Local Tandem Repeat Expansion in Xist RNA as a Model for the Functionalisation of ncRNA. *Noncoding RNA* **2018**, *4* (4), 28.
(123) Pandya-Jones, A.; Markaki, Y.; Serizay, J.; Chitiashvili, T.; Mancia Leon, W. R.; Damianov, A.; Chronis, C.; Papp, B.; Chen, C.-K.; McKee, R.; Wang, X.-J.; Chau, A.; Sabri, S.; Leonhardt, H.; Zheng, S.; Guttman, M.; Black, D. L.; Plath, K. A Protein Assembly Mediates Xist Localization and Gene Silencing. *Nature* **2020**, *587* (7832), 145−151.
(124) Liu, E. Y.; Cali, C. P.; Lee, E. B. RNA Metabolism in Neurodegenerative Disease. *Dis. Model. Mech.* **2017**, *10* (5), 509−518.
(125) Buratti, E.; Baralle, F. E. The Molecular Links between TDP-43 Dysfunction and Neurodegeneration. *Adv. Genet.* **2009**, *66*, 1−34.
(126) Conlon, E. G.; Manley, J. L. RNA-Binding Proteins in Neurodegeneration: Mechanisms in Aggregate. *Genes Dev.* **2017**, *31* (15), 1509−1528.
(127) Jeon, P.; Lee, J. A. Dr. Jekyll and Mr. Hyde? Physiology and Pathology of Neuronal Stress Granules. *Front Cell Dev Biol.* **2021**, *9*, 609698.
(128) Farrawell, N. E.; Lambert-Smith, I. A.; Warraich, S. T.; Blair, I. P.; Saunders, D. N.; Hatters, D. M.; Yerbury, J. J. Distinct Partitioning of ALS Associated TDP-43, FUS and SOD1Mutants into Cellular Inclusions. *Sci. Rep.* **2015**, *5*, 13416.
(129) Ishiguro, A.; Lu, J.; Ozawa, D.; Nagai, Y.; Ishihama, A. ALS-Linked FUS Mutations Dysregulate G-Quadruplex-Dependent Liquid-Liquid Phase Separation and Liquid-to-Solid Transition. *J. Biol. Chem.* **2021**, *297* (5), 101284.
(130) Waelter, S.; Boeddrich, A.; Lurz, R.; Scherzinger, E.; Lueder, G.; Lehrach, H.; Wanker, E. E. Accumulation of Mutant Huntingtin Fragments in Aggresome-like Inclusion Bodies as a Result of Insufficient Protein Degradation. *Mol. Biol. Cell* **2001**, *12* (5), 1393−1407.
(131) Goggin, K.; Beaudoin, S.; Grenier, C.; Brown, A.-A.; Roucou, X. Prion Protein Aggresomes Are poly(A)+ Ribonucleoprotein Complexes That Induce a PKR-Mediated Deficient Cell Stress Response. *Biochim. Biophys. Acta* **2008**, *1783* (3), 479−491.
(132) Apicco, D. J.; Ash, P. E. A.; Maziuk, B.; LeBlang, C.; Medalla, M.; Al Abdullatif, A.; Ferragud, A.; Botelho, E.; Ballance, H. I.; Dhawan, U.; Boudeau, S.; Cruz, A. L.; Kashy, D.; Wong, A.; Goldberg, L. R.; Yazdani, N.; Zhang, C.; Ung, C. Y.; Tripodis, Y.; Kanaan, N. M.; Ikezu, T.; Cottone, P.; Leszyk, J.; Li, H.; Luebke, J.; Bryant, C. D.; Wolozin, B. Reducing the RNA Binding Protein TIA1 Protects against Tau-Mediated Neurodegeneration in Vivo. *Nat. Neurosci.* **2018**, *21* (1), 72−80.
(133) Nussbacher, J. K.; Tabet, R.; Yeo, G. W.; Lagier-Tourenne, C. Disruption of RNA Metabolism in Neurological Diseases and Emerging Therapeutic Interventions. *Neuron* **2019**, *102* (2), 294−320.
(134) Polymenidou, M.; Lagier-Tourenne, C.; Hutt, K. R.; Huelga, S. C.; Moran, J.; Liang, T. Y.; Ling, S.-C.; Sun, E.; Wancewicz, E.; Mazur, C.; Kordasiewicz, H.; Sedaghat, Y.; Donohue, J. P.; Shiue, L.; Bennett, C. F.; Yeo, G. W.; Cleveland, D. W. Long Pre-mRNA Depletion and RNA Missplicing Contribute to Neuronal Vulnerability from Loss of TDP-43. *Nat. Neurosci.* **2011**, *14* (4), 459−468.

https://doi.org/10.1021/acs.chemrev.3c00575
Chem. Rev. XXXX, XXX, XXX−XXX

(135) Chen, H.-J.; Topp, S. D.; Hui, H. S.; Zacco, E.; Katarya, M.; McLoughlin, C.; King, A.; Smith, B. N.; Troakes, C.; Pastore, A.; Shaw, C. E. RRM Adjacent TARDBP Mutations Disrupt RNA Binding and Enhance TDP-43 Proteinopathy. *Brain* **2019**, *142* (12), 3753−3770.
(136) Savas, J. N.; Ma, B.; Deinhardt, K.; Culver, B. P.; Restituito, S.; Wu, L.; Belasco, J. G.; Chao, M. V.; Tanese, N. A Role for Huntington Disease Protein in Dendritic RNA Granules. *J. Biol. Chem.* **2010**, *285* (17), 13142−13153.
(137) Bentmann, E.; Haass, C.; Dormann, D. Stress Granules in Neurodegeneration–Lessons Learnt from TAR DNA Binding Protein of 43 kDa and Fused in Sarcoma. *FEBS J.* **2013**, *280* (18), 4348−4370.
(138) Nonhoff, U.; Ralser, M.; Welzel, F.; Piccini, I.; Balzereit, D.; Yaspo, M.-L.; Lehrach, H.; Krobitsch, S. Ataxin-2 Interacts with the DEAD/H-Box RNA Helicase DDX6 and Interferes with P-Bodies and Stress Granules. *Mol. Biol. Cell* **2007**, *18* (4), 1385−1396.
(139) Mackenzie, I. R.; Nicholson, A. M.; Sarkar, M.; Messing, J.; Purice, M. D.; Pottier, C.; Annu, K.; Baker, M.; Perkerson, R. B.; Kurti, A.; Matchett, B. J.; Mittag, T.; Temirov, J.; Hsiung, G.-Y. R.; Krieger, C.; Murray, M. E.; Kato, M.; Fryer, J. D.; Petrucelli, L.; Zinman, L.; Weintraub, S.; Mesulam, M.; Keith, J.; Zivkovic, S. A.; Hirsch-Reinshagen, V.; Roos, R. P.; Züchner, S.; Graff-Radford, N. R.; Petersen, R. C.; Caselli, R. J.; Wszolek, Z. K.; Finger, E.; Lippa, C.; Lacomis, D.; Stewart, H.; Dickson, D. W.; Kim, H. J.; Rogaeva, E.; Bigio, E.; Boylan, K. B.; Taylor, J. P.; Rademakers, R. TIA1Mutations in Amyotrophic Lateral Sclerosis and Frontotemporal Dementia Promote Phase Separation and Alter Stress Granule Dynamics. *Neuron* **2017**, *95* (4), 808−816.e9.
(140) Wolozin, B.; Ivanov, P. Stress Granules and Neurodegeneration. *Nat. Rev. Neurosci.* **2019**, *20* (11), 649−666.
(141) Panas, M. D.; Ivanov, P.; Anderson, P. Mechanistic Insights into Mammalian Stress Granule Dynamics. *J. Cell Biol.* **2016**, *215* (3), 313−323.
(142) Sebastià, J.; Kieran, D.; Breen, B.; King, M. A.; Netteland, D. F.; Joyce, D.; Fitzpatrick, S. F.; Taylor, C. T.; Prehn, J. H. M. Angiogenin Protects Motoneurons against Hypoxic Injury. *Cell Death Differ.* **2009**, *16* (9), 1238−1247.
(143) Skorupa, A.; King, M. A.; Aparicio, I. M.; Dussmann, H.; Coughlan, K.; Breen, B.; Kieran, D.; Concannon, C. G.; Marin, P.; Prehn, J. H. M. Motoneurons Secrete Angiogenin to Induce RNA Cleavage in Astroglia. *J. Neurosci.* **2012**, *32* (15), 5024−5038.
(144) Ivanov, P.; O'Day, E.; Emara, M. M.; Wagner, G.; Lieberman, J.; Anderson, P. G-Quadruplex Structures Contribute to the Neuroprotective Effects of Angiogenin-Induced tRNA Fragments. *Proc. Natl. Acad. Sci. U. S. A.* **2014**, *111* (51), 18201−18206.
(145) Ratti, A.; Corrado, L.; Castellotti, B.; Del Bo, R.; Fogh, I.; Cereda, C.; Tiloca, C.; D'Ascenzo, C.; Bagarotti, A.; Pensato, V.; Ranieri, M.; Gagliardi, S.; Calini, D.; Mazzini, L.; Taroni, F.; Corti, S.; Ceroni, M.; Oggioni, G. D.; Lin, K.; Powell, J. F.; Sorarù, G.; Ticozzi, N.; Comi, G. P.; D'Alfonso, S.; Gellera, C.; Silani, V. SLAGEN Consortium. C9ORF72 Repeat Expansion in a Large Italian ALS Cohort: Evidence of a Founder Effect. *Neurobiol. Aging* **2012**, *33* (10), 2528.e7−e14.
(146) Mizielinska, S.; Lashley, T.; Norona, F. E.; Clayton, E. L.; Ridler, C. E.; Fratta, P.; Isaacs, A. M. C9orf72 Frontotemporal Lobar Degeneration Is Characterised by Frequent Neuronal Sense and Antisense RNA Foci. *Acta Neuropathol.* **2013**, *126* (6), 845−857.
(147) Mori, K.; Lammich, S.; Mackenzie, I. R. A.; Forné, I.; Zilow, S.; Kretzschmar, H.; Edbauer, D.; Janssens, J.; Kleinberger, G.; Cruts, M.; Herms, J.; Neumann, M.; Van Broeckhoven, C.; Arzberger, T.; Haass, C. hnRNP A3 Binds to GGGGCC Repeats and Is a Constituent of p62-positive/TDP43-Negative Inclusions in the Hippocampus of Patients with C9orf72 Mutations. *Acta Neuropathol.* **2013**, *125* (3), 413−423.
(148) Emara, M. M.; Ivanov, P.; Hickman, T.; Dawra, N.; Tisdale, S.; Kedersha, N.; Hu, G.-F.; Anderson, P. Angiogenin-Induced tRNA-Derived Stress-Induced RNAs Promote Stress-Induced Stress Granule Assembly. *J. Biol. Chem.* **2010**, *285* (14), 10959−10968.
(149) Kocabalkan, O.; Ozgür, F.; Erk, Y.; Gürsu, K. G.; Güngen, Y. Malignant Melanoma in Xeroderma Pigmentosum Patients: Report of Five Cases. *Eur. J. Surg. Oncol.* **1997**, *23* (1), 43−47.
(150) Sofola, O. A.; Jin, P.; Qin, Y.; Duan, R.; Liu, H.; de Haro, M.; Nelson, D. L.; Botas, J. RNA-Binding Proteins hnRNP A2/B1 and CUGBP1 Suppress Fragile X CGG Premutation Repeat-Induced Neurodegeneration in a Drosophila Model of FXTAS. *Neuron* **2007**, *55* (4), 565−571.
(151) Zhang, X.; Lin, Y.; Eschmann, N. A.; Zhou, H.; Rauch, J. N.; Hernandez, I.; Guzman, E.; Kosik, K. S.; Han, S. RNA Stores Tau Reversibly in Complex Coacervates. *PLoS Biol.* **2017**, *15* (7), No. e2002183.
(152) Gunawardana, C. G.; Mehrabian, M.; Wang, X.; Mueller, I.; Lubambo, I. B.; Jonkman, J. E. N.; Wang, H.; Schmitt-Ulms, G. The Human Tau Interactome: Binding to the Ribonucleoproteome, and Impaired Binding of the Proline-to-Leucine Mutant at Position 301 (P301L) to Chaperones and the Proteasome. *Mol. Cell. Proteomics* **2015**, *14* (11), 3000−3014.
(153) Chen, J.-A.; Wichterle, H. Apoptosis of Limb Innervating Motor Neurons and Erosion of Motor Pool Identity upon Lineage Specific Dicer Inactivation. *Front. Neurosci.* **2012**, *6*, 69.
(154) Hubstenberger, A.; Courel, M.; Bénard, M.; Souquere, S.; Ernoult-Lange, M.; Chouaib, R.; Yi, Z.; Morlot, J.-B.; Munier, A.; Fradet, M.; Daunesse, M.; Bertrand, E.; Pierron, G.; Mozziconacci, J.; Kress, M.; Weil, D. P-Body Purification Reveals the Condensation of Repressed mRNA Regulons. *Mol. Cell* **2017**, *68* (1), 144−157.e5.
(155) De Felice, B.; Guida, M.; Guida, M.; Coppola, C.; De Mieri, G.; Cotrufo, R. A miRNA Signature in Leukocytes from Sporadic Amyotrophic Lateral Sclerosis. *Gene* **2012**, *508* (1), 35−40.
(156) Wang, W.-X.; Rajeev, B. W.; Stromberg, A. J.; Ren, N.; Tang, G.; Huang, Q.; Rigoutsos, I.; Nelson, P. T. The Expression of microRNA miR-107 Decreases Early in Alzheimer's Disease and May Accelerate Disease Progression through Regulation of Beta-Site Amyloid Precursor Protein-Cleaving Enzyme 1. *J. Neurosci.* **2008**, *28* (5), 1213−1223.
(157) Basavaraju, M.; de Lencastre, A. Alzheimer's Disease: Presence and Role of microRNAs. *Biomol. Concepts* **2016**, *7* (4), 241−252.
(158) Smith, P. Y.; Hernandez-Rapp, J.; Jolivette, F.; Lecours, C.; Bisht, K.; Goupil, C.; Dorval, V.; Parsi, S.; Morin, F.; Planel, E.; Bennett, D. A.; Fernandez-Gomez, F.-J.; Sergeant, N.; Buée, L.; Tremblay, M.-È.; Calon, F.; Hébert, S. S. miR-132/212 Deficiency Impairs Tau Metabolism and Promotes Pathological Aggregation in Vivo. *Hum. Mol. Genet.* **2015**, *24* (23), 6721−6735.
(159) Vanderweyde, T.; Apicco, D. J.; Youmans-Kidder, K.; Ash, P. E. A.; Cook, C.; Lummertz da Rocha, E.; Jansen-West, K.; Frame, A. A.; Citro, A.; Leszyk, J. D.; Ivanov, P.; Abisambra, J. F.; Steffen, M.; Li, H.; Petrucelli, L.; Wolozin, B. Interaction of Tau with the RNA-Binding Protein TIA1 Regulates Tau Pathophysiology and Toxicity. *Cell Rep.* **2016**, *15* (7), 1455−1466.
(160) Weiss, J. M. The Promise and Peril of Targeting Cell Metabolism for Cancer Therapy. *Cancer Immunol. Immunother.* **2020**, *69* (2), 255−261.
(161) Bradner, J. E.; Hnisz, D.; Young, R. A. Transcriptional Addiction in Cancer. *Cell* **2017**, *168* (4), 629−643.
(162) Cho, W.-K.; Spille, J.-H.; Hecht, M.; Lee, C.; Li, C.; Grube, V.; Cisse, I. I. Mediator and RNA Polymerase II Clusters Associate in Transcription-Dependent Condensates. *Science* **2018**, *361* (6400), 412−415.
(163) Bouchard, J. J.; Otero, J. H.; Scott, D. C.; Szulc, E.; Martin, E. W.; Sabri, N.; Granata, D.; Marzahn, M. R.; Lindorff-Larsen, K.; Salvatella, X.; Schulman, B. A.; Mittag, T. Cancer Mutations of the Tumor Suppressor SPOP Disrupt the Formation of Active, Phase-Separated Compartments. *Mol. Cell* **2018**, *72* (1), 19−36.e8.
(164) Zhu, H.-H.; Wu, C.; Sun, Y.; Hu, J. PML Mutation in PML-Rarα Alters PML Nuclear Body Organization and Induces ATRA Resistance in Acute Promyelocytic Leukemia. *Blood* **2018**, *132*, 3923−3923.
(165) Lin, C. Y.; Lovén, J.; Rahl, P. B.; Paranal, R. M.; Burge, C. B.; Bradner, J. E.; Lee, T. I.; Young, R. A. Transcriptional Amplification in Tumor Cells with Elevated c-Myc. *Cell* **2012**, *151* (1), 56−67.
(166) Barbieri, I.; Kouzarides, T. Role of RNA Modifications in Cancer. *Nat. Rev. Cancer* **2020**, *20* (6), 303−322.

https://doi.org/10.1021/acs.chemrev.3c00575
Chem. Rev. XXXX, XXX, XXX−XXX

(167) Wang, E.; Aifantis, I. RNA Splicing and Cancer. *Trends Cancer Res.* **2020**, *6* (8), 631−644.
(168) Boija, A.; Klein, I. A.; Young, R. A. Biomolecular Condensates and Cancer. *Cancer Cell* **2021**, *39* (2), 174−192.
(169) El-Naggar, A. M.; Sorensen, P. H. Translational Control of Aberrant Stress Responses as a Hallmark of Cancer. *J. Pathol.* **2018**, *244* (5), 650−666.
(170) Yang, C.; Li, Z.; Li, Y.; Xu, R.; Wang, Y.; Tian, Y.; Chen, W. Long Non-Coding RNA NEAT1 Overexpression Is Associated with Poor Prognosis in Cancer Patients: A Systematic Review and Meta-Analysis. *Oncotarget* **2017**, *8* (2), 2672−2680.
(171) Idogawa, M.; Ohashi, T.; Sasaki, Y.; Nakase, H.; Tokino, T. Long Non-Coding RNA NEAT1 Is a Transcriptional Target of p53 and Modulates p53-Induced Transactivation and Tumor-Suppressor Function. *Int. J. Cancer* **2017**, *140* (12), 2785−2791.
(172) Mello, S. S.; Sinow, C.; Raj, N.; Mazur, P. K.; Bieging-Rolett, K.; Broz, D. K.; Imam, J. F. C.; Vogel, H.; Wood, L. D.; Sage, J.; Hirose, T.; Nakagawa, S.; Rinn, J.; Attardi, L. D. Neat1 Is a p53-Inducible lincRNA Essential for Transformation Suppression. *Genes Dev.* **2017**, *31* (11), 1095−1108.
(173) Adriaens, C.; Standaert, L.; Barra, J.; Latil, M.; Verfaillie, A.; Kalev, P.; Boeckx, B.; Wijnhoven, P. W. G.; Radaelli, E.; Vermi, W.; Leucci, E.; Lapouge, G.; Beck, B.; van den Oord, J.; Nakagawa, S.; Hirose, T.; Sablina, A. A.; Lambrechts, D.; Aerts, S.; Blanpain, C.; Marine, J.-C. p53 Induces Formation of NEAT1 lncRNA-Containing Paraspeckles That Modulate Replication Stress Response and Chemosensitivity. *Nat. Med.* **2016**, *22* (8), 861−868.
(174) Laplante, M.; Sabatini, D. M. mTOR Signaling in Growth Control and Disease. *Cell* **2012**, *149* (2), 274−293.
(175) Thedieck, K.; Holzwarth, B.; Prentzell, M. T.; Boehlke, C.; Kläsener, K.; Ruf, S.; Sonntag, A. G.; Maerz, L.; Grellscheid, S.-N.; Kremmer, E.; Nitschke, R.; Kuehn, E. W.; Jonker, J. W.; Groen, A. K.; Reth, M.; Hall, M. N.; Baumeister, R. Inhibition of mTORC1 by Astrin and Stress Granules Prevents Apoptosis in Cancer Cells. *Cell* **2013**, *154* (4), 859−874.
(176) Polunovsky, V. A.; Bitterman, P. B. The Cap-Dependent Translation Apparatus Integrates and Amplifies Cancer Pathways. *RNA Biol.* **2006**, *3* (1), 10−17.
(177) Frydryskova, K.; Masek, T.; Borcin, K.; Mrvova, S.; Venturi, V.; Pospisek, M. Distinct Recruitment of Human eIF4E Isoforms to Processing Bodies and Stress Granules. *BMC Mol. Biol.* **2016**, *17* (1), 21.
(178) Evdokimova, V.; Tognon, C.; Ng, T.; Ruzanov, P.; Melnyk, N.; Fink, D.; Sorokin, A.; Ovchinnikov, L. P.; Davicioni, E.; Triche, T. J.; Sorensen, P. H. B. Translational Activation of snail1 and Other Developmentally Regulated Transcription Factors by YB-1 Promotes an Epithelial-Mesenchymal Transition. *Cancer Cell* **2009**, *15* (5), 402−415.
(179) Shih, J.-W.; Wang, W.-T.; Tsai, T.-Y.; Kuo, C.-Y.; Li, H.-K.; Wu Lee, Y.-H. Critical Roles of RNA Helicase DDX3 and Its Interactions with eIF4E/PABP1 in Stress Granule Assembly and Stress Response. *Biochem. J.* **2012**, *441* (1), 119−129.
(180) Fujimura, K.; Wright, T.; Strnadel, J.; Kaushal, S.; Metildi, C.; Lowy, A. M.; Bouvet, M.; Kelber, J. A.; Klemke, R. L. A Hypusine-eIF5A-PEAK1 Switch Regulates the Pathogenesis of Pancreatic Cancer. *Cancer Res.* **2014**, *74* (22), 6671−6681.
(181) Hayes, J.; Peruzzi, P. P.; Lawler, S. MicroRNAs in Cancer: Biomarkers, Functions and Therapy. *Trends Mol. Med.* **2014**, *20* (8), 460−469.
(182) El Yacoubi, B.; Bailly, M.; de Crécy-Lagard, V. Biosynthesis and Function of Posttranscriptional Modifications of Transfer RNAs. *Annu. Rev. Genet.* **2012**, *46*, 69−95.
(183) Dominissini, D.; Moshitch-Moshkovitz, S.; Schwartz, S.; Salmon-Divon, M.; Ungar, L.; Osenberg, S.; Cesarkas, K.; Jacob-Hirsch, J.; Amariglio, N.; Kupiec, M.; Sorek, R.; Rechavi, G. Topology of the Human and Mouse m6A RNA Methylomes Revealed by m6A-Seq. *Nature* **2012**, *485* (7397), 201−206.
(184) Meyer, K. D.; Saletore, Y.; Zumbo, P.; Elemento, O.; Mason, C. E.; Jaffrey, S. R. Comprehensive Analysis of mRNA Methylation Reveals Enrichment in 3′ UTRs and near Stop Codons. *Cell* **2012**, *149* (7), 1635−1646.
(185) Hajnic, M.; Ruiter, A. de; Polyansky, A. A.; Zagrovic, B. Inosine Nucleobase Acts as Guanine in Interactions with Protein Side Chains. *J. Am. Chem. Soc.* **2016**, *138* (17), 5519−5522.
(186) Liu, J.; Yue, Y.; Han, D.; Wang, X.; Fu, Y.; Zhang, L.; Jia, G.; Yu, M.; Lu, Z.; Deng, X.; Dai, Q.; Chen, W.; He, C. A METTL3-METTL14 Complex Mediates Mammalian Nuclear RNA N6-Adenosine Methylation. *Nat. Chem. Biol.* **2014**, *10* (2), 93−95.
(187) Ping, X.-L.; Sun, B.-F.; Wang, L.; Xiao, W.; Yang, X.; Wang, W.-J.; Adhikari, S.; Shi, Y.; Lv, Y.; Chen, Y.-S.; Zhao, X.; Li, A.; Yang, Y.; Dahal, U.; Lou, X.-M.; Liu, X.; Huang, J.; Yuan, W.-P.; Zhu, X.-F.; Cheng, T.; Zhao, Y.-L.; Wang, X.; Rendtlew Danielsen, J. M.; Liu, F.; Yang, Y.-G. Mammalian WTAP Is a Regulatory Subunit of the RNA N6-Methyladenosine Methyltransferase. *Cell Res.* **2014**, *24* (2), 177−189.
(188) Schwartz, S.; Mumbach, M. R.; Jovanovic, M.; Wang, T.; Maciag, K.; Bushkin, G. G.; Mertins, P.; Ter-Ovanesyan, D.; Habib, N.; Cacchiarelli, D.; Sanjana, N. E.; Freinkman, E.; Pacold, M. E.; Satija, R.; Mikkelsen, T. S.; Hacohen, N.; Zhang, F.; Carr, S. A.; Lander, E. S.; Regev, A. Perturbation of m6A Writers Reveals Two Distinct Classes of mRNA Methylation at Internal and 5′ Sites. *Cell Rep.* **2014**, *8* (1), 284−296.
(189) Xiao, W.; Adhikari, S.; Dahal, U.; Chen, Y.-S.; Hao, Y.-J.; Sun, B.-F.; Sun, H.-Y.; Li, A.; Ping, X.-L.; Lai, W.-Y.; Wang, X.; Ma, H.-L.; Huang, C.-M.; Yang, Y.; Huang, N.; Jiang, G.-B.; Wang, H.-L.; Zhou, Q.; Wang, X.-J.; Zhao, Y.-L.; Yang, Y.-G. Nuclear m(6)A Reader YTHDC1 Regulates mRNA Splicing. *Mol. Cell* **2016**, *61* (4), 507−519.
(190) Wang, X.; Zhao, B. S.; Roundtree, I. A.; Lu, Z.; Han, D.; Ma, H.; Weng, X.; Chen, K.; Shi, H.; He, C. N(6)-Methyladenosine Modulates Messenger RNA Translation Efficiency. *Cell* **2015**, *161* (6), 1388−1399.
(191) Jia, G.; Fu, Y.; Zhao, X.; Dai, Q.; Zheng, G.; Yang, Y.; Yi, C.; Lindahl, T.; Pan, T.; Yang, Y.-G.; He, C. N6-Methyladenosine in Nuclear RNA Is a Major Substrate of the Obesity-Associated FTO. *Nat. Chem. Biol.* **2011**, *7* (12), 885−887.
(192) Zheng, G.; Dahl, J. A.; Niu, Y.; Fedorcsak, P.; Huang, C.-M.; Li, C. J.; Vagbo, C. B.; Shi, Y.; Wang, W.-L.; Song, S.-H.; Lu, Z.; Bosmans, R. P. G.; Dai, Q.; Hao, Y.-J.; Yang, X.; Zhao, W.-M.; Tong, W.-M.; Wang, X.-J.; Bogdan, F.; Furu, K.; Fu, Y.; Jia, G.; Zhao, X.; Liu, J.; Krokan, H. E.; Klungland, A.; Yang, Y.-G.; He, C. ALKBH5 Is a Mammalian RNA Demethylase That Impacts RNA Metabolism and Mouse Fertility. *Mol. Cell* **2013**, *49* (1), 18−29.
(193) Wang, J.; Wang, L.; Diao, J.; Shi, Y. G.; Shi, Y.; Ma, H.; Shen, H. Binding to m6A RNA Promotes YTHDF2-Mediated Phase Separation. *Protein Cell* **2020**, *11* (4), 304−307.
(194) Patil, D. P.; Pickering, B. F.; Jaffrey, S. R. Reading m6A in the Transcriptome: m6A-Binding Proteins. *Trends Cell Biol.* **2018**, *28* (2), 113−127.
(195) Gao, Y.; Pei, G.; Li, D.; Li, R.; Shao, Y.; Zhang, Q. C.; Li, P. Multivalent m6A Motifs Promote Phase Separation of YTHDF Proteins. *Cell Res.* **2019**, *29* (9), 767−769.
(196) Fu, Y.; Zhuang, X. m6A-Binding YTHDF Proteins Promote Stress Granule Formation. *Nat. Chem. Biol.* **2020**, *16* (9), 955−963.
(197) Anders, M.; Chelysheva, I.; Goebel, I.; Trenkner, T.; Zhou, J.; Mao, Y.; Verzini, S.; Qian, S.-B.; Ignatova, Z. Dynamic m6A Methylation Facilitates mRNA Triaging to Stress Granules. *Life Sci. Alliance* **2018**, *1* (4), No. e201800113.
(198) Cheng, Y.; Xie, W.; Pickering, B. F.; Chu, K. L.; Savino, A. M.; Yang, X.; Luo, H.; Nguyen, D. T.; Mo, S.; Barin, E.; Velleca, A.; Rohwetter, T. M.; Patel, D. J.; Jaffrey, S. R.; Kharas, M. G. N6-Methyladenosine on mRNA Facilitates a Phase-Separated Nuclear Body That Suppresses Myeloid Leukemic Differentiation. *Cancer Cell* **2021**, *39* (7), 958−972.e8.
(199) Wang, X.; Liu, C.; Zhang, S.; Yan, H.; Zhang, L.; Jiang, A.; Liu, Y.; Feng, Y.; Li, D.; Guo, Y.; Hu, X.; Lin, Y.; Bu, P.; Li, D. N6-Methyladenosine Modification of MALAT1 Promotes Metastasis via Reshaping Nuclear Speckles. *Dev. Cell* **2021**, *56* (5), 702−715.e8.

https://doi.org/10.1021/acs.chemrev.3c00575
Chem. Rev. XXXX, XXX, XXX−XXX

(200) Linder, B.; Grozhik, A. V.; Olarerin-George, A. O.; Meydan, C.; Mason, C. E.; Jaffrey, S. R. Single-Nucleotide-Resolution Mapping of m6A and m6Am throughout the Transcriptome. *Nat. Methods* **2015**, *12* (8), 767−772.
(201) Liu, N.; Dai, Q.; Zheng, G.; He, C.; Parisien, M.; Pan, T. N(6)-Methyladenosine-Dependent RNA Structural Switches Regulate RNA-Protein Interactions. *Nature* **2015**, *518* (7540), 560−564.
(202) Han, D.; Longhini, A. P.; Zhang, X.; Hoang, V.; Wilson, M. Z.; Kosik, K. S. Dynamic Assembly of the mRNA m6A Methyltransferase Complex Is Regulated by METTL3 Phase Separation. *PLoS Biol.* **2022**, *20* (2), No. e3001535.
(203) Alriquet, M.; Martínez-Limón, A.; Hanspach, G.; Hengesbach, M.; Tartaglia, G. G.; Calloni, G.; Vabulas, R. M. Assembly of Proteins by Free RNA during the Early Phase of Proteostasis Stress. *J. Proteome Res.* **2019**, *18* (7), 2835−2847.
(204) Zhou, H.; Kimsey, I. J.; Nikolova, E. N.; Sathyamoorthy, B.; Grazioli, G.; McSally, J.; Bai, T.; Wunderlich, C. H.; Kreutz, C.; Andricioaei, I.; Al-Hashimi, H. M. m(1)A and m(1)G Disrupt A-RNA Structure through the Intrinsic Instability of Hoogsteen Base Pairs. *Nat. Struct. Mol. Biol.* **2016**, *23* (9), 803−810.
(205) Dominissini, D.; Nachtergaele, S.; Moshitch-Moshkovitz, S.; Peer, E.; Kol, N.; Ben-Haim, M. S.; Dai, Q.; Di Segni, A.; Salmon-Divon, M.; Clark, W. C.; Zheng, G.; Pan, T.; Solomon, O.; Eyal, E.; Hershkovitz, V.; Han, D.; Doré, L. C.; Amariglio, N.; Rechavi, G.; He, C. The Dynamic N(1)-Methyladenosine Methylome in Eukaryotic Messenger RNA. *Nature* **2016**, *530* (7591), 441−446.
(206) Zhang, Z.; Carmichael, G. G. The Fate of dsRNA in the Nucleus: A p54(nrb)-Containing Complex Mediates the Nuclear Retention of Promiscuously A-to-I Edited RNAs. *Cell* **2001**, *106* (4), 465−475.
(207) Chen, L.-L.; DeCerbo, J. N.; Carmichael, G. G. Alu Element-Mediated Gene Silencing. *EMBO J.* **2008**, *27* (12), 1694−1705.
(208) Fox, A. H.; Bond, C. S.; Lamond, A. I. P54nrb Forms a Heterodimer with PSP1 That Localizes to Paraspeckles in an RNA-Dependent Manner. *Mol. Biol. Cell* **2005**, *16* (11), 5304−5315.
(209) Fox, A. H.; Lam, Y. W.; Leung, A. K. L.; Lyon, C. E.; Andersen, J.; Mann, M.; Lamond, A. I. Paraspeckles: A Novel Nuclear Domain. *Curr. Biol.* **2002**, *12* (1), 13−25.
(210) Hutchinson, J. N.; Ensminger, A. W.; Clemson, C. M.; Lynch, C. R.; Lawrence, J. B.; Chess, A. A Screen for Nuclear Transcripts Identifies Two Linked Noncoding RNAs Associated with SC35 Splicing Domains. *BMC Genomics* **2007**, *8*, 39.
(211) Vlachogiannis, N. I.; Sachse, M.; Georgiopoulos, G.; Zormpas, E.; Bampatsias, D.; Delialis, D.; Bonini, F.; Galyfos, G.; Sigala, F.; Stamatelopoulos, K.; Gatsiou, A.; Stellos, K. Adenosine-to-Inosine Alu RNA Editing Controls the Stability of the pro-Inflammatory Long Noncoding RNA NEAT1 in Atherosclerotic Cardiovascular Disease. *J. Mol. Cell. Cardiol.* **2021**, *160*, 111−120.
(212) Delli Ponti, R.; Broglia, L.; Vandelli, A.; Armaos, A.; Burgas, M. T.; Sanchez de Groot, N.; Tartaglia, G. G. A High-Throughput Approach to Predict A-to-I Effects on RNA Structure Indicates a Change of Double-Stranded Content in Noncoding RNAs. *IUBMB Life* **2023**, *75* (5), 411−426.
(213) Okonski, K. M.; Samuel, C. E. Stress Granule Formation Induced by Measles Virus Is Protein Kinase PKR Dependent and Impaired by RNA Adenosine Deaminase ADAR1. *J. Virol.* **2013**, *87* (2), 756−766.
(214) Saar, K. L.; Qian, D.; Good, L. L.; Morgunov, A. S.; Collepardo-Guevara, R.; Best, R. B.; Knowles, T. P. J. Theoretical and Data-Driven Approaches for Biomolecular Condensates. *Chem. Rev.* **2023**, *123* (14), 8988−9009.
(215) Riback, J. A.; Zhu, L.; Ferrolino, M. C.; Tolbert, M.; Mitrea, D. M.; Sanders, D. W.; Wei, M.-T.; Kriwacki, R. W.; Brangwynne, C. P. Composition-Dependent Thermodynamics of Intracellular Phase Separation. *Nature* **2020**, *581* (7807), 209−214.
(216) Shin, Y.; Chang, Y.-C.; Lee, D. S. W.; Berry, J.; Sanders, D. W.; Ronceray, P.; Wingreen, N. S.; Haataja, M.; Brangwynne, C. P. Liquid Nuclear Condensates Mechanically Sense and Restructure the Genome. *Cell* **2018**, *175* (6), 1481−1491.e13.
(217) Wu, X.; Ganzella, M.; Zhou, J.; Zhu, S.; Jahn, R.; Zhang, M. Vesicle Tethering on the Surface of Phase-Separated Active Zone Condensates. *Mol. Cell* **2021**, *81* (1), 13−24.e7.
(218) Van Lindt, J.; Bratek-Skicki, A.; Nguyen, P. N.; Pakravan, D.; Durán-Armenta, L. F.; Tantos, A.; Pancsa, R.; Van Den Bosch, L.; Maes, D.; Tompa, P. A Generic Approach to Study the Kinetics of Liquid-Liquid Phase Separation under near-Native Conditions. *Commun. Biol.* **2021**, *4* (1), 77.
(219) Kroschwald, S.; Maharana, S.; Mateju, D.; Malinovska, L.; Nüske, E.; Poser, I.; Richter, D.; Alberti, S. Promiscuous Interactions and Protein Disaggregases Determine the Material State of Stress-Inducible RNP Granules. *Elife* **2015**, *4*, No. e06807.
(220) Gibson, B. A.; Doolittle, L. K.; Schneider, M. W. G.; Jensen, L. E.; Gamarra, N.; Henry, L.; Gerlich, D. W.; Redding, S.; Rosen, M. K. Organization of Chromatin by Intrinsic and Regulated Phase Separation. *Cell* **2019**, *179* (2), 470−484.e21.
(221) Lyu, X.; Wang, J.; Wang, J.; Yin, Y.-S.; Zhu, Y.; Li, L.-L.; Huang, S.; Peng, S.; Xue, B.; Liao, R.; Wang, S.-Q.; Long, M.; Wohland, T.; Chua, B. T.; Sun, Y.; Li, P.; Chen, X.-W.; Xu, L.; Chen, F.-J.; Li, P. A Gel-like Condensation of Cidec Generates Lipid-Permeable Plates for Lipid Droplet Fusion. *Dev. Cell* **2021**, *56* (18), 2592−2606.e7.
(222) Wang, H.; Zhou, F.; Guo, Y.; Ju, L. A. Micropipette-Based Biomechanical Nanotools on Living Cells. *Eur. Biophys. J.* **2022**, *51* (2), 119−133.
(223) Portet, T.; Gordon, S. E.; Keller, S. L. Increasing Membrane Tension Decreases Miscibility Temperatures; an Experimental Demonstration via Micropipette Aspiration. *Biophys. J.* **2012**, *103* (8), L35−L37.
(224) Ju, L.; Chen, Y.; Rushdi, M. N.; Chen, W.; Zhu, C. Two-Dimensional Analysis of Cross-Junctional Molecular Interaction by Force Probes. *Methods Mol. Biol.* **2017**, *1584*, 231−258.
(225) Kapanidis, A. N.; Strick, T. Biology, One Molecule at a Time. *Trends Biochem. Sci.* **2009**, *34* (5), 234−243.
(226) Hill, C. H.; Pekarek, L.; Napthine, S.; Kibe, A.; Firth, A. E.; Graham, S. C.; Caliskan, N.; Brierley, I. Structural and Molecular Basis for Cardiovirus 2A Protein as a Viral Gene Expression Switch. *Nat. Commun.* **2021**, *12* (1), 7166.
(227) Scull, C. E.; Dandpat, S. S.; Romero, R. A.; Walter, N. G. Transcriptional Riboswitches Integrate Timescales for Bacterial Gene Expression Control. *Front Mol. Biosci* **2021**, *7*, 607158.
(228) Ghosh, A.; Zhou, H.-X. Determinants for Fusion Speed of Biomolecular Droplets. *Angew. Chem., Int. Ed. Engl.* **2020**, *59* (47), 20837−20840.
(229) Wang, M.; Zhao, C.; Miao, X.; Zhao, Y.; Rufo, J.; Liu, Y. J.; Huang, T. J.; Zheng, Y. Plasmofluidics: Merging Light and Fluids at the Micro-/Nanoscale. *Small* **2015**, *11* (35), 4423−4444.
(230) Papale, A.; Smrek, J.; Rosa, A. Nanorheology of Active-Passive Polymer Mixtures Differentiates between Linear and Ring Polymer Topology. *Soft Matter* **2021**, *17* (30), 7111−7117.
(231) Alshareedah, I.; Moosa, M. M.; Raju, M.; Potoyan, D. A.; Banerjee, P. R. Phase Transition of RNA-Protein Complexes into Ordered Hollow Condensates. *Proc. Natl. Acad. Sci. U. S. A.* **2020**, *117* (27), 15650−15658.
(232) Kaur, T.; Alshareedah, I.; Wang, W.; Ngo, J.; Moosa, M. M.; Banerjee, P. R. Molecular Crowding Tunes Material States of Ribonucleoprotein Condensates. *Biomolecules* **2019**, *9* (2), 71.
(233) Saito, T.; Matsunaga, D.; Deguchi, S. Long-Term Fluorescence Recovery After Photobleaching (FRAP). *Methods Mol. Biol.* **2023**, *2600*, 311−322.
(234) Soranno, A. The Trap in the FRAP: A Cautionary Tale about Transport Measurements in Biomolecular Condensates. *Biophys. J.* **2019**, *117* (11), 2041−2042.
(235) Taylor, N. O.; Wei, M.-T.; Stone, H. A.; Brangwynne, C. P. Quantifying Dynamics in Phase-Separated Condensates Using Fluorescence Recovery after Photobleaching. *Biophys. J.* **2019**, *117* (7), 1285−1300.
(236) Brangwynne, C. P.; Mitchison, T. J.; Hyman, A. A. Active Liquid-like Behavior of Nucleoli Determines Their Size and Shape in

https://doi.org/10.1021/acs.chemrev.3c00575
Chem. Rev. XXXX, XXX, XXX−XXX

Xenopus Laevis Oocytes. *Proc. Natl. Acad. Sci. U. S. A.* **2011**, *108* (11), 4334−4339.
(237) Braga, J.; McNally, J. G.; Carmo-Fonseca, M. A Reaction-Diffusion Model to Study RNA Motion by Quantitative Fluorescence Recovery after Photobleaching. *Biophys. J.* **2007**, *92* (8), 2694−2703.
(238) Zhang, H.; Keane, S. C. Advances That Facilitate the Study of Large RNA Structure and Dynamics by Nuclear Magnetic Resonance Spectroscopy. *Wiley Interdiscip. Rev. RNA* **2019**, *10* (5), No. e1541.
(239) Jackson, R. W.; Smathers, C. M.; Robart, A. R. General Strategies for RNA X-Ray Crystallography. *Molecules* **2023**, *28* (5), 2111.
(240) Le Brun, E.; Arluison, V.; Wien, F. Application of Synchrotron Radiation Circular Dichroism for RNA Structural Analysis. *Methods Mol. Biol.* **2020**, *2113*, 135−148.
(241) Geinguenaud, F.; Militello, V.; Arluison, V. Application of FTIR Spectroscopy to Analyze RNA Structure. *Methods Mol. Biol.* **2020**, *2113*, 119−133.
(242) Strobel, E. J.; Yu, A. M.; Lucks, J. B. High-Throughput Determination of RNA Structures. *Nat. Rev. Genet.* **2018**, *19* (10), 615−634.
(243) Wilkinson, K. A.; Merino, E. J.; Weeks, K. M. Selective 2'-Hydroxyl Acylation Analyzed by Primer Extension (SHAPE): Quantitative RNA Structure Analysis at Single Nucleotide Resolution. *Nat. Protoc.* **2006**, *1* (3), 1610−1616.
(244) Lu, Z.; Zhang, Q. C.; Lee, B.; Flynn, R. A.; Smith, M. A.; Robinson, J. T.; Davidovich, C.; Gooding, A. R.; Goodrich, K. J.; Mattick, J. S.; Mesirov, J. P.; Cech, T. R.; Chang, H. Y. RNA Duplex Map in Living Cells Reveals Higher-Order Transcriptome Structure. *Cell* **2016**, *165* (5), 1267−1279.
(245) Minton, A. P. Recent Applications of Light Scattering Measurement in the Biological and Biopharmaceutical Sciences. *Anal. Biochem.* **2016**, *501*, 4−22.
(246) Simon, J. R.; Carroll, N. J.; Rubinstein, M.; Chilkoti, A.; López, G. P. Programming Molecular Self-Assembly of Intrinsically Disordered Proteins Containing Sequences of Low Complexity. *Nat. Chem.* **2017**, *9* (6), 509−515.
(247) Stetefeld, J.; McKenna, S. A.; Patel, T. R. Dynamic Light Scattering: A Practical Guide and Applications in Biomedical Sciences. *Biophys. Rev.* **2016**, *8* (4), 409−427.
(248) Riback, J. A.; Katanski, C. D.; Kear-Scott, J. L.; Pilipenko, E. V.; Rojek, A. E.; Sosnick, T. R.; Drummond, D. A. Stress-Triggered Phase Separation Is an Adaptive, Evolutionarily Tuned Response. *Cell* **2017**, *168* (6), 1028−1040.e19.
(249) Dutagaci, B.; Nawrocki, G.; Goodluck, J.; Ashkarran, A. A.; Hoogstraten, C. G.; Lapidus, L. J.; Feig, M. Charge-Driven Condensation of RNA and Proteins Suggests Broad Role of Phase Separation in Cytoplasmic Environments. *Elife* **2021**, *10*, e64004 DOI: 10.7554/eLife.64004.
(250) Bernadó, P.; Shimizu, N.; Zaccai, G.; Kamikubo, H.; Sugiyama, M. Solution Scattering Approaches to Dynamical Ordering in Biomolecular Systems. *Biochim. Biophys. Acta Gen. Subj.* **2018**, *1862* (2), 253−274.
(251) Chaudhuri, B. N. Emerging Applications of Small Angle Solution Scattering in Structural Biology. *Protein Sci.* **2015**, *24* (3), 267−276.
(252) Svergun, D. I. Small-Angle X-Ray and Neutron Scattering as a Tool for Structural Systems Biology. *Biol. Chem.* **2010**, *391* (7), 737−743.
(253) Gommes, C. J.; Jaksch, S.; Frielinghaus, H. Small-Angle Scattering for Beginners. *J. Appl. Crystallogr.* **2021**, *54* (6), 1832−1843.
(254) Kilburn, D.; Behrouzi, R.; Lee, H.-T.; Sarkar, K.; Briber, R. M.; Woodson, S. A. Entropic Stabilization of Folded RNA in Crowded Solutions Measured by SAXS. *Nucleic Acids Res.* **2016**, *44* (19), 9452−9461.
(255) He, W.; Naleem, N.; Kleiman, D.; Kirmizialtin, S. Refining the RNA Force Field with Small-Angle X-Ray Scattering of Helix-Junction-Helix RNA. *J. Phys. Chem. Lett.* **2022**, *13* (15), 3400−3408.
(256) Lapinaite, A.; Carlomagno, T.; Gabel, F. Small-Angle Neutron Scattering of RNA-Protein Complexes. *Methods Mol. Biol.* **2020**, *2113*, 165−188.
(257) Krueger, S. Small-Angle Neutron Scattering Contrast Variation Studies of Biological Complexes: Challenges and Triumphs. *Curr. Opin. Struct. Biol.* **2022**, *74*, 102375.
(258) Sasmal, D. K.; Pulido, L. E.; Kasal, S.; Huang, J. Single-Molecule Fluorescence Resonance Energy Transfer in Molecular Biology. *Nanoscale* **2016**, *8* (48), 19928−19944.
(259) Wei, M.-T.; Elbaum-Garfinkle, S.; Holehouse, A. S.; Chen, C. C.-H.; Feric, M.; Arnold, C. B.; Priestley, R. D.; Pappu, R. V.; Brangwynne, C. P. Phase Behaviour of Disordered Proteins Underlying Low Density and High Permeability of Liquid Organelles. *Nat. Chem.* **2017**, *9* (11), 1118−1125.
(260) Sekar, R. B.; Periasamy, A. Fluorescence Resonance Energy Transfer (FRET) Microscopy Imaging of Live Cell Protein Localizations. *J. Cell Biol.* **2003**, *160* (5), 629−633.
(261) Roy, R.; Hohng, S.; Ha, T. A Practical Guide to Single-Molecule FRET. *Nat. Methods* **2008**, *5* (6), 507−516.
(262) Hadzic, M. C. A. S.; Sigel, R. K. O.; Börner, R. Single-Molecule Kinetic Studies of Nucleic Acids by Förster Resonance Energy Transfer. *Methods Mol. Biol.* **2022**, *2439*, 173−190.
(263) Elson, E. L. Fluorescence Correlation Spectroscopy: Past, Present. *Future. Biophys. J.* **2011**, *101* (12), 2855−2870.
(264) Wang, Z.; Zhang, H.; Jian, L.; Ding, B.; Huang, K.; Zhang, W.; Xiao, Q.; Huang, S. Principles of Fluorescence Correlation Spectroscopy Applied to Studies of Biomolecular Liquid-Liquid Phase Separation. *Biophys Rep* **2022**, *8* (2), 100−118.
(265) Mateu-Regué, A.; Christiansen, J.; Bagger, F. O.; Hellriegel, C.; Nielsen, F. C. Unveiling mRNP Composition by Fluorescence Correlation and Cross-Correlation Spectroscopy Using Cell Lysates. *Nucleic Acids Res.* **2021**, *49* (20), No. e119.
(266) Politz, J. C.; Browne, E. S.; Wolf, D. E.; Pederson, T. Intranuclear Diffusion and Hybridization State of Oligonucleotides Measured by Fluorescence Correlation Spectroscopy in Living Cells. *Proc. Natl. Acad. Sci. U. S. A.* **1998**, *95* (11), 6043−6048.
(267) Fujita, H.; Oikawa, R.; Hayakawa, M.; Tomoike, F.; Kimura, Y.; Okuno, H.; Hatashita, Y.; Fiallos Oliveros, C.; Bito, H.; Ohshima, T.; Tsuneda, S.; Abe, H.; Inoue, T. Quantification of Native mRNA Dynamics in Living Neurons Using Fluorescence Correlation Spectroscopy and Reduction-Triggered Fluorescent Probes. *J. Biol. Chem.* **2020**, *295* (23), 7923−7940.
(268) Neuman, K. C.; Nagy, A. Single-Molecule Force Spectroscopy: Optical Tweezers, Magnetic Tweezers and Atomic Force Microscopy. *Nat. Methods* **2008**, *5* (6), 491−505.
(269) Drake, B.; Prater, C. B.; Weisenhorn, A. L.; Gould, S. A.; Albrecht, T. R.; Quate, C. F.; Cannell, D. S.; Hansma, H. G.; Hansma, P. K. Imaging Crystals, Polymers, and Processes in Water with the Atomic Force Microscope. *Science* **1989**, *243* (4898), 1586−1589.
(270) Binnig, G.; Quate, C. F.; Gerber, C. Atomic Force Microscope. *Phys. Rev. Lett.* **1986**, *56* (9), 930−933.
(271) Ando, T.; Kodera, N.; Takai, E.; Maruyama, D.; Saito, K.; Toda, A. A High-Speed Atomic Force Microscope for Studying Biological Macromolecules. *Proc. Natl. Acad. Sci. U. S. A.* **2001**, *98* (22), 12468−12472.
(272) Cordova, J. C.; Das, D. K.; Manning, H. W.; Lang, M. J. Combining Single-Molecule Manipulation and Single-Molecule Detection. *Curr. Opin. Struct. Biol.* **2014**, *28*, 142−148.
(273) Qamar, S.; Wang, G.; Randle, S. J.; Ruggeri, F. S.; Varela, J. A.; Lin, J. Q.; Phillips, E. C.; Miyashita, A.; Williams, D.; Ströhl, F.; Meadows, W.; Ferry, R.; Dardov, V. J.; Tartaglia, G. G.; Farrer, L. A.; Kaminski Schierle, G. S.; Kaminski, C. F.; Holt, C. E.; Fraser, P. E.; Schmitt-Ulms, G.; Klenerman, D.; Knowles, T.; Vendruscolo, M.; St, George-Hyslop P. FUS Phase Separation Is Modulated by a Molecular Chaperone and Methylation of Arginine Cation-π Interactions. *Cell* **2018**, *173* (3), 720−734.e15.
(274) Singatulina, A. S.; Hamon, L.; Sukhanova, M. V.; Desforges, B.; Joshi, V.; Bouhss, A.; Lavrik, O. I.; Pastré, D. PARP-1 Activation Directs

FUS to DNA Damage Sites to Form PARG-Reversible Compartments Enriched in Damaged DNA. *Cell Rep.* **2019**, *27* (6), 1809−1821.e5.
(275) Boyko, S.; Surewicz, K.; Surewicz, W. K. Regulatory Mechanisms of Tau Protein Fibrillation under the Conditions of Liquid-Liquid Phase Separation. *Proc. Natl. Acad. Sci. U. S. A.* **2020**, *117* (50), 31882−31890.
(276) Ruiz-Robles, J. F.; Longoria-Hernández, A. M.; Gerling, N.; Vazquez-Martinez, E.; Sanchez-Diaz, L. E.; Cadena-Nava, R. D.; Villagrana-Escareño, M. V.; Reynaga-Hernández, E.; Ivlev, B. I.; Ruiz-Garcia, J. Spontaneous Condensation of RNA into Nanoring and Globular Structures. *ACS Omega* **2022**, *7* (18), 15404−15410.
(277) Sajja, S.; Chandler, M.; Fedorov, D.; Kasprzak, W. K.; Lushnikov, A.; Viard, M.; Shah, A.; Dang, D.; Dahl, J.; Worku, B.; Dobrovolskaia, M. A.; Krasnoslobodtsev, A.; Shapiro, B. A.; Afonin, K. A. Dynamic Behavior of RNA Nanoparticles Analyzed by AFM on a Mica/Air Interface. *Langmuir* **2018**, *34* (49), 15099−15108.
(278) Orlova, E. V.; Saibil, H. R. Structural Analysis of Macromolecular Assemblies by Electron Microscopy. *Chem. Rev.* **2011**, *111* (12), 7710−7748.
(279) Kato, M.; Han, T. W.; Xie, S.; Shi, K.; Du, X.; Wu, L. C.; Mirzaei, H.; Goldsmith, E. J.; Longgood, J.; Pei, J.; Grishin, N. V.; Frantz, D. E.; Schneider, J. W.; Chen, S.; Li, L.; Sawaya, M. R.; Eisenberg, D.; Tycko, R.; McKnight, S. L. Cell-Free Formation of RNA Granules: Low Complexity Sequence Domains Form Dynamic Fibers within Hydrogels. *Cell* **2012**, *149* (4), 753−767.
(280) Lin, Y.; Mori, E.; Kato, M.; Xiang, S.; Wu, L.; Kwon, I.; McKnight, S. L. Toxic PR Poly-Dipeptides Encoded by the C9orf72 Repeat Expansion Target LC Domain Polymers. *Cell* **2016**, *167* (3), 789−802.e12.
(281) Souquere, S.; Weil, D.; Pierron, G. Comparative Ultrastructure of CRM1-Nucleolar Bodies (CNoBs), Intranucleolar Bodies (INBs) and Hybrid PML/p62 Bodies Uncovers New Facets of Nuclear Body Dynamic and Diversity. *Nucleus* **2015**, *6* (4), 326−338.
(282) Bazett-Jones, D. P.; Hendzel, M. J. Electron Spectroscopic Imaging of Chromatin. *Methods* **1999**, *17* (2), 188−200.
(283) Gall, J. G.; Bellini, M.; Wu, Z.; Murphy, C. Assembly of the Nuclear Transcription and Processing Machinery: Cajal Bodies (coiled Bodies) and Transcriptosomes. *Mol. Biol. Cell* **1999**, *10* (12), 4385−4402.
(284) Bounedjah, O.; Desforges, B.; Wu, T.-D.; Pioche-Durieu, C.; Marco, S.; Hamon, L.; Curmi, P. A.; Guerquin-Kern, J.-L.; Piétrement, O.; Pastré, D. Free mRNA in Excess upon Polysome Dissociation Is a Scaffold for Protein Multimerization to Form Stress Granules. *Nucleic Acids Res.* **2014**, *42* (13), 8678−8691.
(285) Souquere, S.; Mollet, S.; Kress, M.; Dautry, F.; Pierron, G.; Weil, D. Unravelling the Ultrastructure of Stress Granules and Associated P-Bodies in Human Cells. *J. Cell Sci.* **2009**, *122* (20), 3619−3626.
(286) de Boer, P.; Hoogenboom, J. P.; Giepmans, B. N. G. Correlated Light and Electron Microscopy: Ultrastructure Lights Up! *Nat. Methods* **2015**, *12* (6), 503−513.
(287) Normand, C.; Berthaud, M.; Gadal, O.; Léger-Silvestre, I. Correlative Light and Electron Microscopy of Nucleolar Transcription in Saccharomyces Cerevisiae. *Methods Mol. Biol.* **2016**, *1455*, 29−40.
(288) Tchelidze, P.; Benassarou, A.; Kaplan, H.; O'Donohue, M.-F.; Lucas, L.; Terryn, C.; Rusishvili, L.; Mosidze, G.; Lalun, N.; Ploton, D. Nucleolar Sub-Compartments in Motion during rRNA Synthesis Inhibition: Contraction of Nucleolar Condensed Chromatin and Gathering of Fibrillar Centers Are Concomitant. *PLoS One* **2017**, *12* (11), No. e0187977.
(289) Oberti, D.; Biasini, A.; Kirschmann, M. A.; Genoud, C.; Stunnenberg, R.; Shimada, Y.; Bühler, M. Dicer and Hsp104 Function in a Negative Feedback Loop to Confer Robustness to Environmental Stress. *Cell Rep.* **2015**, *10* (1), 47−61.
(290) Liu, S.; Hoess, P.; Ries, J. Super-Resolution Microscopy for Structural Cell Biology. *Annu. Rev. Biophys.* **2022**, *51*, 301−326.
(291) Vicidomini, G.; Bianchini, P.; Diaspro, A. STED Super-Resolved Microscopy. *Nat. Methods* **2018**, *15* (3), 173−182.
(292) Yang, Z.; Sharma, A.; Qi, J.; Peng, X.; Lee, D. Y.; Hu, R.; Lin, D.; Qu, J.; Kim, J. S. Super-Resolution Fluorescent Materials: An Insight into Design and Bioimaging Applications. *Chem. Soc. Rev.* **2016**, *45* (17), 4651−4667.
(293) Steffens, H.; Wegner, W.; Willig, K. I. In Vivo STED Microscopy: A Roadmap to Nanoscale Imaging in the Living Mouse. *Methods* **2020**, *174*, 42−48.
(294) Spahn, C.; Grimm, J. B.; Lavis, L. D.; Lampe, M.; Heilemann, M. Whole-Cell, 3D, and Multicolor STED Imaging with Exchangeable Fluorophores. *Nano Lett.* **2019**, *19* (1), 500−505.
(295) Sydor, A. M.; Czymmek, K. J.; Puchner, E. M.; Mennella, V. Super-Resolution Microscopy: From Single Molecules to Supramolecular Assemblies. *Trends Cell Biol.* **2015**, *25* (12), 730−748.
(296) Ha, T.; Tinnefeld, P. Photophysics of Fluorescent Probes for Single-Molecule Biophysics and Super-Resolution Imaging. *Annu. Rev. Phys. Chem.* **2012**, *63*, 595−617.
(297) Jain, S.; Wheeler, J. R.; Walters, R. W.; Agrawal, A.; Barsic, A.; Parker, R. ATPase-Modulated Stress Granules Contain a Diverse Proteome and Substructure. *Cell* **2016**, *164* (3), 487−498.
(298) Tingey, M.; Schnell, S. J.; Yu, W.; Saredy, J.; Junod, S.; Patel, D.; Alkurdi, A. A.; Yang, W. Technologies Enabling Single-Molecule Super-Resolution Imaging of mRNA. *Cells* **2022**, *11* (19), 3079.
(299) Liu, Z.; Xing, D.; Su, Q. P.; Zhu, Y.; Zhang, J.; Kong, X.; Xue, B.; Wang, S.; Sun, H.; Tao, Y.; Sun, Y. Super-Resolution Imaging and Tracking of Protein-Protein Interactions in Sub-Diffraction Cellular Space. *Nat. Commun.* **2014**, *5*, 4443.
(300) Van Treeck, B.; Parker, R. Principles of Stress Granules Revealed by Imaging Approaches. *Cold Spring Harb. Perspect. Biol.* **2019**, *11* (2), a033068.
(301) Sunwoo, H.; Wu, J. Y.; Lee, J. T. The Xist RNA-PRC2 Complex at 20-Nm Resolution Reveals a Low Xist Stoichiometry and Suggests a Hit-and-Run Mechanism in Mouse Cells. *Proc. Natl. Acad. Sci. U. S. A.* **2015**, *112* (31), E4216−E4225.
(302) Ramanathan, M.; Porter, D. F.; Khavari, P. A. Methods to Study RNA-Protein Interactions. *Nat. Methods* **2019**, *16* (3), 225−234.
(303) Marchese, D.; de Groot, N. S.; Lorenzo Gotor, N.; Livi, C. M.; Tartaglia, G. G. Advances in the Characterization of RNA-Binding Proteins. *Wiley Interdiscip. Rev. RNA* **2016**, *7* (6), 793−810.
(304) Young, A. P.; Jackson, D. J.; Wyeth, R. C. A Technical Review and Guide to RNA Fluorescence in Situ Hybridization. *PeerJ.* **2020**, *8*, No. e8806.
(305) Pardue, M. L.; Gall, J. G. Molecular Hybridization of Radioactive DNA to the DNA of Cytological Preparations. *Proc. Natl. Acad. Sci. U. S. A.* **1969**, *64* (2), 600−604.
(306) Rudkin, G. T.; Stollar, B. D. High Resolution Detection of DNA-RNA Hybrids in Situ by Indirect Immunofluorescence. *Nature* **1977**, *265* (5593), 472−473.
(307) Singer, R. H.; Ward, D. C. Actin Gene Expression Visualized in Chicken Muscle Tissue Culture by Using in Situ Hybridization with a Biotinated Nucleotide Analog. *Proc. Natl. Acad. Sci. U. S. A.* **1982**, *79* (23), 7331−7335.
(308) Femino, A. M.; Fay, F. S.; Fogarty, K.; Singer, R. H. Visualization of Single RNA Transcripts in Situ. *Science* **1998**, *280* (5363), 585−590.
(309) Kucho, K.-I.; Yoneda, H.; Harada, M.; Ishiura, M. Determinants of Sensitivity and Specificity in Spotted DNA Microarrays with Unmodified Oligonucleotides. *Genes Genet. Syst.* **2004**, *79* (4), 189−197.
(310) Chong, S.; Graham, T. G. W.; Dugast-Darzacq, C.; Dailey, G. M.; Darzacq, X.; Tjian, R. Tuning Levels of Low-Complexity Domain Interactions to Modulate Endogenous Oncogenic Transcription. *Mol. Cell* **2022**, *82* (11), 2084−2097.e5.
(311) Xing, Z.; Xue, J.; Ma, X.; Han, C.; Wang, Z.; Luo, S.; Wang, C.; Dong, L.; Zhang, J. Intracellular mRNA Phase Separation Induced by Cationic Polymers for Tumor Immunotherapy. *J. Nanobiotechnology* **2022**, *20* (1), 442.
(312) Cochard, A.; Garcia-Jove Navarro, M.; Piroska, L.; Kashida, S.; Kress, M.; Weil, D.; Gueroui, Z. RNA at the Surface of Phase-Separated Condensates Impacts Their Size and Number. *Biophys. J.* **2022**, *121* (9), 1675−1690.

https://doi.org/10.1021/acs.chemrev.3c00575
Chem. Rev. XXXX, XXX, XXX−XXX

(313) Andersen, J. S.; Lam, Y. W.; Leung, A. K. L.; Ong, S.-E.; Lyon, C. E.; Lamond, A. I.; Mann, M. Nucleolar Proteome Dynamics. *Nature* **2005**, *433* (7021), 77−83.
(314) Sanz, E.; Yang, L.; Su, T.; Morris, D. R.; McKnight, G. S.; Amieux, P. S. Cell-Type-Specific Isolation of Ribosome-Associated mRNA from Complex Tissues. *Proc. Natl. Acad. Sci. U. S. A.* **2009**, *106* (33), 13939−13944.
(315) Shaalan, A. K.; Ellison-Hughes, G. M. A Protocol for Extracting Immunolabeled Murine Cardiomyocytes of High-Quality RNA by Laser Capture Microdissection. *STAR Protoc* **2022**, *3* (1), 101231.
(316) Li, W.; Jiang, C.; Zhang, E. Advances in the Phase Separation-Organized Membraneless Organelles in Cells: A Narrative Review. *Transl. Cancer Res.* **2021**, *10* (11), 4929−4946.
(317) Pina, A. S.; Batalha, Í. L.; Dias, A. M. G. C.; Roque, A. C. A. Affinity Tags in Protein Purification and Peptide Enrichment: An Overview. *Methods Mol. Biol.* **2021**, *2178*, 107−132.
(318) Srisawat, C.; Goldstein, I. J.; Engelke, D. R. Sephadex-Binding RNA Ligands: Rapid Affinity Purification of RNA from Complex RNA Mixtures. *Nucleic Acids Res.* **2001**, *29* (2), E4.
(319) Sil, S.; Keegan, S.; Ettefa, F.; Denes, L. T.; Boeke, J. D.; Holt, L. J. Condensation of LINE-1 Is Critical for Retrotransposition. *Elife* **2023**, *12*, e82991 DOI: 10.7554/eLife.82991.
(320) Aznaourova, M.; Schmerer, N.; Schmeck, B.; Schulte, L. N. Disease-Causing Mutations and Rearrangements in Long Non-Coding RNA Gene Loci. *Front. Genet.* **2020**, *11*, 527484.
(321) Srisawat, C.; Engelke, D. R. RNA Affinity Tags for Purification of RNAs and Ribonucleoprotein Complexes. *Methods* **2002**, *26* (2), 156−161.
(322) Fox, A. H.; Nakagawa, S.; Hirose, T.; Bond, C. S. Paraspeckles: Where Long Noncoding RNA Meets Phase Separation. *Trends Biochem. Sci.* **2018**, *43* (2), 124−135.
(323) Sasaki, Y. T. F.; Ideue, T.; Sano, M.; Mituyama, T.; Hirose, T. MENepsilon/beta Noncoding RNAs Are Essential for Structural Integrity of Nuclear Paraspeckles. *Proc. Natl. Acad. Sci. U. S. A.* **2009**, *106* (8), 2525−2530.
(324) Mao, Y. S.; Sunwoo, H.; Zhang, B.; Spector, D. L. Direct Visualization of the Co-Transcriptional Assembly of a Nuclear Body by Noncoding RNAs. *Nat. Cell Biol.* **2011**, *13* (1), 95−101.
(325) Chujo, T.; Yamazaki, T.; Kawaguchi, T.; Kurosaka, S.; Takumi, T.; Nakagawa, S.; Hirose, T. Unusual Semi-Extractability as a Hallmark of Nuclear Body-Associated Architectural Noncoding RNAs. *EMBO J.* **2017**, *36* (10), 1447−1462.
(326) Mito, M.; Kawaguchi, T.; Hirose, T.; Nakagawa, S. Simultaneous Multicolor Detection of RNA and Proteins Using Super-Resolution Microscopy. *Methods* **2016**, *98*, 158−165.
(327) Naganuma, T.; Hirose, T. Paraspeckle Formation during the Biogenesis of Long Non-Coding RNAs. *RNA Biol.* **2013**, *10* (3), 456−461.
(328) Kawaguchi, T.; Tanigawa, A.; Naganuma, T.; Ohkawa, Y.; Souquere, S.; Pierron, G.; Hirose, T. SWI/SNF Chromatin-Remodeling Complexes Function in Noncoding RNA-Dependent Assembly of Nuclear Bodies. *Proc. Natl. Acad. Sci. U. S. A.* **2015**, *112* (14), 4304−4309.
(329) Souquere, S.; Beauclair, G.; Harper, F.; Fox, A.; Pierron, G. Highly Ordered Spatial Organization of the Structural Long Noncoding NEAT1 RNAs within Paraspeckle Nuclear Bodies. *Mol. Biol. Cell* **2010**, *21* (22), 4020−4027.
(330) West, J. A.; Mito, M.; Kurosaka, S.; Takumi, T.; Tanegashima, C.; Chujo, T.; Yanaka, K.; Kingston, R. E.; Hirose, T.; Bond, C.; Fox, A.; Nakagawa, S. Structural, Super-Resolution Microscopy Analysis of Paraspeckle Nuclear Body Organization. *J. Cell Biol.* **2016**, *214* (7), 817−830.
(331) Yamazaki, T.; Souquere, S.; Chujo, T.; Kobelke, S.; Chong, Y. S.; Fox, A. H.; Bond, C. S.; Nakagawa, S.; Pierron, G.; Hirose, T. Functional Domains of NEAT1 Architectural lncRNA Induce Paraspeckle Assembly through Phase Separation. *Mol. Cell* **2018**, *70* (6), 1038−1053.e7.
(332) Tycowski, K. T.; Shu, M.-D.; Borah, S.; Shi, M.; Steitz, J. A. Conservation of a Triple-Helix-Forming RNA Stability Element in Noncoding and Genomic RNAs of Diverse Viruses. *Cell Rep.* **2012**, *2* (1), 26−32.
(333) Knott, G. J.; Bond, C. S.; Fox, A. H. The DBHS Proteins SFPQ, NONO and PSPC1: A Multipurpose Molecular Scaffold. *Nucleic Acids Res.* **2016**, *44* (9), 3989−4004.
(334) Uversky, V. N. Recent Developments in the Field of Intrinsically Disordered Proteins: Intrinsic Disorder-Based Emergence in Cellular Biology in Light of the Physiological and Pathological Liquid-Liquid Phase Transitions. *Annu. Rev. Biophys.* **2021**, *50*, 135−156.
(335) Hennig, S.; Kong, G.; Mannen, T.; Sadowska, A.; Kobelke, S.; Blythe, A.; Knott, G. J.; Iyer, K. S.; Ho, D.; Newcombe, E. A.; Hosoki, K.; Goshima, N.; Kawaguchi, T.; Hatters, D.; Trinkle-Mulcahy, L.; Hirose, T.; Bond, C. S.; Fox, A. H. Prion-like Domains in RNA Binding Proteins Are Essential for Building Subnuclear Paraspeckles. *J. Cell Biol.* **2015**, *210* (4), 529−539.
(336) Mai, Y.; Eisenberg, A. Self-Assembly of Block Copolymers. *Chem. Soc. Rev.* **2012**, *41* (18), 5969−5985.
(337) Moughton, A. O.; Hillmyer, M. A.; Lodge, T. P. Multicompartment Block Polymer Micelles. *Macromolecules* **2012**, *45* (1), 2−19.
(338) Yamazaki, T.; Yamamoto, T.; Yoshino, H.; Souquere, S.; Nakagawa, S.; Pierron, G.; Hirose, T. Paraspeckles Are Constructed as Block Copolymer Micelles. *EMBO J.* **2021**, *40* (12), No. e107270.
(339) Passon, D. M.; Lee, M.; Rackham, O.; Stanley, W. A.; Sadowska, A.; Filipovska, A.; Fox, A. H.; Bond, C. S. Structure of the Heterodimer of Human NONO and Paraspeckle Protein Component 1 and Analysis of Its Role in Subnuclear Body Formation. *Proc. Natl. Acad. Sci. U. S. A.* **2012**, *109* (13), 4846−4850.
(340) Jacobson, E. C.; Pandya-Jones, A.; Plath, K. A Lifelong Duty: How Xist Maintains the Inactive X Chromosome. *Curr. Opin. Genet. Dev.* **2022**, *75*, 101927.
(341) Sahakyan, A.; Yang, Y.; Plath, K. The Role of Xist in X-Chromosome Dosage Compensation. *Trends Cell Biol.* **2018**, *28* (12), 999−1013.
(342) Pintacuda, G.; Cerase, A. X Inactivation Lessons from Differentiating Mouse Embryonic Stem Cells. *Stem Cell Rev. Rep* **2015**, *11* (5), 699−705.
(343) Brockdorff, N.; Bowness, J. S.; Wei, G. Progress toward Understanding Chromosome Silencing by Xist RNA. *Genes Dev.* **2020**, *34* (11−12), 733−744.
(344) Engreitz, J. M.; Pandya-Jones, A.; McDonel, P.; Shishkin, A.; Sirokman, K.; Surka, C.; Kadri, S.; Xing, J.; Goren, A.; Lander, E. S.; Plath, K.; Guttman, M. The Xist lncRNA Exploits Three-Dimensional Genome Architecture to Spread across the X Chromosome. *Science* **2013**, *341* (6147), 1237973.
(345) Cerase, A.; Pintacuda, G.; Tattermusch, A.; Avner, P. Xist Localization and Function: New Insights from Multiple Levels. *Genome Biol.* **2015**, *16* (1), 166.
(346) Robert Finestra, T.; Gribnau, J. X Chromosome Inactivation: Silencing, Topology and Reactivation. *Curr. Opin. Cell Biol.* **2017**, *46*, 54−61.
(347) Mira-Bontenbal, H.; Gribnau, J. New Xist-Interacting Proteins in X-Chromosome Inactivation. *Curr. Biol.* **2016**, *26* (8), R338−R342.
(348) Borsani, G.; Tonlorenzi, R.; Simmler, M. C.; Dandolo, L.; Arnaud, D.; Capra, V.; Grompe, M.; Pizzuti, A.; Muzny, D.; Lawrence, C.; Willard, H. F.; Avner, P.; Ballabio, A. Characterization of a Murine Gene Expressed from the Inactive X Chromosome. *Nature* **1991**, *351* (6324), 325−329.
(349) Brown, C. J.; Ballabio, A.; Rupert, J. L.; Lafreniere, R. G.; Grompe, M.; Tonlorenzi, R.; Willard, H. F. A Gene from the Region of the Human X Inactivation Centre Is Expressed Exclusively from the Inactive X Chromosome. *Nature* **1991**, *349* (6304), 38−44.
(350) Ballabio, A.; Willard, H. F. Mammalian X-Chromosome Inactivation and the XIST Gene. *Curr. Opin. Genet. Dev.* **1992**, *2* (3), 439−447.
(351) Pintacuda, G.; Young, A. N.; Cerase, A. Function by Structure: Spotlights on Xist Long Non-Coding RNA. *Front Mol. Biosci* **2017**, *4*, 90.
(352) Cerase, A.; Tartaglia, G. G. Long Non-Coding RNA-Polycomb Intimate Rendezvous. *Open Biol.* **2020**, *10* (9), 200126.

https://doi.org/10.1021/acs.chemrev.3c00575
Chem. Rev. XXXX, XXX, XXX−XXX

(353) Wutz, A.; Rasmussen, T. P.; Jaenisch, R. Chromosomal Silencing and Localization Are Mediated by Different Domains of Xist RNA. *Nat. Genet.* **2002**, *30* (2), 167−174.
(354) McHugh, C. A.; Chen, C.-K.; Chow, A.; Surka, C. F.; Tran, C.; McDonel, P.; Pandya-Jones, A.; Blanco, M.; Burghard, C.; Moradian, A.; Sweredoski, M. J.; Shishkin, A. A.; Su, J.; Lander, E. S.; Hess, S.; Plath, K.; Guttman, M. The Xist lncRNA Interacts Directly with SHARP to Silence Transcription through HDAC3. *Nature* **2015**, *521* (7551), 232−236.
(355) Chu, C.; Zhang, Q. C.; da Rocha, S. T.; Flynn, R. A.; Bharadwaj, M.; Calabrese, J. M.; Magnuson, T.; Heard, E.; Chang, H. Y. Systematic Discovery of Xist RNA Binding Proteins. *Cell* **2015**, *161* (2), 404−416.
(356) Monfort, A.; Di Minin, G.; Wutz, A. Screening for Factors Involved in X Chromosome Inactivation Using Haploid ESCs. *Methods Mol. Biol.* **2018**, *1861*, 1−18.
(357) Dossin, F.; Pinheiro, I.; Żylicz, J. J.; Roensch, J.; Collombet, S.; Le Saux, A.; Chelmicki, T.; Attia, M.; Kapoor, V.; Zhan, Y.; Dingli, F.; Loew, D.; Mercher, T.; Dekker, J.; Heard, E. SPEN Integrates Transcriptional and Epigenetic Control of X-Inactivation. *Nature* **2020**, *578* (7795), 455−460.
(358) Cerase, A.; Young, A. N.; Ruiz, N. B.; Buness, A.; Sant, G. M.; Arnold, M.; Di Giacomo, M.; Ascolani, M.; Kumar, M.; Hierholzer, A.; Trigiante, G.; Marzi, S. J.; Avner, P. Chd8 Regulates X Chromosome Inactivation in Mouse through Fine-Tuning Control of Xist Expression. *Commun. Biol.* **2021**, *4* (1), 485.
(359) Jachowicz, J. W.; Strehle, M.; Banerjee, A. K.; Blanco, M. R.; Thai, J.; Guttman, M. Xist Spatially Amplifies SHARP/SPEN Recruitment to Balance Chromosome-Wide Silencing and Specificity to the X Chromosome. *Nat. Struct. Mol. Biol.* **2022**, *29* (3), 239−249.
(360) Patil, D. P.; Chen, C.-K.; Pickering, B. F.; Chow, A.; Jackson, C.; Guttman, M.; Jaffrey, S. R. m(6)A RNA Methylation Promotes XIST-Mediated Transcriptional Repression. *Nature* **2016**, *537* (7620), 369−373.
(361) Nesterova, T. B.; Wei, G.; Coker, H.; Pintacuda, G.; Bowness, J. S.; Zhang, T.; Almeida, M.; Bloechl, B.; Moindrot, B.; Carter, E. J.; Alvarez Rodrigo, I.; Pan, Q.; Bi, Y.; Song, C.-X.; Brockdorff, N. Systematic Allelic Analysis Defines the Interplay of Key Pathways in X Chromosome Inactivation. *Nat. Commun.* **2019**, *10* (1), 3129.
(362) da Rocha, S. T.; Boeva, V.; Escamilla-Del-Arenal, M.; Ancelin, K.; Granier, C.; Matias, N. R.; Sanulli, S.; Chow, J.; Schulz, E.; Picard, C.; Kaneko, S.; Helin, K.; Reinberg, D.; Stewart, A. F.; Wutz, A.; Margueron, R.; Heard, E. Jarid2 Is Implicated in the Initial Xist-Induced Targeting of PRC2 to the Inactive X Chromosome. *Mol. Cell* **2014**, *53* (2), 301−316.
(363) Jansz, N.; Nesterova, T.; Keniry, A.; Iminitoff, M.; Hickey, P. F.; Pintacuda, G.; Masui, O.; Kobelke, S.; Geoghegan, N.; Breslin, K. A.; Willson, T. A.; Rogers, K.; Kay, G. F.; Fox, A. H.; Koseki, H.; Brockdorff, N.; Murphy, J. M.; Blewitt, M. E. Smchd1 Targeting to the Inactive X Is Dependent on the Xist-HnrnpK-PRC1 Pathway. *Cell Rep.* **2018**, *25* (7), 1912−1923.e9.
(364) Blewitt, M. E.; Gendrel, A.-V.; Pang, Z.; Sparrow, D. B.; Whitelaw, N.; Craig, J. M.; Apedaile, A.; Hilton, D. J.; Dunwoodie, S. L.; Brockdorff, N.; Kay, G. F.; Whitelaw, E. SmcHD1, Containing a Structural-Maintenance-of-Chromosomes Hinge Domain, Has a Critical Role in X Inactivation. *Nat. Genet.* **2008**, *40* (5), 663−669.
(365) Wang, C.-Y.; Colognori, D.; Sunwoo, H.; Wang, D.; Lee, J. T. PRC1 Collaborates with SMCHD1 to Fold the X-Chromosome and Spread Xist RNA between Chromosome Compartments. *Nat. Commun.* **2019**, *10* (1), 2950.
(366) Ridings-Figueroa, R.; Stewart, E. R.; Nesterova, T. B.; Coker, H.; Pintacuda, G.; Godwin, J.; Wilson, R.; Haslam, A.; Lilley, F.; Ruigrok, R.; Bageghni, S. A.; Albadrani, G.; Mansfield, W.; Roulson, J.-A.; Brockdorff, N.; Ainscough, J. F. X.; Coverley, D. The Nuclear Matrix Protein CIZ1 Facilitates Localization of Xist RNA to the Inactive X-Chromosome Territory. *Genes Dev.* **2017**, *31* (9), 876−888.
(367) Markaki, Y.; Chong, J. G.; Wang, Y.; Jacobson, E. C.; Luong, C.; Tan, S. Y. X.; Jachowicz, J. W.; Strehle, M.; Maestrini, D.; Banerjee, A. K.; Mistry, B. A.; Dror, I.; Dossin, F.; Schöneberg, J.; Heard, E.; Guttman, M.; Chou, T.; Plath, K. Xist Nucleates Local Protein Gradients to Propagate Silencing across the X Chromosome. *Cell* **2021**, *184* (25), 6212.
(368) Rodermund, L.; Coker, H.; Oldenkamp, R.; Wei, G.; Bowness, J.; Rajkumar, B.; Nesterova, T.; Susano Pinto, D. M.; Schermelleh, L.; Brockdorff, N. Time-Resolved Structured Illumination Microscopy Reveals Key Principles of Xist RNA Spreading. *Science* **2021**, *372* (6547), eabe7500 DOI: 10.1126/science.abe7500.
(369) Csankovszki, G.; Nagy, A.; Jaenisch, R. Synergism of Xist RNA, DNA Methylation, and Histone Hypoacetylation in Maintaining X Chromosome Inactivation. *J. Cell Biol.* **2001**, *153* (4), 773−784.
(370) Lu, Z.; Guo, J. K.; Wei, Y.; Dou, D. R.; Zarnegar, B.; Ma, Q.; Li, R.; Zhao, Y.; Liu, F.; Choudhry, H.; Khavari, P. A.; Chang, H. Y. Structural Modularity of the XIST Ribonucleoprotein Complex. *Nat. Commun.* **2020**, *11* (1), 6163.
(371) Lin, Y.; Protter, D. S. W.; Rosen, M. K.; Parker, R. Formation and Maturation of Phase-Separated Liquid Droplets by RNA-Binding Proteins. *Mol. Cell* **2015**, *60* (2), 208−219.
(372) Carey, J. L.; Guo, L. Liquid-Liquid Phase Separation of TDP-43 and FUS in Physiology and Pathology of Neurodegenerative Diseases. *Front Mol. Biosci* **2022**, *9*, 826719.
(373) Sofi, S.; Williamson, L.; Turvey, G. L.; Scoynes, C.; Hirst, C.; Godwin, J.; Brockdorff, N.; Ainscough, J.; Coverley, D. Prion-like Domains Drive CIZ1 Assembly Formation at the Inactive X Chromosome. *J. Cell Biol.* **2022**, *221* (4), e202103185 DOI: 10.1083/jcb.202103185.
(374) Loda, A.; Collombet, S.; Heard, E. Gene Regulation in Time and Space during X-Chromosome Inactivation. *Nat. Rev. Mol. Cell Biol.* **2022**, *23* (4), 231−249.
(375) Almeida, M.; Pintacuda, G.; Masui, O.; Koseki, Y.; Gdula, M.; Cerase, A.; Brown, D.; Mould, A.; Innocent, C.; Nakayama, M.; Schermelleh, L.; Nesterova, T. B.; Koseki, H.; Brockdorff, N. PCGF3/5-PRC1 Initiates Polycomb Recruitment in X Chromosome Inactivation. *Science* **2017**, *356* (6342), 1081−1084.
(376) Smeets, D.; Markaki, Y.; Schmid, V. J.; Kraus, F.; Tattermusch, A.; Cerase, A.; Sterr, M.; Fiedler, S.; Demmerle, J.; Popken, J.; Leonhardt, H.; Brockdorff, N.; Cremer, T.; Schermelleh, L.; Cremer, M. Three-Dimensional Super-Resolution Microscopy of the Inactive X Chromosome Territory Reveals a Collapse of Its Active Nuclear Compartment Harboring Distinct Xist RNA Foci. *Epigenetics Chromatin* **2014**, *7*, 8.
(377) Cerase, A.; Smeets, D.; Tang, Y. A.; Gdula, M.; Kraus, F.; Spivakov, M.; Moindrot, B.; Leleu, M.; Tattermusch, A.; Demmerle, J.; Nesterova, T. B.; Green, C.; Otte, A. P.; Schermelleh, L.; Brockdorff, N. Spatial Separation of Xist RNA and Polycomb Proteins Revealed by Superresolution Microscopy. *Proc. Natl. Acad. Sci. U. S. A.* **2014**, *111* (6), 2235−2240.
(378) Hasegawa, Y.; Brockdorff, N.; Kawano, S.; Tsutui, K.; Tsutui, K.; Nakagawa, S. The Matrix Protein hnRNP U Is Required for Chromosomal Localization of Xist RNA. *Dev. Cell* **2010**, *19* (3), 469−476.
(379) Ng, K.; Daigle, N.; Bancaud, A.; Ohhata, T.; Humphreys, P.; Walker, R.; Ellenberg, J.; Wutz, A. A System for Imaging the Regulatory Noncoding Xist RNA in Living Mouse Embryonic Stem Cells. *Mol. Biol. Cell* **2011**, *22* (14), 2634−2645.
(380) Chow, J. C.; Ciaudo, C.; Fazzari, M. J.; Mise, N.; Servant, N.; Glass, J. L.; Attreed, M.; Avner, P.; Wutz, A.; Barillot, E.; Greally, J. M.; Voinnet, O.; Heard, E. LINE-1 Activity in Facultative Heterochromatin Formation during X Chromosome Inactivation. *Cell* **2010**, *141* (6), 956−969.
(381) Banani, S. F.; Lee, H. O.; Hyman, A. A.; Rosen, M. K. Biomolecular Condensates: Organizers of Cellular Biochemistry. *Nat. Rev. Mol. Cell Biol.* **2017**, *18* (5), 285−298.
(382) Cerase, A.; Calabrese, J. M.; Tartaglia, G. G. Phase Separation Drives X-Chromosome Inactivation. *Nat. Struct. Mol. Biol.* **2022**, *29* (3), 183−185.
(383) Moindrot, B.; Cerase, A.; Coker, H.; Masui, O.; Grijzenhout, A.; Pintacuda, G.; Schermelleh, L.; Nesterova, T. B.; Brockdorff, N. A Pooled shRNA Screen Identifies Rbm15, Spen, and Wtap as Factors

Required for Xist RNA-Mediated Silencing. *Cell Rep.* **2015**, *12* (4), 562−572.
(384) Zacco, E.; Graña-Montes, R.; Martin, S. R.; de Groot, N. S.; Alfano, C.; Tartaglia, G. G.; Pastore, A. RNA as a Key Factor in Driving or Preventing Self-Assembly of the TAR DNA-Binding Protein 43. *J. Mol. Biol.* **2019**, *431* (8), 1671−1688.
(385) Jones, A. N.; Sattler, M. Challenges and Perspectives for Structural Biology of lncRNAs-the Example of the Xist lncRNA A-Repeats. *J. Mol. Cell Biol.* **2019**, *11* (10), 845−859.
(386) Duszczyk, M. M.; Sattler, M. ^{1}H, ^{13}C, ^{15}N and ^{31}P Chemical Shift Assignments of a Human Xist RNA A-Repeat Tetraloop Hairpin Essential for X-Chromosome Inactivation. *Biomol. NMR Assign.* **2012**, *6* (1), 75−77.
(387) Duszczyk, M. M.; Wutz, A.; Rybin, V.; Sattler, M. The Xist RNA A-Repeat Comprises a Novel AUCG Tetraloop Fold and a Platform for Multimerization. *RNA* **2011**, *17* (11), 1973−1982.
(388) Fang, R.; Moss, W. N.; Rutenberg-Schoenberg, M.; Simon, M. D. Probing Xist RNA Structure in Cells Using Targeted Structure-Seq. *PLoS Genet.* **2015**, *11* (12), No. e1005668.
(389) Maenner, S.; Blaud, M.; Fouillen, L.; Savoye, A.; Marchand, V.; Dubois, A.; Sanglier-Cianférani, S.; Van Dorsselaer, A.; Clerc, P.; Avner, P.; Visvikis, A.; Branlant, C. 2-D Structure of the A Region of Xist RNA and Its Implication for PRC2 Association. *PLoS Biol.* **2010**, *8* (1), No. e1000276.
(390) Smola, M. J.; Christy, T. W.; Inoue, K.; Nicholson, C. O.; Friedersdorf, M.; Keene, J. D.; Lee, D. M.; Calabrese, J. M.; Weeks, K. M. SHAPE Reveals Transcript-Wide Interactions, Complex Structural Domains, and Protein Interactions across the Xist lncRNA in Living Cells. *Proc. Natl. Acad. Sci. U. S. A.* **2016**, *113* (37), 10322−10327.
(391) Johnson, B. S.; Snead, D.; Lee, J. J.; McCaffery, J. M.; Shorter, J.; Gitler, A. D. TDP-43 Is Intrinsically Aggregation-Prone, and Amyotrophic Lateral Sclerosis-Linked Mutations Accelerate Aggregation and Increase Toxicity. *J. Biol. Chem.* **2009**, *284* (30), 20329−20339.
(392) Stofer, E.; Chipot, C.; Lavery, R. Free Energy Calculations of Watson−Crick Base Pairing in Aqueous Solution. *J. Am. Chem. Soc.* **1999**, *121* (41), 9503−9508.
(393) Sponer, J.; Sponer, J. E.; Mládek, A.; Jurečka, P.; Banáš, P.; Otyepka, M. Nature and Magnitude of Aromatic Base Stacking in DNA and RNA: Quantum Chemistry, Molecular Mechanics, and Experiment. *Biopolymers* **2013**, *99* (12), 978−988.
(394) Chawla, M.; Chermak, E.; Zhang, Q.; Bujnicki, J. M.; Oliva, R.; Cavallo, L. Occurrence and Stability of Lone Pair-π Stacking Interactions between Ribose and Nucleobases in Functional RNAs. *Nucleic Acids Res.* **2017**, *45* (19), 11019−11032.
(395) Deng, J.-H.; Luo, J.; Mao, Y.-L.; Lai, S.; Gong, Y.-N.; Zhong, D.-C.; Lu, T.-B. π-π Stacking Interactions: Non-Negligible Forces for Stabilizing Porous Supramolecular Frameworks. *Sci. Adv.* **2020**, *6* (2), No. eaax9976.
(396) Sivasakthi, V.; Anbarasu, A.; Ramaiah, S. π-π Interactions in Structural Stability: Role in RNA Binding Proteins. *Cell Biochem. Biophys.* **2013**, *67* (3), 853−863.
(397) Cirillo, D.; Blanco, M.; Armaos, A.; Buness, A.; Avner, P.; Guttman, M.; Cerase, A.; Tartaglia, G. G. Quantitative Predictions of Protein Interactions with Long Noncoding RNAs. *Nat. Methods* **2017**, *14* (1), 5−6.
(398) Trigiante, G.; Blanes Ruiz, N.; Cerase, A. Emerging Roles of Repetitive and Repeat-Containing RNA in Nuclear and Chromatin Organization and Gene Expression. *Front Cell Dev Biol.* **2021**, *9*, 735527.
(399) Draper, D. E. A Guide to Ions and RNA Structure. *RNA* **2004**, *10* (3), 335−343.
(400) Hou, Q.; Jaffrey, S. R. Synthetic Biology Tools to Promote the Folding and Function of RNA Aptamers in Mammalian Cells. *RNA Biol.* **2023**, *20* (1), 198−206.
(401) Chen, C.-K.; Blanco, M.; Jackson, C.; Aznauryan, E.; Ollikainen, N.; Surka, C.; Chow, A.; Cerase, A.; McDonel, P.; Guttman, M. Xist Recruits the X Chromosome to the Nuclear Lamina to Enable Chromosome-Wide Silencing. *Science* **2016**, *354* (6311), 468−472.
(402) Young, A. N.; Perlas, E.; Ruiz-Blanes, N.; Hierholzer, A.; Pomella, N.; Martin-Martin, B.; Liverziani, A.; Jachowicz, J. W.; Giannakouros, T.; Cerase, A. Deletion of LBR N-Terminal Domains Recapitulates Pelger-Huet Anomaly Phenotypes in Mouse without Disrupting X Chromosome Inactivation. *Commun. Biol.* **2021**, *4* (1), 478.
(403) Isono, K.; Endo, T. A.; Ku, M.; Yamada, D.; Suzuki, R.; Sharif, J.; Ishikura, T.; Toyoda, T.; Bernstein, B. E.; Koseki, H. SAM Domain Polymerization Links Subnuclear Clustering of PRC1 to Gene Silencing. *Dev. Cell* **2013**, *26* (6), 565−577.
(404) Nepita, I.; Piazza, S.; Ruglioni, M.; Cristiani, S.; Bosurgi, E.; Salvadori, T.; Vicidomini, G.; Diaspro, A.; Castello, M.; Cerase, A.; Bianchini, P.; Storti, B.; Bizzarri, R. On the Advent of Super-Resolution Microscopy in the Realm of Polycomb Proteins. *Biology* **2023**, *12* (3), 374.
(405) Clemson, C. M.; McNeil, J. A.; Willard, H. F.; Lawrence, J. B. XIST RNA Paints the Inactive X Chromosome at Interphase: Evidence for a Novel RNA Involved in Nuclear/chromosome Structure. *J. Cell Biol.* **1996**, *132* (3), 259−275.
(406) Collombet, S.; Rall, I.; Dugast-Darzacq, C.; Heckert, A.; Halavatyi, A.; Le Saux, A.; Dailey, G.; Darzacq, X.; Heard, E. RNA Polymerase II Depletion from the Inactive X Chromosome Territory Is Not Mediated by Physical Compartmentalization. *Nat. Struct. Mol. Biol.* **2023**, *30*, 1216.
(407) Espinosa, J. R.; Joseph, J. A.; Sanchez-Burgos, I.; Garaizar, A.; Frenkel, D.; Collepardo-Guevara, R. Liquid Network Connectivity Regulates the Stability and Composition of Biomolecular Condensates with Many Components. *Proc. Natl. Acad. Sci. U. S. A.* **2020**, *117* (24), 13238−13247.
(408) Polyansky, A. A.; Gallego, L. D.; Efremov, R. G.; Köhler, A.; Zagrovic, B. Protein Compactness and Interaction Valency Define the Architecture of a Biomolecular Condensate across Scales. *Elife* **2023**, *12*, e80038 DOI: 10.7554/eLife.80038.
(409) Conti, B. A.; Oppikofer, M. Biomolecular Condensates: New Opportunities for Drug Discovery and RNA Therapeutics. *Trends Pharmacol. Sci.* **2022**, *43* (10), 820−837.
(410) Hallegger, M.; Chakrabarti, A. M.; Lee, F. C. Y.; Lee, B. L.; Amalietti, A. G.; Odeh, H. M.; Copley, K. E.; Rubien, J. D.; Portz, B.; Kuret, K.; Huppertz, I.; Rau, F.; Patani, R.; Fawzi, N. L.; Shorter, J.; Luscombe, N. M.; Ule, J. TDP-43 Condensation Properties Specify Its RNA-Binding and Regulatory Repertoire. *Cell* **2021**, *184* (18), 4680−4696.e22.
(411) Louka, A.; Zacco, E.; Temussi, P. A.; Tartaglia, G. G.; Pastore, A. RNA as the Stone Guest of Protein Aggregation. *Nucleic Acids Res.* **2020**, *48* (21), 11880−11889.
(412) Meier, U. T. RNA Modification in Cajal Bodies. *RNA Biol.* **2017**, *14* (6), 693−700.
(413) Zhang, D.-H.; Fujimoto, T.; Saxena, S.; Yu, H.-Q.; Miyoshi, D.; Sugimoto, N. Monomorphic RNA G-Quadruplex and Polymorphic DNA G-Quadruplex Structures Responding to Cellular Environmental Factors. *Biochemistry* **2010**, *49* (21), 4554−4563.
(414) Guo, W.; Ji, D.; Kinghorn, A. B.; Chen, F.; Pan, Y.; Li, X.; Li, Q.; Huck, W. T. S.; Kwok, C. K.; Shum, H. C. Tuning Material States and Functionalities of G-Quadruplex-Modulated RNA-Peptide Condensates. *J. Am. Chem. Soc.* **2023**, *145* (4), 2375−2385.
(415) Lyons, S. M.; Gudanis, D.; Coyne, S. M.; Gdaniec, Z.; Ivanov, P. Identification of Functional Tetramolecular RNA G-Quadruplexes Derived from Transfer RNAs. *Nat. Commun.* **2017**, *8* (1), 1127.
(416) Suzuki, T. The Expanding World of tRNA Modifications and Their Disease Relevance. *Nat. Rev. Mol. Cell Biol.* **2021**, *22* (6), 375−392.
(417) Akiyama, Y.; Kharel, P.; Abe, T.; Anderson, P.; Ivanov, P. Isolation and Initial Structure-Functional Characterization of Endogenous tRNA-Derived Stress-Induced RNAs. *RNA Biol.* **2020**, *17* (8), 1116−1124.
(418) Edupuganti, R. R.; Geiger, S.; Lindeboom, R. G. H.; Shi, H.; Hsu, P. J.; Lu, Z.; Wang, S.-Y.; Baltissen, M. P. A.; Jansen, P. W. T. C.; Rossa, M.; Müller, M.; Stunnenberg, H. G.; He, C.; Carell, T.; Vermeulen, M. N6-Methyladenosine (m6A) Recruits and Repels

AQ

Proteins to Regulate mRNA Homeostasis. *Nat. Struct. Mol. Biol.* **2017**, *24* (10), 870−878.
(419) Arguello, A. E.; DeLiberto, A. N.; Kleiner, R. E. RNA Chemical Proteomics Reveals the N6-Methyladenosine (m6A)-Regulated Protein-RNA Interactome. *J. Am. Chem. Soc.* **2017**, *139* (48), 17249−17252.
(420) Pandolfini, L.; Barbieri, I.; Bannister, A. J.; Hendrick, A.; Andrews, B.; Webster, N.; Murat, P.; Mach, P.; Brandi, R.; Robson, S. C.; Migliori, V.; Alendar, A.; d'Onofrio, M.; Balasubramanian, S.; Kouzarides, T. METTL1 Promotes Let-7 MicroRNA Processing via m7G Methylation. *Mol. Cell* **2019**, *74* (6), 1278−1290.e9.
(421) Wang, J.; Wang, J.; Gu, Q.; Ma, Y.; Yang, Y.; Zhu, J.; Zhang, Q. The Biological Function of m6A Demethylase ALKBH5 and Its Role in Human Disease. *Cancer Cell Int.* **2020**, *20*, 347.
(422) Jiang, X.; Liu, B.; Nie, Z.; Duan, L.; Xiong, Q.; Jin, Z.; Yang, C.; Chen, Y. The Role of m6A Modification in the Biological Functions and Diseases. *Signal Transduct Target Ther* **2021**, *6* (1), 74.
(423) Morgan, M.; Much, C.; DiGiacomo, M.; Azzi, C.; Ivanova, I.; Vitsios, D. M.; Pistolic, J.; Collier, P.; Moreira, P. N.; Benes, V.; Enright, A. J.; O'Carroll, D. mRNA 3′ Uridylation and poly(A) Tail Length Sculpt the Mammalian Maternal Transcriptome. *Nature* **2017**, *548* (7667), 347−351.
(424) Roundtree, I. A.; Evans, M. E.; Pan, T.; He, C. Dynamic RNA Modifications in Gene Expression Regulation. *Cell* **2017**, *169* (7), 1187−1200.
(425) Hiragami-Hamada, K.; Fischle, W. RNAs - Physical and Functional Modulators of Chromatin Reader Proteins. *Biochim. Biophys. Acta* **2014**, *1839* (8), 737−742.
(426) Jones, A. N.; Tikhaia, E.; Mourão, A.; Sattler, M. Structural Effects of m6A Modification of the Xist A-Repeat AUCG Tetraloop and Its Recognition by YTHDC1. *Nucleic Acids Res.* **2022**, *50* (4), 2350−2362.
(427) Bolognesi, B.; Lorenzo Gotor, N.; Dhar, R.; Cirillo, D.; Baldrighi, M.; Tartaglia, G. G.; Lehner, B. A Concentration-Dependent Liquid Phase Separation Can Cause Toxicity upon Increased Protein Expression. *Cell Rep.* **2016**, *16* (1), 222−231.
(428) Bellucci, M.; Agostini, F.; Masin, M.; Tartaglia, G. G. Predicting Protein Associations with Long Noncoding RNAs. *Nat. Methods* **2011**, *8* (6), 444−445.
(429) Tartaglia, G. G.; Pawar, A. P.; Campioni, S.; Dobson, C. M.; Chiti, F.; Vendruscolo, M. Prediction of Aggregation-Prone Regions in Structured Proteins. *J. Mol. Biol.* **2008**, *380* (2), 425−436.
(430) Feig, M.; Sugita, Y. Whole-Cell Models and Simulations in Molecular Detail. *Annu. Rev. Cell Dev. Biol.* **2019**, *35*, 191−211.
(431) Vernon, R. M.; Chong, P. A.; Tsang, B.; Kim, T. H.; Bah, A.; Farber, P.; Lin, H.; Forman-Kay, J. D. Pi-Pi Contacts Are an Overlooked Protein Feature Relevant to Phase Separation. *Elife* **2018**, *7*, e31486 DOI: 10.7554/eLife.31486.
(432) Paloni, M.; Bailly, R.; Ciandrini, L.; Barducci, A. Unraveling Molecular Interactions in Liquid-Liquid Phase Separation of Disordered Proteins by Atomistic Simulations. *J. Phys. Chem. B* **2020**, *124* (41), 9009−9016.
(433) Laghmach, R.; Malhotra, I.; Potoyan, D. A. Multiscale Modeling of Protein-RNA Condensation in and Out of Equilibrium. *Methods Mol. Biol.* **2023**, *2563*, 117−133.

https://doi.org/10.1021/acs.chemrev.3c00575
Chem. Rev. XXXX, XXX, XXX−XXX